AFCRL—71—0012 •

DEPARTMENT OF ELECTRICAL ENGINEERING
Colorado State University
Fort Collins, Colorado 80521

MICROWAVE REENTRY PLASMA DIAGNOSTICS

By James P. Rybak

Contract No. F19628—70—C—0035 Project No. 7260

PROJECT THEMIS

Scientific Report No.3 January 1971

CONTRACT MONITOR: WALTER ROTMAN MICROWAVE PHYSICS LABORATORY

PREPARED FOR

AIR FORCE CAMBRIDGE RESEARCH LABORATORIES
AIR FORCE SYSTEMS COMMAND UNITED STATES AIR FORCE
BEDFORD, MASSACHUSETTS 01730

AFCRL-71-0012

Department of Electrical Engineering

Colorado State University - Fort Collins, Colorado 80521

MICROWAVE REENTRY PLASMA DIAGNOSTICS

By
James P. Rybak

Contract No. F19628-70-C-0035

Project No. 7260

PROJECT THEMIS

Scientific Report No. 3

January 1971

Contract Monitor: Walter Rotman
Microwave Physics Laboratory

Prepared
for

AIR FORCE CAMBRIDGE RESEARCH LABORATORIES

AIR FORCE SYSTEMS COMMAND

UNITED STATES AIR FORCE

BEDFORD, MASSACHUSETTS 01730

ABSTRACT

An analysis of surface-mounted aperture antenna admittance has been performed in this study to determine the conditions under which admittance measurements can be used for reentry plasma diagnostics. The primary contribution of the present work is the determination that the admittance of a thin, microwave aperture antenna, located on the surface of a reentry vehicle, can be used to obtain the values of the electron density, electron collision frequency, ion sheath thickness and electron temperature of the reentry plasma. It is further demonstrated, by using admittance measurements made during a reentry test flight as reported by Mayhan et al. (1968 IEEE Trans. Antennas and Propagation, AP-17, 573), that open-ended-waveguide antenna admittances can be used to determine the plasma electron density, electron collision frequency and plasma stand-off distance when the reentry plasma is separated, due to aerodynamic boundary layer effects, from the surface of the reentry vehicle.

TABLE OF CONTENTS

LIST OF TABLES

LIST OF FIGURES

CHAPTER 1

INTRODUCTION

The problems which arise during the atmospheric reentry of a spacecraft or missile are myriad and by no means insignificant. The primary problem associated with the reentry plasma sheath is the "communications blackout" which in many cases results in a complete loss or at least a severe decrease in the strength of radio frequency signals between the reentry vehicle and the ground. This problem is of importance due to the loss of voice communications and data telemetry during the reentry of manned space vehicles and the loss of electronic countermeasures capability during the reentry of military ballistic missile payloads (Jacavanco 1969). No less important are the concomitant antenna electrical breakdown and antenna pattern distortion which can also occur before and after the blackout period. This problem lasts for up to ten minutes during what is often the most crucial part of the vehicle's flight. The "shuttle" reentry vehicles of the future will spend longer times in the reentry phase of flight and consequently will experience even more prolonged periods of reentry communications problems.

Considerable effort has been directed toward determining ways to alleviate the problems associated with the reentry plasma sheath. The most promising techniques to lessen the reentry plasma problem involve the injection of electrophilic chemicals into the reentry plasma flow field upstream from the antenna locations and the changing of the plasma flow field by aerodynamic shaping (Huber and Sims 1964). These alleviation techniques are in the developmental stage and a number of problems still must be solved. A thorough knowledge of the plasma sheath properties is needed in order to develop systems which can maintain communications during reentry. Unfortunately, the reentry plasma sheath is the result of chemical and thermodynamic processes which are not well understood. In addition, the conditions which control the rates at which these chemical and thermody-

namic processes occur change rapidly during reentry, further complicating the picture. Consequently, a complete understanding of the plasma sheath cannot be obtained from analytical approaches. Rather, it is necessary to make accurate in-flight measurements of the reentry plasma sheath properties.

Ideally, one would like to determine continuously the spatial variation of the electron density, electron collision frequency and electron temperature in the inhomogeneous plasma sheath from the surface of the reentry vehicle out to the point where the effect of the plasma upon the electromagnetic waves of interest becomes negligible. However, the severe environmental conditions which exist at all but the earliest stages of reentry preclude the use of probes extending into the plasma to determine the spatial variation of the plasma properties. Consequently, it is highly desirable to use sensors which are flush mounted on the surface of the vehicle. These sensors do not perturb the plasma flow field and are not subject to severe environmental conditions. Unfortunately, measurements from flush mounted sensors lack the spatial resolution of probe measurements. Nevertheless, surface mounted sensor measurements are the most practical means of determining the properties of the reentry plasma sheath.

The radiation patterns and admittances of surface mounted aperture antennas are changed markedly by the presence of a reentry plasma sheath. Consequently, measurements of aperture antenna admittance can be used to determine the properties of the reentry plasma sheath. The subject of in-flight measurements which can be related to the properties of the reentry plasma sheath is only in its elementary stages of development. Much more needs to be known about the performance of the surface mounted sensors in the reentry environment and the proper interpretation of the data acquired from them.

The original work described in this report has been directed toward furthering the knowledge and understanding of the behavior of surface mounted aperture antennas in a reentry plasma environment and developing techniques which enable one to use aperture antenna admittance measurements to determine directly the properties of the reentry plasma sheath.

These properties include the electron density, electron collision frequency, electron temperature and the thickness of the boundary layer which separates the plasma sheath from the reentry vehicle. Some aperture antenna configurations are able to excite efficiently longitudinal or electroacoustic waves in addition to transverse waves in a warm or compressible plasma (i.e. a plasma with a non-zero electron temperature). Consequently, the analysis of the aperture antenna sensors is based upon compressible plasma theory, where appropriate, in preference to the simpler but less accurate incompressible plasma theory which is commonly used.

The techniques developed in this study are applied successfully to measurements of aperture antenna admittance made during the reentry of a Trailblazer II rocket.

The equations appearing in this report are written in terms of rationalized mks units, exclusively. Aerospace and plasma physics jargon however is not based upon a consistent set of units. Data therefore, are presented with commonly accepted units.

CHAPTER II

APERTURE ADMITTANCE FOR A RIGID BOUNDARY

The input admittance expression for a rectangular aperture on a perfectly conducting ground plane separated from a compressible plasma half-space by an ion sheath of thickness z_o is formulated as a boundary-value problem in the current study. The sheath layer thickness is assumed to be of the order of a Debye length (see Appendix I), the sheath region permittivity is taken to be that of free space and the sheath boundary is assumed to be rigid. The aperture admittance is evaluated for a number of aperture dimensions and plasma conditions. The plasma conditions have been chosen to represent, realistically, those encountered during reentry. These reentry plasma conditions are given in Table II-1.

The admittance expression for an open-ended-waveguide antenna located on a ground plane covered with an incompressible (cold) plasma has been formulated and evaluated by Galejs (1965), Villeneuve (1965), Compton (1964), Swift (1967) and Mayhan (1967). A similar problem has been treated by Galejs (1966) for a compressible plasma layer. Galejs considered apertures with wave-guide dimensions only and did not investigate the aperture admittance at frequencies below the plasma frequency.

The determination of the aperture admittance expression in this chapter is based upon methods similar to those used by Compton (1964) and Swift (1967), with modifications included to account for the compressible plasma effects. It is felt that this formulation provides more insight concerning the problem than does the formulation developed by Galejs (1966).

A. Aperture Admittance Expression The geometry of the problem is shown in Figure II-1. The rectangular aperture is assumed to have a prescribed field distribution given by

$$E_x = \frac{V_o}{a} \cos(\pi y/b) \qquad \text{(II-1)}$$

TABLE II-1

TYPICAL REENTRY PLASMA PARAMETERS

Peak Plasma Frequency	$10 \lesssim \frac{\omega_p}{2\pi} \lesssim 1000$ GHz
Normalized Collision Frequency	$10^{-3} \lesssim \nu/\omega_p \lesssim 10^{-1}$
Electron Temperature	$T_e \lesssim 12{,}000°K$

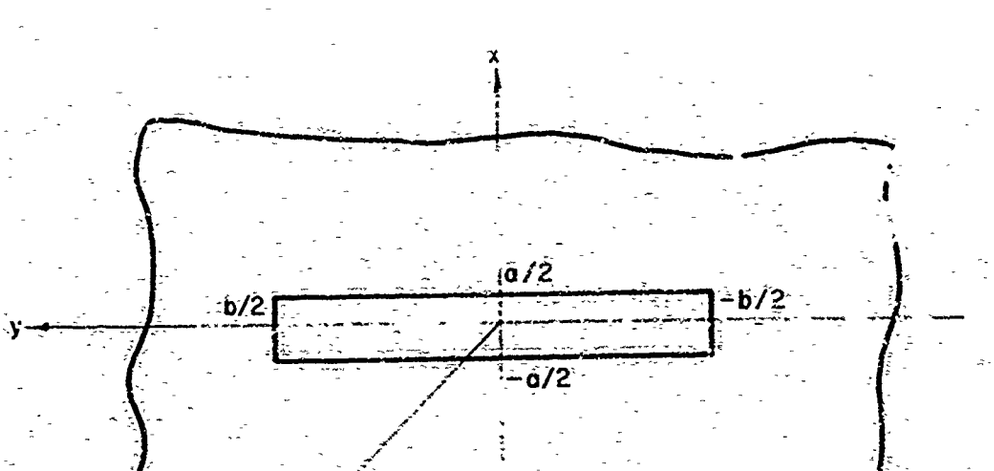

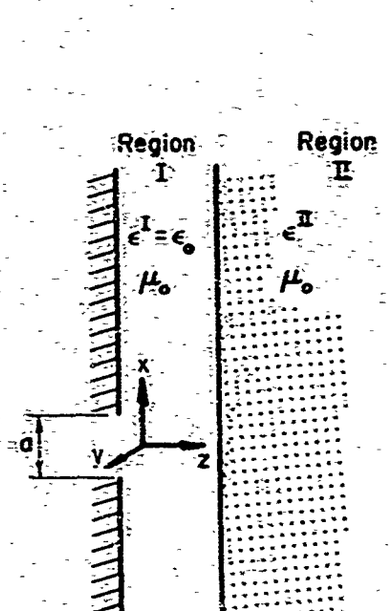

Figure II-1. Geometry for admittance calculations.

$$E_y = 0 \qquad \text{(II-2)}$$

for $-a/2 \leq x \leq a/2$ and $-b/2 \leq y \leq b/2$ where V_o is the aperture voltage. The aperture field distributions given by (II-1) and (II-2) are valid for thin $(a < \lambda_o/10)$ apertures of any length b or for wider apertures with $b = \lambda_o/2$ (Galejs 1969). The tangential electric field is assumed to be identically zero on the perfectly conducting ground plane.

The effect of surface waves on the aperture field distribution has been neglected in this study. Galejs (1966) has shown that these surface waves significantly affect the open-ended-waveguide antenna field distribution only when the aperture width is a multiple of surface half-wavelengths. Galejs found that this effect is reduced as the plasma electron collision frequency is increased. The effect of surface waves upon the aperture field distribution can be assumed negligible for the values of electron collision frequency experienced during reentry.

The field equations for the plasma regions are obtained by rewriting the linearized hydrodynamic equations (Oster 1960) in the form

$$\nabla \times \vec{E} = i\omega\mu_o \vec{H} \qquad \text{(II-3)}$$

$$\nabla \times \vec{H} = -i\omega\varepsilon_o \vec{\vec{E}} - N_o e\vec{v} \qquad \text{(II-4)}$$

$$(-i\omega+\nu)mN_o\vec{v} = -N_o e\vec{E} - \nabla P \qquad \text{(II-5)}$$

$$u^2 mN_o \nabla \cdot \vec{v} = i\omega P \qquad \text{(II-6)}$$

The electric field $\vec{E}$ and electron velocity $\vec{v}$ can be obtained in terms of $\vec{H}$ and P by eliminating either $\vec{v}$ or $\vec{E}$ from equations (II-4) and (II-5). The expressions for $\vec{E}$ and $\vec{v}$ are then written

$$\vec{E} = \frac{-1}{i\omega\varepsilon} (\nabla \times \vec{H}) + \frac{(\varepsilon_o - \varepsilon)}{N_o e \varepsilon} \nabla P \qquad \text{(II-7)}$$

$$\vec{v} = \frac{(\varepsilon_o - \varepsilon)}{N_o e \varepsilon} [\nabla \times \vec{H} - \frac{i\omega\varepsilon_o}{N_o e} \nabla P] \qquad \text{(II-8)}$$

where

$$\varepsilon = \left(1 - \frac{\omega_p^2}{\omega(\omega+i\nu)} \right) \varepsilon_o \quad . \qquad \text{(II-9)}$$

It is well known that the vector components of $\vec{H}$ can be separated into TE and TM parts which are derived from two potential functions, ψ_z and ψ_z^*. The components of $\vec{H}$ are related to ψ_z and ψ_z^* by

$$H_x = \frac{1}{\mu_o} \frac{\partial \psi_z}{\partial y} - \frac{1}{i\omega\mu_o} \frac{\partial^2 \psi_z^*}{\partial x \partial z} \qquad \text{(II-10)}$$

$$H_y = \frac{-1}{\mu_o} \frac{\partial \psi_z}{\partial x} - \frac{1}{i\omega\mu_o} \frac{\partial^2 \psi_z^*}{\partial y \partial z} \qquad \text{(II-11)}$$

$$H_z = \frac{1}{i\omega\mu_o} \left[\frac{\partial^2 \psi_z^*}{\partial x^2} + \frac{\partial^2 \psi_z^*}{\partial y^2} \right] \quad . \qquad \text{(II-12)}$$

Similarly, the components of $\vec{E}$ can be written

$$E_x = -\frac{\partial \psi_z^*}{\partial y} - \frac{1}{i\omega\mu_o\varepsilon} \frac{\partial^2 \psi_z}{\partial x \partial z} + \frac{(\varepsilon_o - \varepsilon)}{N_o e \varepsilon} \frac{\partial P}{\partial x} \qquad \text{(II-13)}$$

$$E_y = \frac{\partial \psi_z^*}{\partial x} - \frac{1}{i\omega\mu_o\varepsilon} \frac{\partial^2 \psi_z}{\partial y \partial z} + \frac{(\varepsilon_o - \varepsilon)}{N_o e \varepsilon} \frac{\partial P}{\partial y} \qquad \text{(II-14)}$$

$$E_z = \frac{1}{i\omega\mu_o\varepsilon}\left[\frac{\partial^2\psi_z}{\partial x^2} + \frac{\partial^2\psi_z}{\partial y^2}\right] + \frac{(\varepsilon_o - \varepsilon)}{N_o e}\frac{\partial P}{\partial z} \quad . \tag{II-15}$$

The potential functions ψ_z and ψ_z^* are those defined by Stratton (1941) and satisfy the partial differential equations

$$\nabla^2\psi_z + \omega^2\mu_o\varepsilon\psi_z = 0 \tag{II-16a}$$

$$\nabla^2\psi_z^* + \omega^2\mu_o\varepsilon\psi_z^* = 0 \quad . \tag{II-16b}$$

Similarly, P satisfies the partial differential equation obtained from equations (II-6) and (II-8)

$$\nabla^2 P + \frac{1}{u^2}\left[\omega(\omega+i\nu) - \omega_p^2\right] P = 0 \quad . \tag{II-17}$$

The potential functions are defined both in region I and in region II by the relations (Harrington 1961)

$$\psi_z^{I,II} = \frac{1}{(2\pi)^2}\iint_{-\infty}^{\infty} \bar{G}^{I,II}(k_x,k_y,z)\,\exp[i(k_x x + k_y y)]dk_x dk_y \tag{II-18}$$

$$\psi_z^{*I,II} = \frac{1}{(2\pi)^2}\iint_{-\infty}^{\infty} \bar{F}^{II}(k_x,k_y,z)\,\exp[i(k_x x + k_y y)]dk_x dk_y \tag{II-19}$$

$$P^{II} = \frac{1}{(2\pi)^2}\iint_{-\infty}^{\infty} \bar{P}^{II}(k_x,k_y,z)\,\exp[i(k_x x + k_y y)]dk_x dk_y \tag{II-20}$$

$$P^{I} \equiv 0 \tag{II-21}$$

$$\bar{F}^{II}(k_x,k_y,z) = A^{II}(k_x,k_y)\exp(ik_{ez}^{II}z) \qquad \text{(II-22)}$$

$$\bar{G}^{II}(k_x,k_y,z) = C^{II}(k_x,k_y)\exp(ik_{ez}^{II}z) \qquad \text{(II-23)}$$

$$\bar{P}^{II}(k_x,k_y,z) = P_o^{II}(k_x,k_y)\exp(ik_{pz}^{II}z) \qquad \text{(II-24)}$$

The propagation coefficients k_{ez} and k_{pz} are defined by

$$k_{ez}^{I,II} = \sqrt{(k_e^{I,II})^2 - k_x^2 - k_y^2} \qquad \text{(II-25)}$$

$$k_{pz}^{II} = \sqrt{(k_p^{II})^2 - k_x^2 - k_y^2} \qquad \text{(II-26)}$$

$$(k_e^{I,II})^2 = \omega^2\mu_o\varepsilon^{I,II} \qquad \text{(II-27)}$$

$$(k_p^{II})^2 = \frac{\omega^2}{(u^{II})^2}\left[1 - \left(\frac{\omega_p^{II}}{\omega}\right)^2 + \frac{i\nu^{II}}{\omega}\right] . \qquad \text{(II-28)}$$

The values of k_{ez} and k_{pz} determined from equations (II-25) and (II-26), respectively, must lie in the first quadrant of the complex plane to satisfy the radiation condition (Sommerfeld 1952) at infinity.

Equations (II-18) through (II-24) are substituted in equation (II-8) and equations (II-10) through (II-15). The boundary conditions (Kritz and Mintzer 1960) which must be satisfied are 1) continuity of E_x, E_y, H_x and H_y at $z = 0$ and at $z = z_o$; and 2) $v_z = 0$ at $z = z_o$ (rigid boundary condition). The mathematics can be simplified by defining the following terms

$$\bar{\bar{f}}(z) = \frac{\bar{\bar{F}}^{I}(z)}{\bar{\bar{F}}^{II}(z_o)} \tag{II-29}$$

$$\bar{\bar{f}}'(z) = \frac{1}{\bar{\bar{F}}^{II}(z_o)} \frac{\partial \bar{\bar{F}}^{I}(z)}{\partial z} \tag{II-30}$$

$$\bar{\bar{g}}(z) = \frac{\bar{\bar{G}}^{I}(z)}{\bar{\bar{G}}^{II}(z_o)} \tag{II-31}$$

$$\bar{\bar{g}}'(z) = \frac{1}{\bar{\bar{G}}^{II}(z_o)} \frac{\partial \bar{\bar{G}}^{I}(z)}{\partial z} \tag{II-32}$$

Using equations (II-29) through (II-32), the boundary conditions can be written in the following form. Continuity of E_x and E_y at $z = z_o$ yields

$$\bar{\bar{f}}(z_o) = 1 \tag{II-33}$$

$$\frac{k_{ez}^{II}}{\omega \mu_o \varepsilon^{II}} \bar{\bar{G}}^{II}(z_o) - \frac{(\varepsilon_o - \varepsilon^{II})}{N_o^{II} e \varepsilon^{II}} \bar{\bar{P}}^{II}(z_o) = - \frac{i \bar{\bar{g}}'(z_o)}{\omega \mu_o \varepsilon_o} \bar{\bar{G}}^{II}(z_o) \quad . \tag{II-34}$$

Continuity of H_x and H_y at $z = z_o$ yields

$$\bar{\bar{g}}(z_o) = 1 \tag{II-35}$$

$$\bar{\bar{f}}'(z_o) = i k_{ez}^{II} \quad . \tag{II-36}$$

The hard boundary condition ($v_z = 0$) at $z = z_o$ results in the relation

$$\frac{(k_x^2 + k_y^2)}{\mu_o} \bar{\bar{G}}^{II}(z_o) + \frac{\omega \varepsilon_G k_{pz}^{II}}{N_o^{II} e} \bar{\bar{P}}^{II}(z_o) = 0 \quad . \tag{II-37}$$

The tangential components of the electric field must be continuous at $z = 0$. Consequently,

$$\bar{\bar{E}}_x = -i\left[k_y \bar{\bar{f}}(o)\bar{\bar{F}}^{II}(z_o) + \frac{k_x \bar{\bar{G}}^{II}(z_o)\bar{\bar{g}}'(o)}{i\omega\mu_o\varepsilon_o}\right] \tag{II-38}$$

$$\bar{\bar{E}}_y = i\left[k_x \bar{\bar{f}}(o)\bar{\bar{F}}^{II}(z_o) - \frac{k_y \bar{\bar{G}}^{II}(z_o)\bar{\bar{g}}'(o)}{i\omega\mu_o\varepsilon_o}\right] \tag{II-39}$$

where E_x and E_y are the Fourier transforms of the tangential electric field at $z = 0$.

The tangential electric fields are identically zero on the perfectly conducting ground plane and are given by equations (II-1) and (II-2) for the aperture regions. The Fourier transforms of the tangential electric fields at $z = 0$ are given by

$$\bar{\bar{E}}_x = \int_{-\frac{b}{2}}^{\frac{b}{2}} \int_{-\frac{a}{2}}^{\frac{a}{2}} \frac{V_o}{a} \cos\left(\frac{\pi y}{b}\right)\{\exp[-i(k_x x + k_y y)]\}\, dk_x dk_y \tag{II-40}$$

$$= 2V_o b\pi \frac{\sin\left(\frac{k_x a}{2}\right)}{\left(\frac{k_x a}{2}\right)} \frac{\cos\left(\frac{k_y b}{2}\right)}{[\pi^2 - (k_y b)^2]}$$

$$\bar{\bar{E}}_y = 0 \tag{II-41}$$

Equation (II-16) and the geometry of the problem indicate that $f(z)$ is of the form

$$\bar{\bar{f}}(z) = A \exp(ik_{ez}^{I} z) + B \exp(-ik_{ez}^{I} z) \quad . \tag{II-42}$$

The values of A and B are determined from equations (II-33) and (II-36) with the result

$$A = \frac{(k_{ez}^{I} + k_{ez}^{II})}{2k_{ez}^{I}} \exp(-ik_{ez}^{I} z_o) \tag{II-43}$$

$$B = \frac{(k_{ez}^{I} - k_{ez}^{II})}{2k_{ez}^{I}} \exp(ik_{ez}^{I} z_o) \quad . \tag{II-44}$$

Equations (II-34) and (II-37) are used to determine

$$\bar{\bar{g}}'(z_o) = \frac{i(k_x^2 + k_y^2)(\varepsilon_o - \varepsilon^{II})}{\varepsilon^{II} k_{pz}^{II}} + \frac{i\varepsilon_o k_{ez}^{II}}{\varepsilon^{II}} \quad . \tag{II-45}$$

The expression for g(z) is likewise of the form

$$\bar{\bar{g}}(z) = C \exp(ik_{ez}^{I} z) + D \exp(-ik_{ez}^{I} z) \quad . \tag{II-46}$$

The values of C and D are determined from equations (II-35) and (II-45) with the result

$$C = \left[\frac{(k_x^2+k_y^2)(\varepsilon_o-\varepsilon^{II})}{\varepsilon^{II} k_{pz}^{II}} + \frac{\varepsilon_o k_{ez}^{II}}{\varepsilon^{II}} + k_{ez}^{I} \right] \frac{\exp(-ik_{ez}^{I} z_o)}{2k_{ez}^{I}} \tag{II-47}$$

$$D = -\left[\frac{(k_x^2+k_y^2)(\varepsilon_o-\varepsilon^{II})}{\varepsilon^{II} k_{pz}^{II}} + \frac{\varepsilon_o k_{ez}^{II}}{\varepsilon^{II}} - k_{ez}^{I} \right] \frac{\exp(+ik_{ez}^{I} z_o)}{2k_{ez}^{I}} \tag{II-48}$$

The expressions for $F^{II}(z_o)$ and $G^{II}(z_o)$ now can be determined from equations (II-38) and (II-39). The results are

$$\bar{\bar{F}}^{II}(z_o) = \frac{ik_y \bar{\bar{E}}_x}{(k_x^2+k_y^2)f(o)} = \frac{ik_y \bar{\bar{E}}_x}{(k_x^2+k_y^2)(A+B)} \qquad \text{(II-49)}$$

$$\bar{\bar{G}}^{II}(z_o) = \frac{-\omega\mu_o\varepsilon_o k_x \bar{\bar{E}}_x}{(k_x^2+k_y^2)g'(o)} = \frac{-\omega\mu_o\varepsilon_o k_x \bar{\bar{E}}_x}{(k_x^2+k_y^2)ik_{ez}^I(C-D)} \qquad \text{(II-50)}$$

with A, B, C, D and $\bar{\bar{E}}_x$ defined by equations (II-43), (II-44), (II-47), (II-48) and (II-40), respectively.

The Fourier transform of H_y at $z = 0$ can be determined from equation (II-11) along with equations (II-49) and (II-50). The result is

$$\bar{\bar{H}}_y = \frac{iY_o \bar{\bar{E}}_x}{(k_x^2+k_y^2)}\left[\frac{k_o(C+D)k_x^2}{ik_{ez}^I(C-D)} - \frac{ik_{ez}(A-B)k_y^2}{k_o(A+B)}\right] \qquad \text{(II-51)}$$

where $Y_o = \sqrt{\frac{\varepsilon_o}{\mu_o}}$ is the characteristic admittance of free space.

The time-averaged, outward normal, flow of power per unit area through the aperture is given by Hessel et al. (1962) in the form

$$\vec{S} = \frac{1}{2}\left[E_x H_y^* + PV_z^*\right]_{z=o^+}\hat{z} \quad . \qquad \text{(II-52)}$$

The pressure term P is identically zero in the sheath region. Consequently, equation (II-52) can be written

$$\vec{S} = \frac{1}{2}\left[E_x H_y^*\right]\Big|_{z=o^+}\hat{z} \quad . \qquad \text{(II-53)}$$

The complex conjugate of the power radiated by the aperture can be expressed using Parseval's theorem (Harrington 1961)

$$W^* = \frac{1}{2} \int_{-\frac{a}{2}}^{\frac{a}{2}} \int_{-\frac{b}{2}}^{\frac{b}{2}} E_x^* H_y \, dx\,dy = \frac{1}{2}\left(\frac{1}{2\pi}\right)^2 \iint_{-\infty}^{\infty} \bar{\bar{E}}_x^* \bar{\bar{H}}_y \, dk_x\,dk_y \tag{II-54}$$

The conjugate admittance Y^* of the aperture is defined by the relation

$$W^* = \frac{1}{2} V_o^2 Y^* \tag{II-55}$$

where V_o is the peak aperture voltage.

Substituting equation (II-51) into equation (II-54) and using equation (II-40) for $\bar{E}_x$, the expression for the conjugate aperture admittance is

$$Y^* = G_c - iB_c = b^2 Y_o \iint_{-\infty}^{\infty} \left[\frac{\sin\left(\frac{k_x a}{2}\right)}{\left(\frac{k_x a}{2}\right)}\right]^2 \left[\frac{\cos\left(\frac{k_y b}{2}\right)}{\pi^2 - (k_y b)^2}\right]^2 \left[\frac{k_o (C+D) k_x^2}{k_{ez}(C-D)} + \frac{k_{ez}(A-B)k_y^2}{k_o(A+B)}\right] \frac{dk_x\,dk_y}{(k_x^2+k_y^2)} \tag{II-56}$$

The quantity G_c is called the calculated aperture conductance and B_c is called the calculated aperture susceptance.

The evaluation of equation (II-56) is simplified considerably by making a transformation from rectangular coordinates to polar coordinates by means of the relations

$$k_x = k_o \beta \cos \alpha \tag{II-57}$$

$$k_y = k_o \beta \sin \alpha \quad . \tag{II-58}$$

Changing the double integral in equation (II-53) from $k_x - k_y$ coordinates to $\alpha - \beta$ coordinates is accomplished using the general formula (Thomas 1953)

$$\iint \xi\,(x,y)\,dx\,dy = \iint \phi\,[f(u,v),\, g(u,v)]\, \frac{\partial(x,y)}{\partial(u,v)}\, du\,dv \tag{II-59}$$

where

$$\frac{\partial(x,y)}{\partial(u,v)} = \begin{vmatrix} \frac{\partial x}{\partial u} & \frac{\partial x}{\partial v} \\ \frac{\partial y}{\partial u} & \frac{\partial y}{\partial v} \end{vmatrix} \tag{II-60}$$

is the "Jacobian" of the transformation.

Equation (II-56) is then written in terms of α and β in the form

$$Y^* = (k_o b)^2 Y_o \int_0^{\infty} \int_0^{2\pi} \beta \left[\frac{\sin\left(\frac{a k_o \beta \cos \alpha}{2} \right)}{\frac{a k_o \beta \cos \alpha}{2}} \right]^2$$

$$\left[\frac{\cos\left(\frac{b k_o \beta \sin \alpha}{2} \right)}{\pi^2 - (b k_o \beta \sin \alpha)^2} \right]^2 \left[\frac{(C+D) \cos^2 \alpha}{(C-D)\sqrt{1-\beta^2}} \right.$$

$$\left. + \frac{(A-B)\sqrt{1-\beta^2}}{(A+B)} \sin^2 \alpha \right] d\alpha\, d\beta \tag{II-61}$$

with equations (II-43) and (II-44), defining A, B, C and D, written in terms of α and β.

B. Evaluation of the Integral The integration of equation (II-61) cannot be done analytically and must be done numerically. The method of numerical integration chosen to evaluate the β integration in equation (II-59) is that used by Richmond (1966). This method is said to combine "the simplicity of the trapezoidal rule with the efficiency of the fifth-order Newton-Cotes formula" and has proven to be quite satisfactory. The numerical integration method is outlined in Appendix II. A conventional Simpson's rule procedure is used for the α integration.

The integration of equation (II-61) is straightforward, provided the plasma is lossy. For a non-lossy plasma, surface wave poles and branch points may occur along the integration path. Seshadri (1964) and Swift (1967) have described the integration procedure which must be followed when poles exist in the path of integration. Only lossy plasmas have been considered in the current study to represent accurately the reentry plasma sheath.

The value of β at which the integration can be terminated depends upon the dimensions of the aperture. It has been found that the integration can be terminated at $\beta = 6.5$ for waveguide size apertures but that the integration must be carried out to about $\beta = 500$ for very thin ($a < .01 \lambda_c$) apertures. The accuracy of the numerical integration is better than one per cent.

C. Numerical Calculations Equation (II-61) has been evaluated numerically for a range of aperture dimensions and plasma parameters. Initially, the ion sheath thickness has been taken to be zero. Figures II-2 and II-3 show the aperture conductance G_c and susceptance B_c, normalized with respect to the admittance of free space Y_o, as functions of K_r, the real part of the complex plasma dielectric coefficient. The value of the abcissa variable K_r in these figures is related to the plasma frequency ω_p and to the antenna excitation frequency ω through the relation

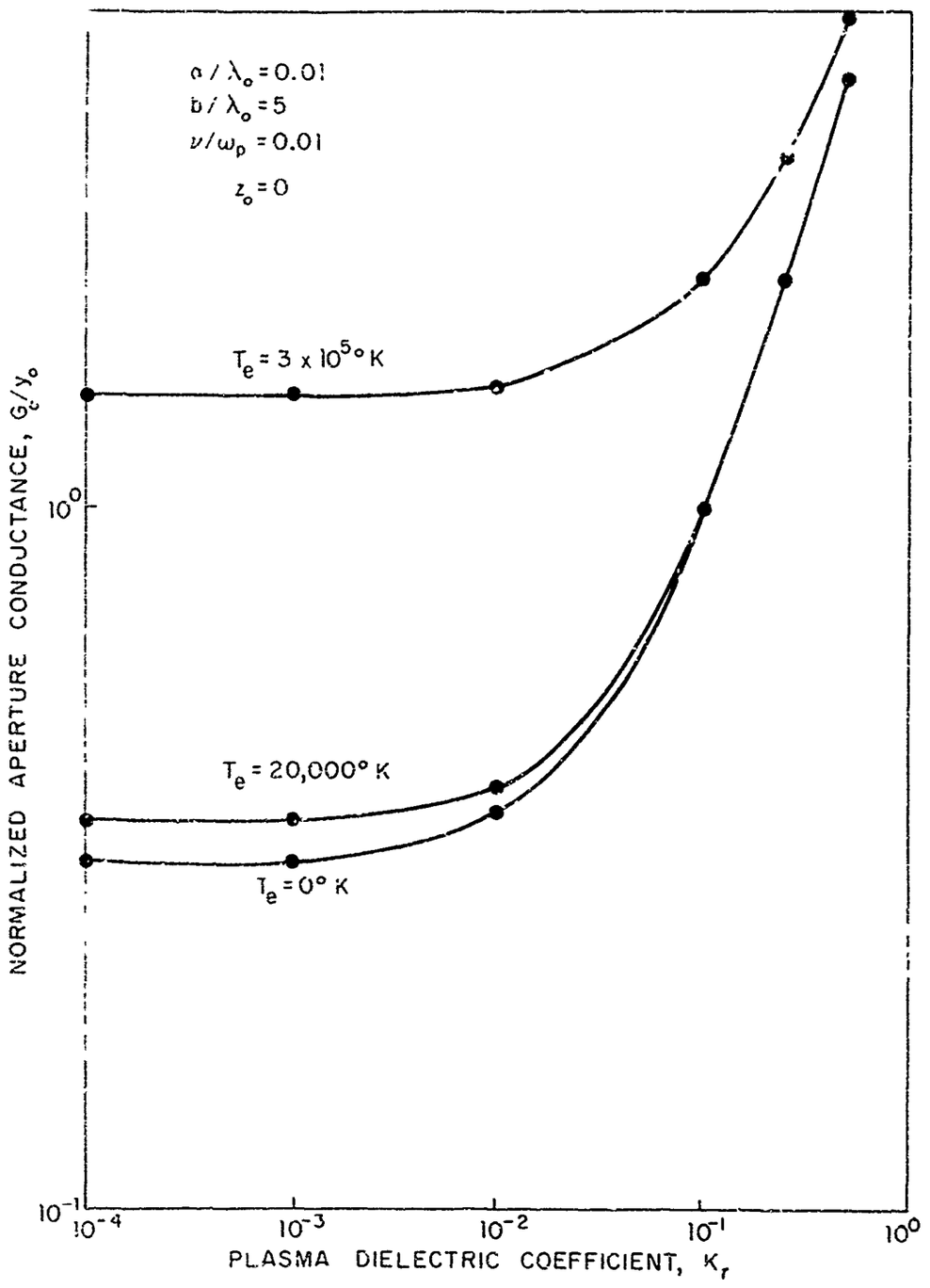

Figure II-2. Normalized conductance of aperture radiating into underdense plasma; effect of dielectric coefficient.

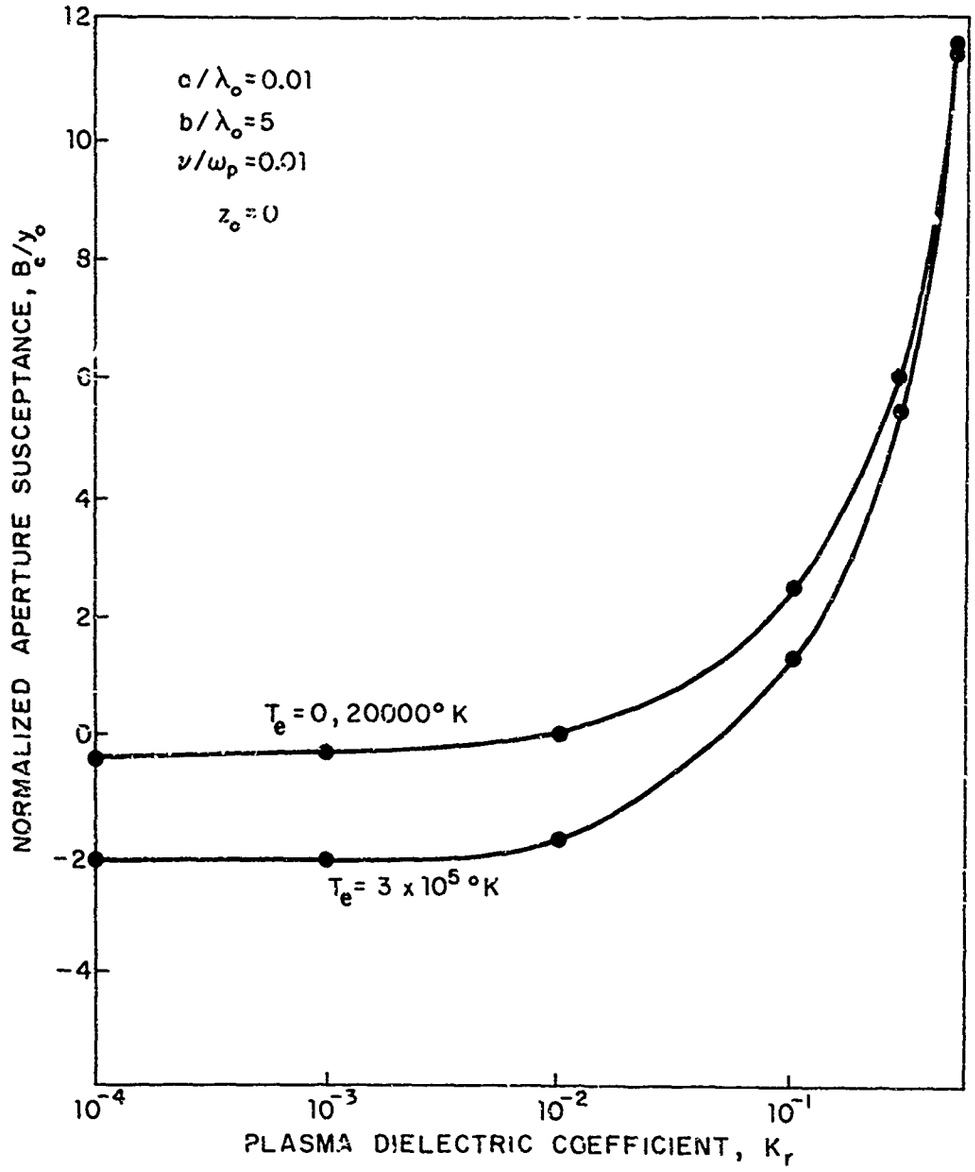

Figure II-3. Normalized susceptance of aperture radiating into underdense plasma; effect of dielectric coefficient.

$$K_r \approx 1 - \left(\frac{\omega_p}{\omega}\right)^2 \quad . \tag{II-62}$$

It is seen from Figures II-2 and II-3 that plasma electron temperature effects, due to the excitation of electroacoustic waves, are small for values of K_r greater than about .50 . More explicitly, electron temperature effects are small for values of the antenna wave frequency only slightly greater than the plasma frequency.

Also apparent from Figures II-2 and II-3 is the fact that the electron temperature, T_e , must be quite high ($\sim 10^{5°}K$) to produce measureable effects upon the aperture admittance. The electron temperature at any location in the reentry plasma sheath probably does not exceed about 12,000°K. This value of electron temperature produces a negligible effect upon the aperture susceptance and only a slight effect upon the aperture conductance.

The effect of the aperture length b upon the calculated aperture admittance is shown in Figures II-4 and II-5. The normalizing factor λ_o is the free space wavelength of the antenna excitation signal. Electron temperature effects upon the aperture susceptance become more important as the aperture length increases for wave frequencies above the plasma frequency. The reason for this behavior is not difficult to understand if one examines equation (II-61). The term

$$\left.\frac{(C+D)}{(C-D)\sqrt{1-\beta^2}}\right|_{z_o=0}$$

$$= \frac{\frac{\varepsilon^{II}}{\varepsilon_o}\sqrt{\left(\frac{c}{u}\right)^2\left[1-\left(\frac{\omega_p}{\omega}\right)^2+i\,\nu/\omega\right]-\beta^2}}{\sqrt{\frac{\varepsilon^{II}}{\varepsilon_o}-\beta^2}\sqrt{\left(\frac{c}{u}\right)^2\left[1-\left(\frac{\omega_p}{\omega}\right)^2+i\,\nu/\omega\right]-\beta^2}+\beta^2\left(1-\frac{\varepsilon^{II}}{\varepsilon_o}\right)} \tag{II-63}$$

produces all the electron temperature effects and is somewhat smaller than the term

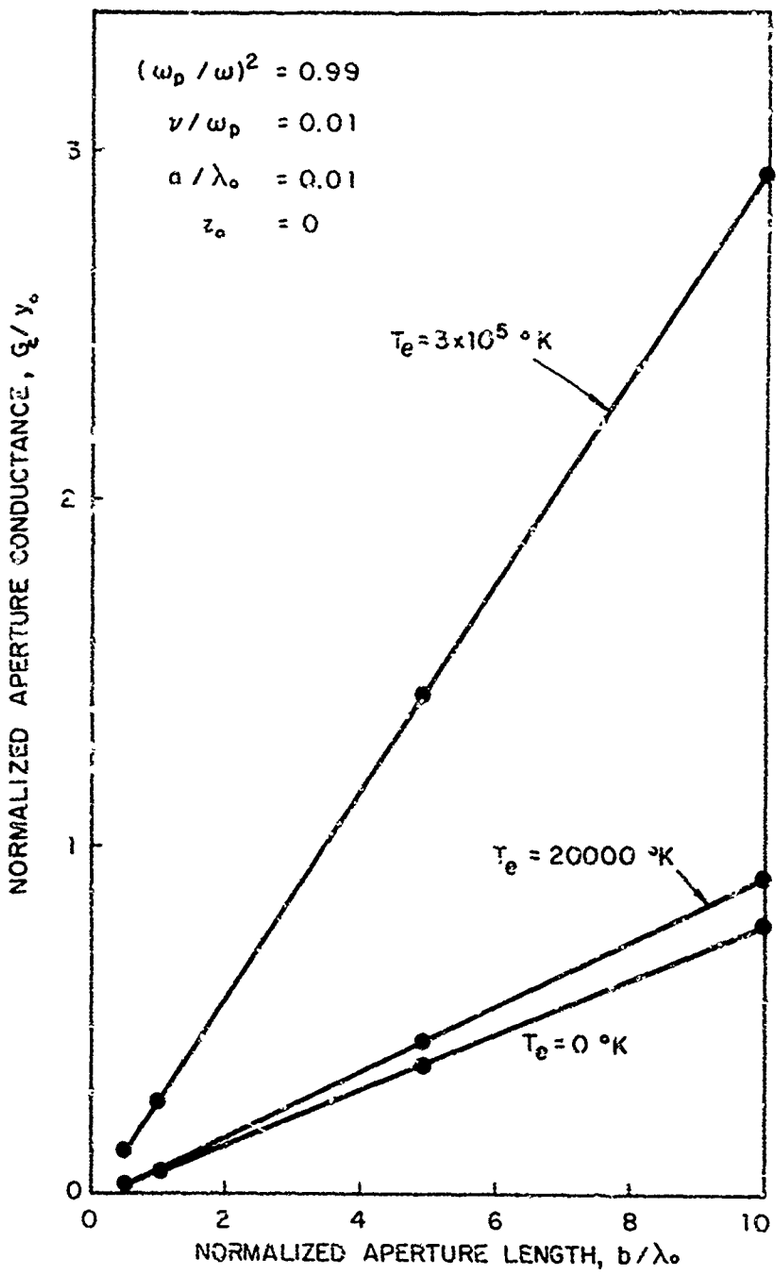

Figure II-4. Normalized conductance of aperture radiating into underdense plasma; effect of aperture length.

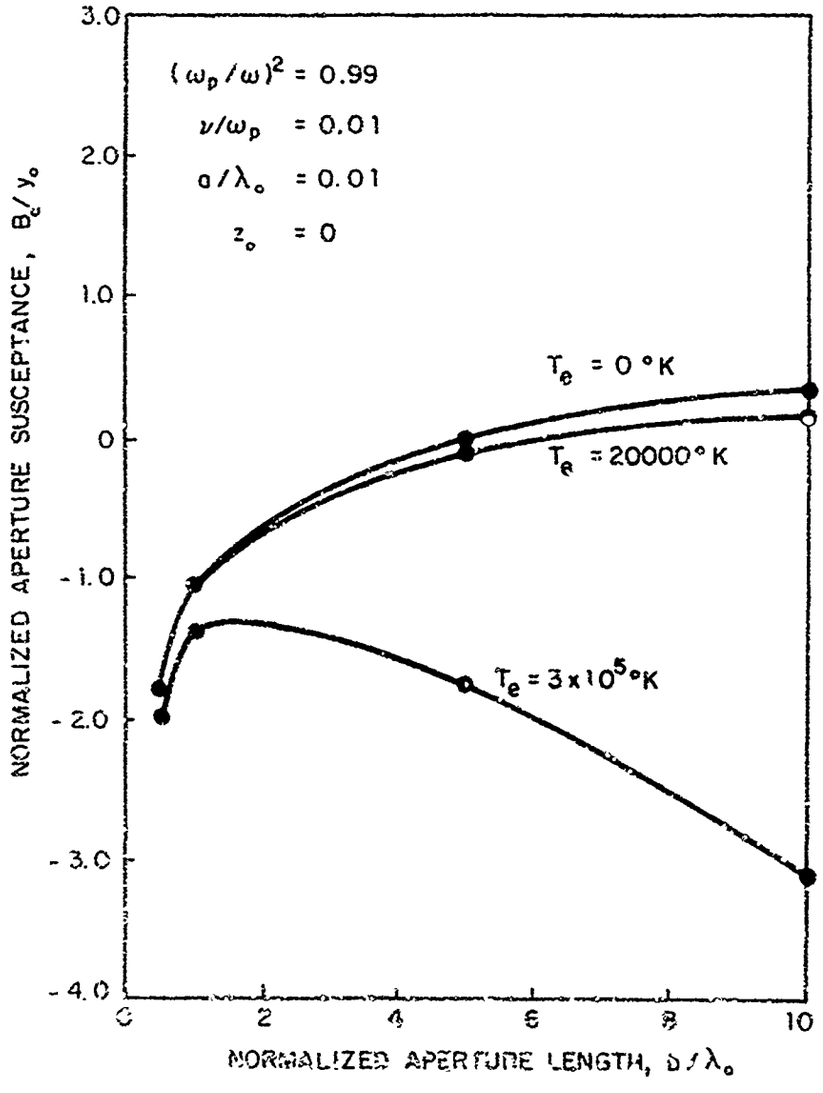

Figure II-5 Normalized susceptance of aperture radiating into underdense plasma; effect of aperture length.

$$\left.\frac{(A-B)\sqrt{1-\beta^2}}{A+B}\right|_{z_o=0} = \sqrt{\frac{\varepsilon^{II}}{\varepsilon_o} - \beta^2} \qquad \text{(II-64)}$$

for values of frequency ω greater than the plasma frequency ω_p. The value of the term

$$\frac{\cos\left(\frac{bk_o \beta \sin\alpha}{2}\right)}{\pi^2 - (bk_o \beta \sin\alpha)^2} \qquad \text{(II-65)}$$

becomes very small for large values of aperture length b except for very small values of α. This produces a weighting factor which increases the importance of term (II-63) with respect to term (II-64) for larger values of b. Term (II-64) contributes significantly only to the aperture susceptance while term (II-63) contributes to both the aperture conductance and susceptance. The result is a linear relationship between the aperture conductance and the aperture length. An examination of equation (II-63) indicates that the contribution of term (II-63) to the integral is linear with b due to the α integration. The electron temperature is observed to determine the coefficient of proportionality between the aperture length and conductance.

The effect of the aperture length upon the component of normalized aperture susceptance B_c' due to the nonzero plasma electron temperature (term II-63) is shown in Figure II-6. The value of B_c' has been obtained by taking the difference

$$B_c'(T_e \neq 0) = B_c(T_e \neq 0) - B_c(T_e = 0) \qquad \text{(II-66)}$$

The value of B_c' is observed to increase linearly with aperture length b, as expected.

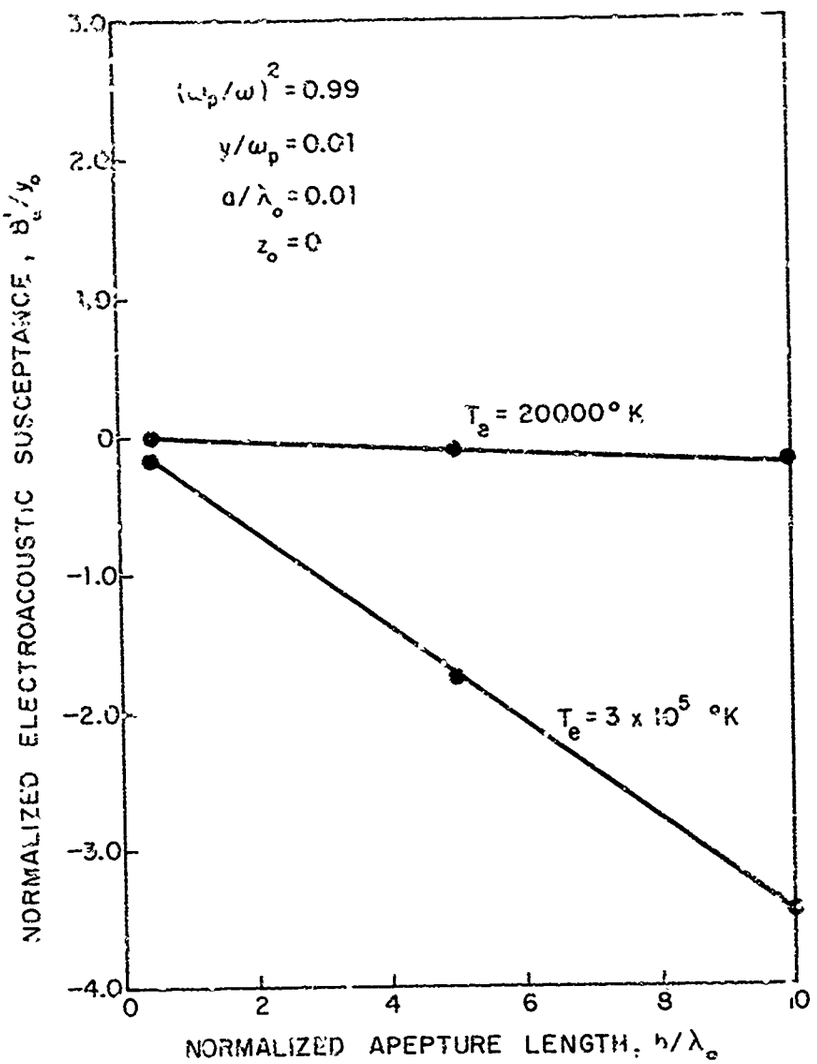

Figure II-6. Normalized electroacoustic susceptance of aperture radiating into underdense plasma; effect of aperture length.

The effect of the aperture width a upon the normalized conductance and susceptance calculated for a sheathless aperture excited at a frequency slightly above the plasma frequency is shown in Figures II-7 and II-8, respectively. The effects of the nonzero plasma electron temperature are diminished as the normalized aperture width increases. Negligible electron temperature effects are observed when the normalized aperture width is .10 or greater.

Electron temperature effects tend to make the calculated aperture susceptance less negative for very thin apertures but tend to make the aperture susceptance more negative for wider apertures. This is due to the effect of the weighting coefficient

$$\left[\frac{\sin\left(\frac{ak_o \beta \cos\alpha}{2}\right)}{\left(\frac{ak_o \beta \cos\alpha}{2}\right)}\right]^2 \qquad \text{(II-67)}$$

upon terms (II-63) and (II-64) in equation (II-61). For large values of the aperture width a , the product of terms (II-65) and (II-67) is small for all but very small values of β . Plasma electron temperature effects in term (II-63), however, are most apparent for somewhat larger values of β . Terms (II-65) and (II-67) tend to suppress the electron temperature effects upon the aperture admittance as the value of the aperture width a increases.

The admittance of an aperture excited at a frequency below the plasma frequency exhibits effects due to the plasma electron temperature somewhat different from those shown in Figures II-2 through II-8. The calculated, normalized aperture conductance and susceptance values shown in Figures II-9 and II-10, respectively, are observed to be measureably affected by plasma electron temperatures encountered during reentry.

Equally interesting are Figures II-11 and II-12 which show the normalized aperture conductance and susceptance, respectively, for various values of the aperture length b . The aperture is excited at a frequency below the

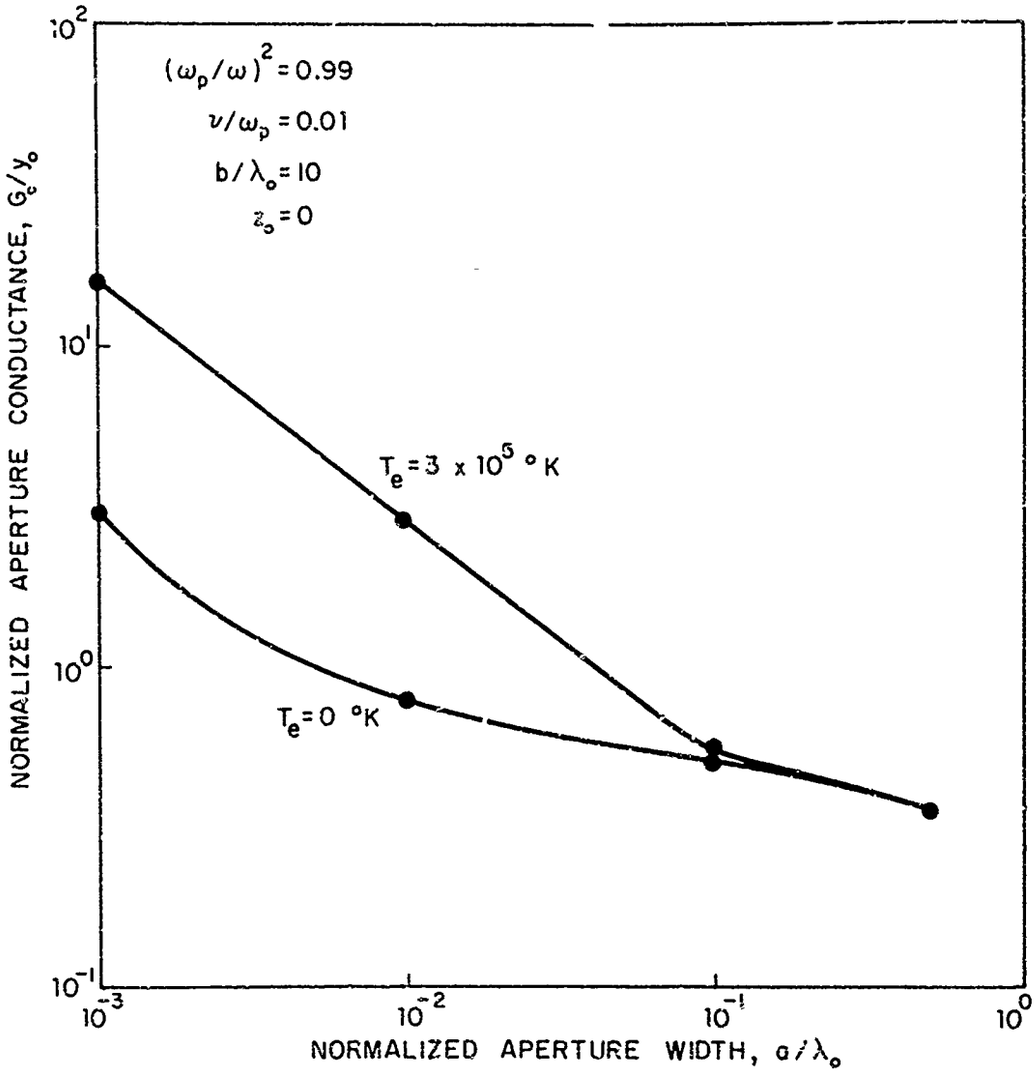

Figure II-7. Normalized conductance aperture radiating into underdense plasma; effect of aperture width.

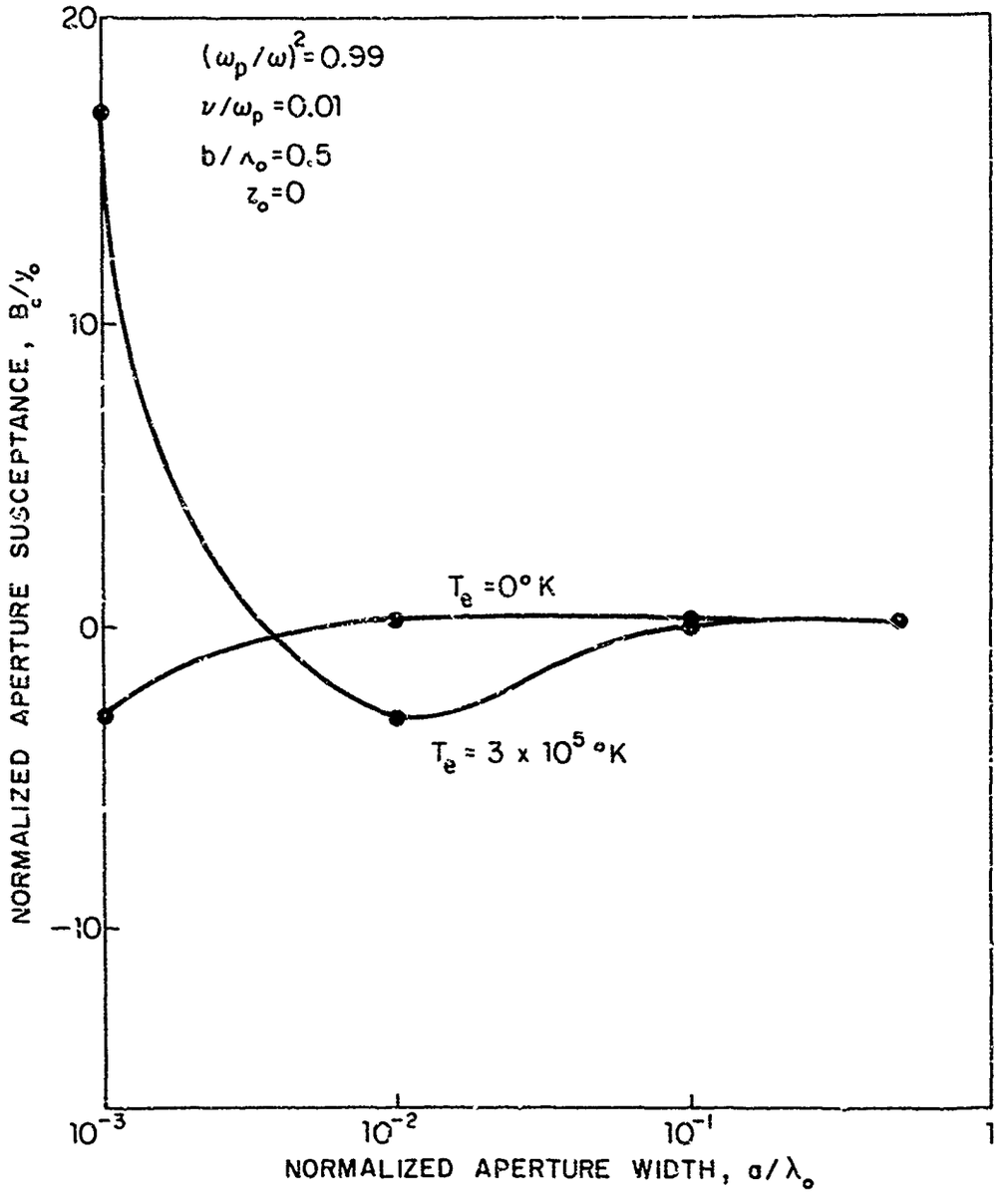

Figure II-8. Normalized susceptance of aperture radiating into underdense plasma; effect of aperture width.

plasma frequency. The normalized aperture susceptance and conductance are observed to vary linearly with the aperture length for both zero and nonzero values of the plasma electron temperature.

The reasons for the increased effect of the plasma electron temperature upon aperture admittance observed in Figures II-9 and II-10 together with the linear relationship of aperture admittance to aperture length observed in Figures II-11 and II-12 are apparent from an examination of equation (II-61). The magnitude of term (II-63) is comparable to or larger than the magnitude of term (II-65) for large, negative values of the plasma permittivity ε, even for small values of the plasma electron temperature. The weighting factor (II-64) along with the $\sin^2 \alpha$ and $\cos^2 \alpha$ coefficients make the contribution of term (II-64) to the integral in equation (II-61) negligible compared to the contribution of term (II-63), even for relatively small values of aperture length b.

The effects of aperture width a upon normalized aperture conductance and susceptance are shown in Figures II-13 and II-14, respectively. The calculated aperture conductance is observed to exhibit smaller electron temperature effects as the aperture width is increased. Negligible electron temperature effects are observed for aperture widths greater than $0.1\ \lambda_o$.

The effect of the plasma electron temperature on the normalized, calculated aperture conductance and susceptance is shown in Figures II-15 through II-17. It is observed that temperature effects become more pronounced as the ratio of the plasma frequency to the antenna excitation frequency becomes larger. Temperature effects, however, are diminished by increased electron collisions.

The reasons for these effects can be seen from an examination of equation (II-61). Term (II-63) becomes large for smaller values of β as the permittivity of the plasma becomes more negative and the electron temperature is held constant. Consequently, a given electron temperature produces a larger effect upon the admittance as the plasma permittivity becomes more negative. An increase in the number of electron collisions increases the imaginary part of the plasma permittivity and limits the magnitude which term (II-63) can attain and, consequently, reduces the effect of a given plasma electron temperature upon the aperture admittance.

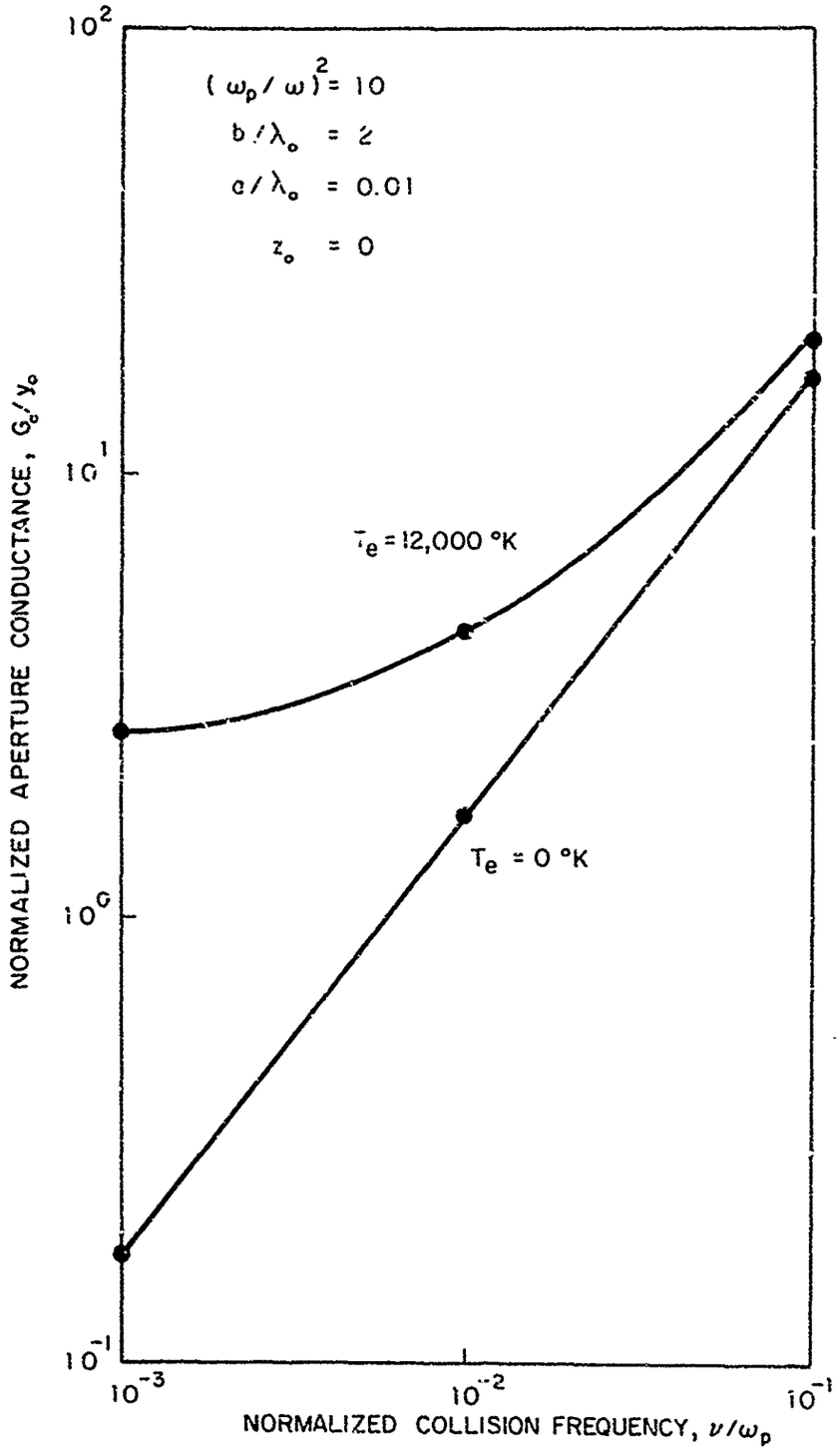

Figure II-9. Normalized conductance of aperture radiaring into overdense plasma; effect of plasma losses.

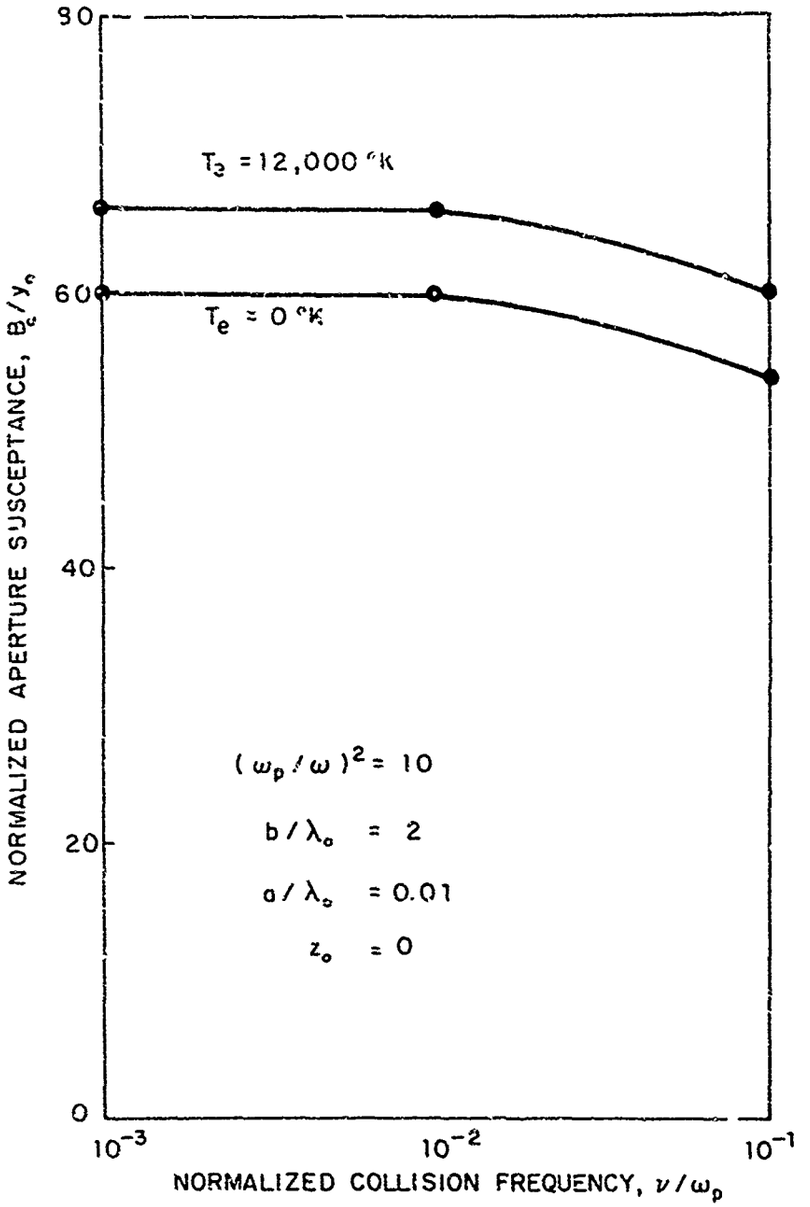

Figure II-10. Normalized susceptance of aperture radiating into overdense plasma; effect of plasma losses.

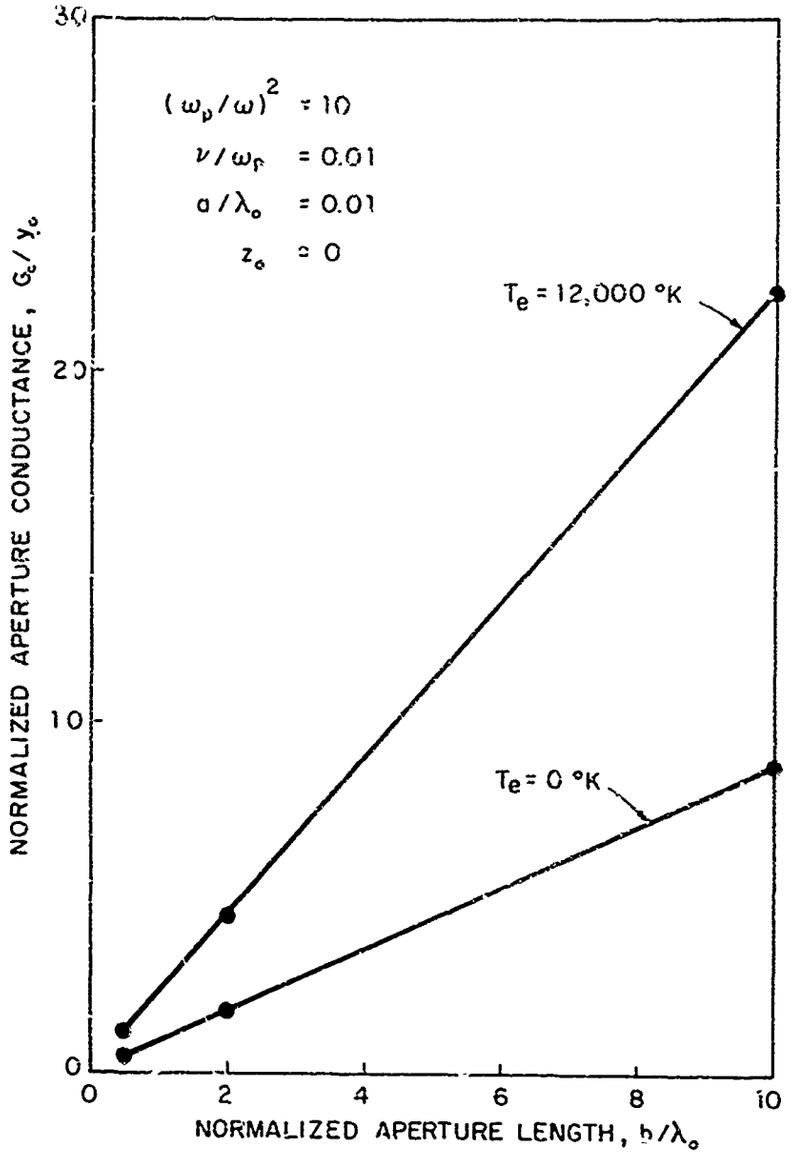

Figure II-11 Normalized conductance of aperture radiating into overdense plasma; effect of aperture length.

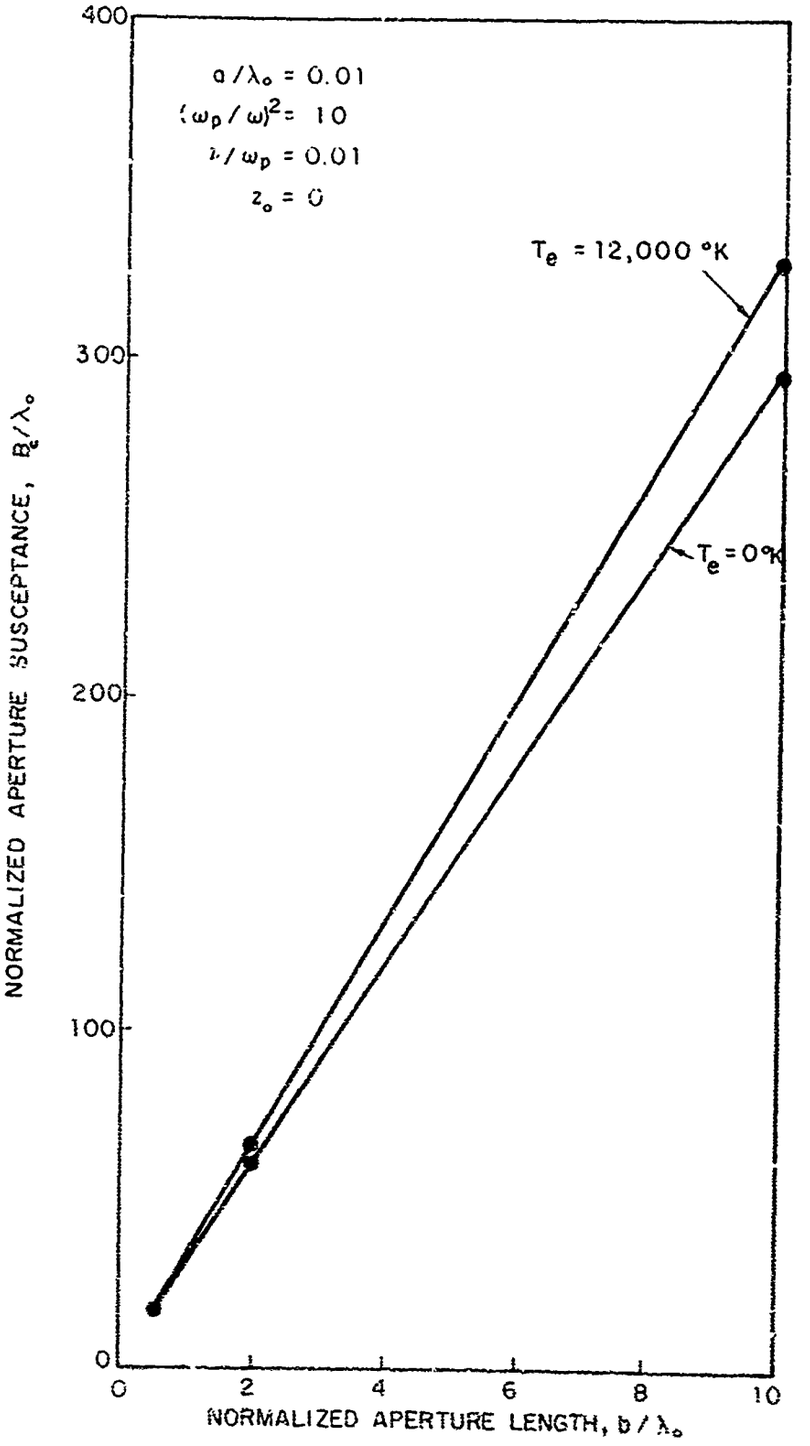

Figure II-12. Normalized susceptance of aperture radiating into overdense plasma; effect of aperture length.

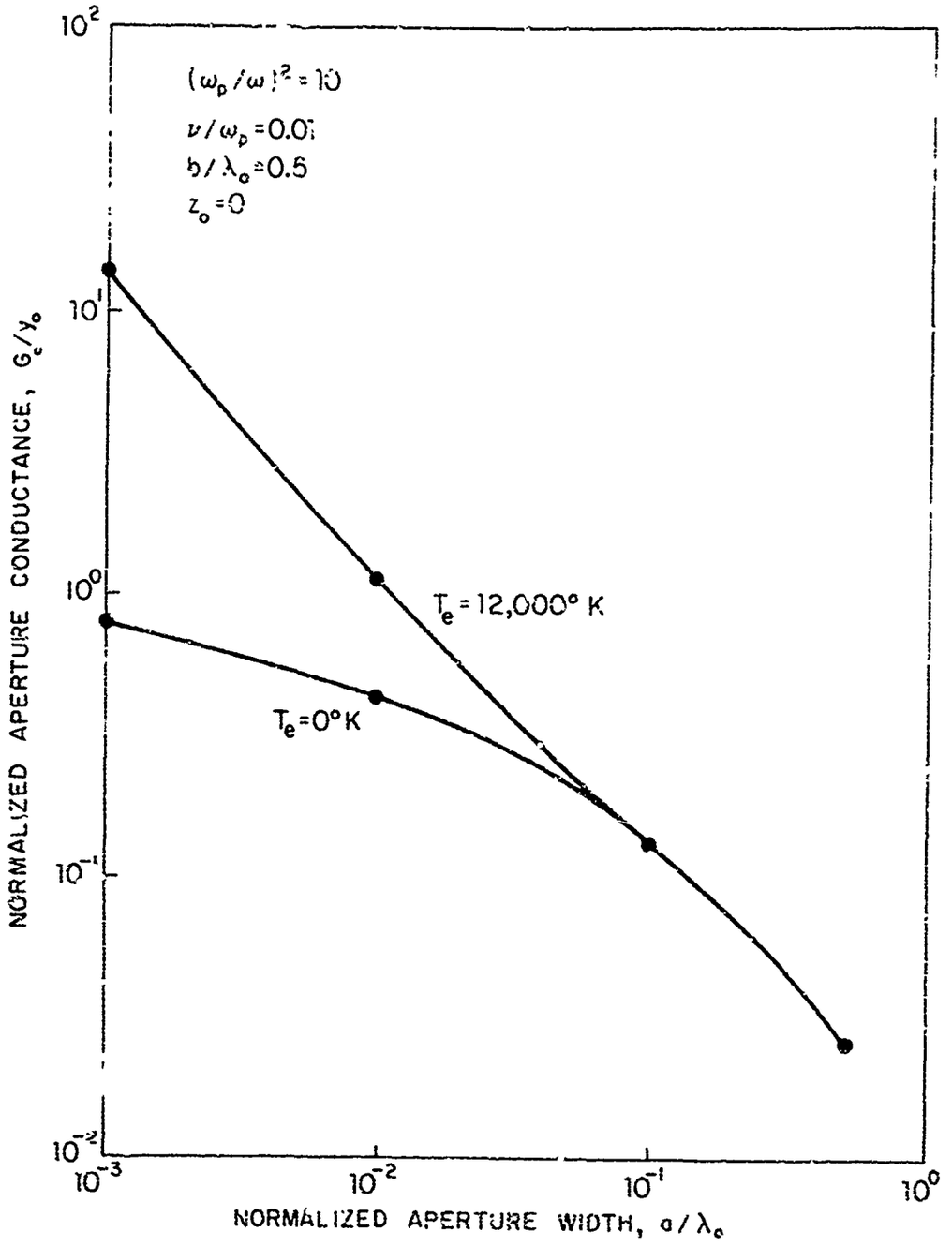

Figure II-13. Normalized conductance of aperture radiating into overdense plasma; effect of aperture width.

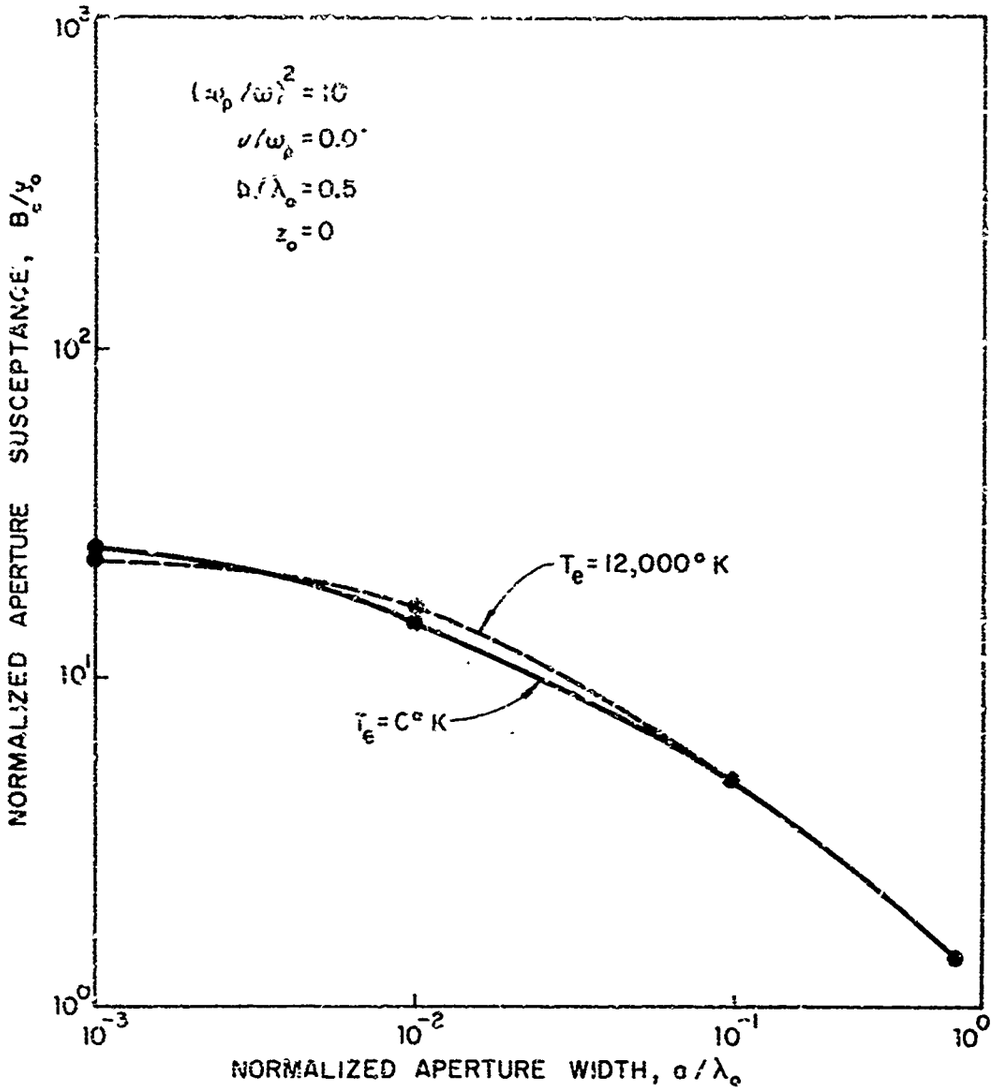

Figure II-14. Normalized susceptance of aperture radiating into overdense plasma; effect of aperture width.

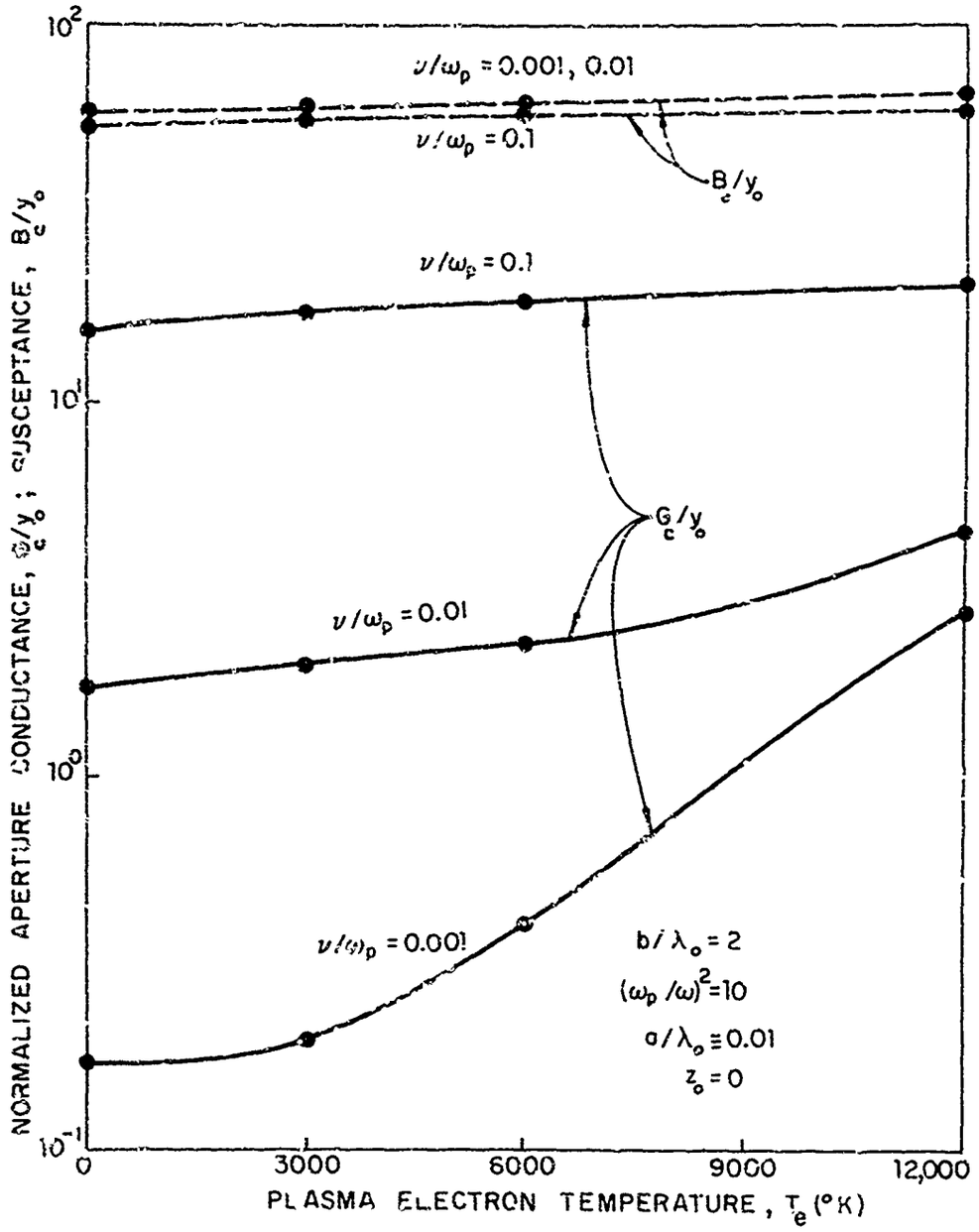

Figure II-15. Normalized conductance and susceptance of aperture radiating into overdense plasma; effect of electron temperature.

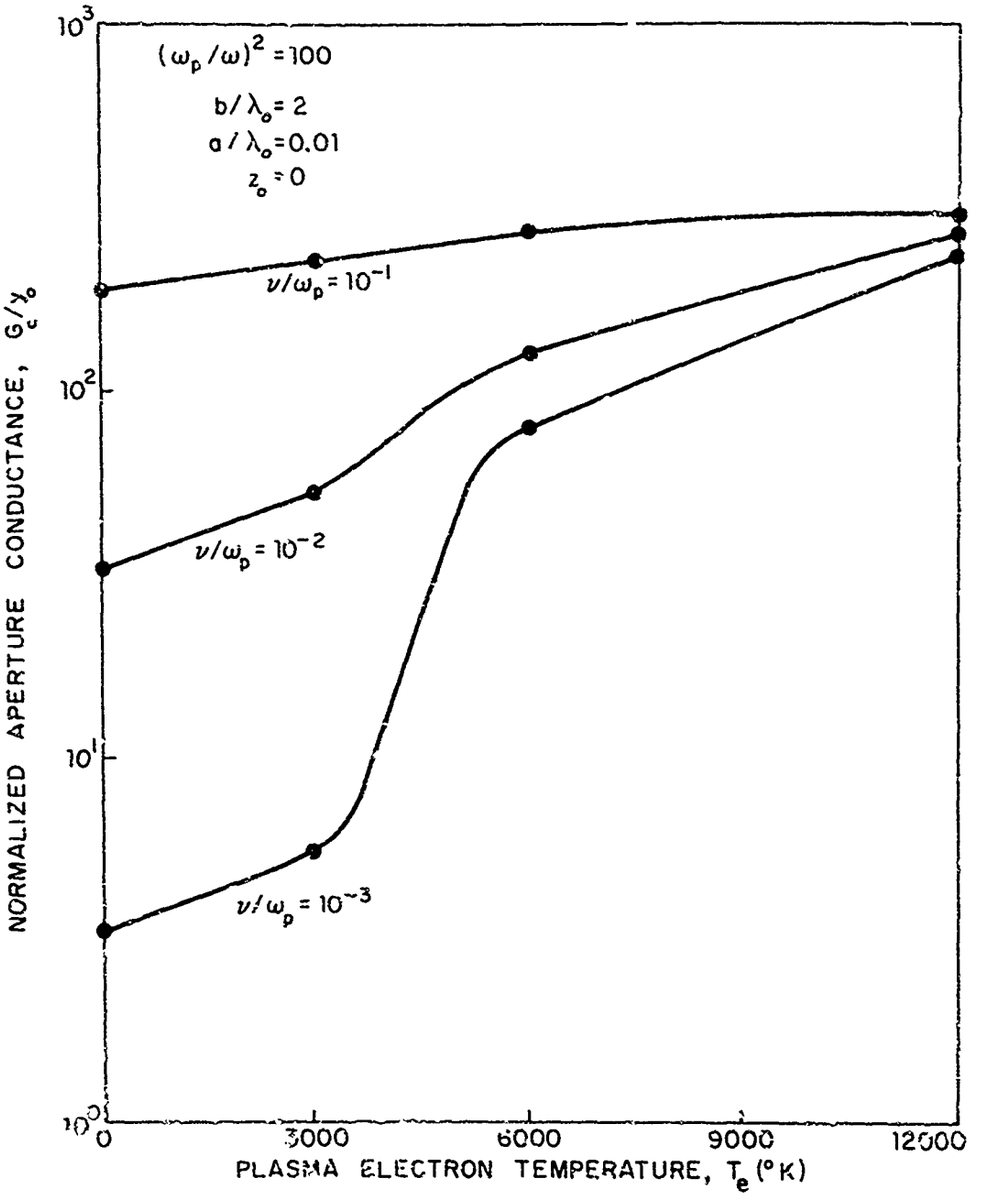

Figure II-16. Normalized conductance of aperture radiating into very overdense plasma; effect of electron temperature.

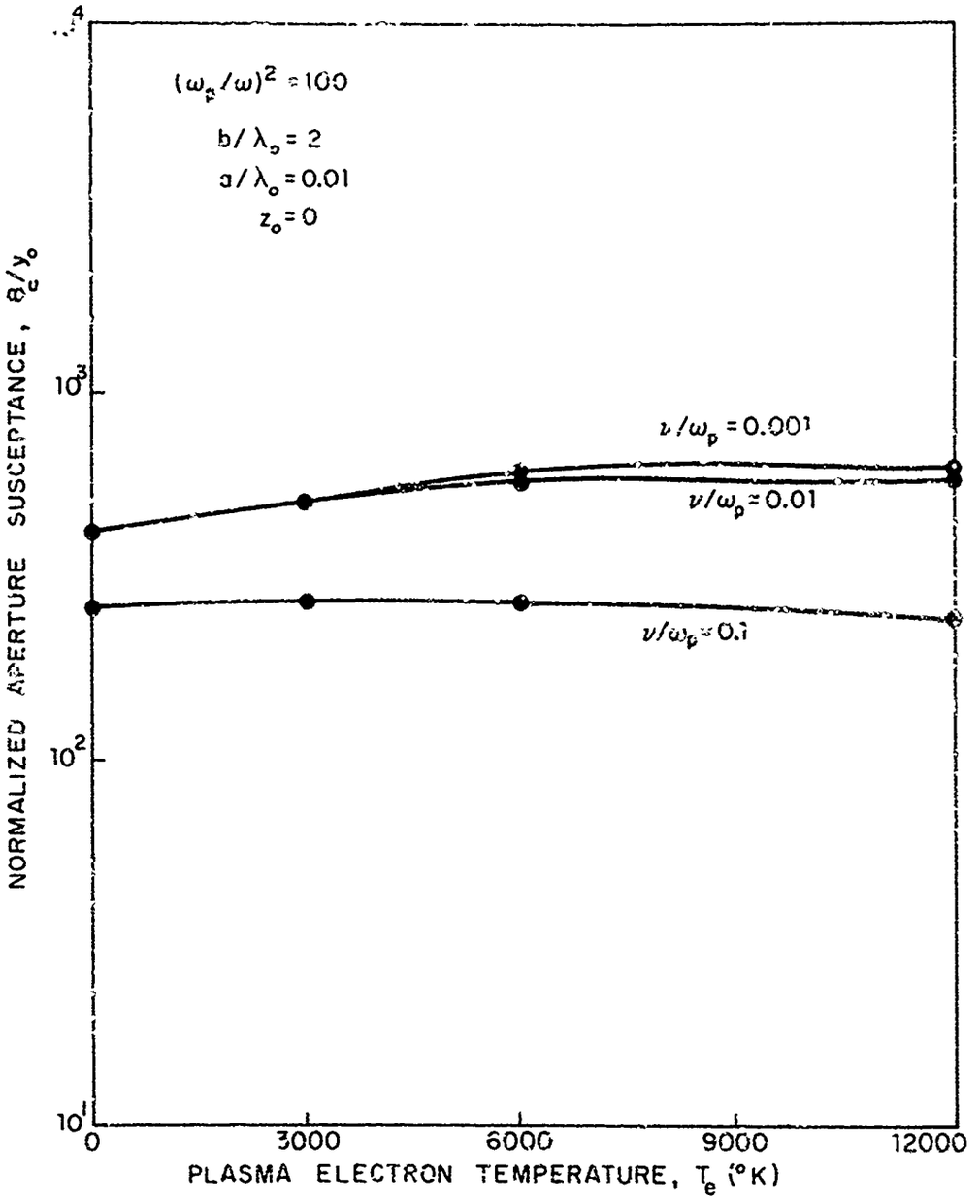

Figure II-17. Normalized susceptance of aperture radiating into very overdense plasma; effect of electron temperature.

The previous admittance calculations have been made neglecting sheath effects at the surface of the ground plane. However, an ion sheath layer will cover any electrically isolated metallic conductor in contact with a plasma (Tanenbaum 1967). The ion sheath thickness is several Debye lengths and may appreciably affect the aperture admittance.

Figures II-18 and II-19 show the effect of an increasing sheath thickness upon the normalized, calculated admittance of an aperture excited at a frequency below the plasma frequency. The sheath thickness z_o is normalized with respect to the free space antenna excitation wave length. The ion sheath has been approximated by a free space layer separating the aperture and ground plane from the plasma. Electron temperature effects upon the admittance are seen to be negligible for sheath thicknesses greater than about .001 λ_o. Values of the sheath thickness in excess of about $3 \times 10^{-5}\ \lambda_o$, however, do have an appreciable effect upon the aperture admittance, regardless of the plasma electron temperature.

It must be remembered that, in reality, the plasma electron temperature and the Debye sheath thickness are not independent quantities. The Debye distance λ_o is related to the plasma electron density N_o and electron temperature T_e through the relation

$$\lambda_o = 69\sqrt{\frac{T_e}{N_o}} \quad . \tag{II-68}$$

The admittance of an aperture excited at a frequency below the plasma frequency and separated from the compressible plasma by an ion sheath is shown in Figures II-20 through II-23 for the range of plasma electron temperature values normally encountered during reentry. Both the sheath thickness and the plasma electron temperature significantly affect the aperture admittance for the typical reentry conditions chosen. The principal effect of the sheath is a large increase in the aperture conductance. Increased electron collisions are observed to reduce the plasma electron temperature effects upon the aperture susceptance. As in the case where the sheath was neglected, electron temperature effects are greater for larger values of $(\omega_p/\omega)^2$.

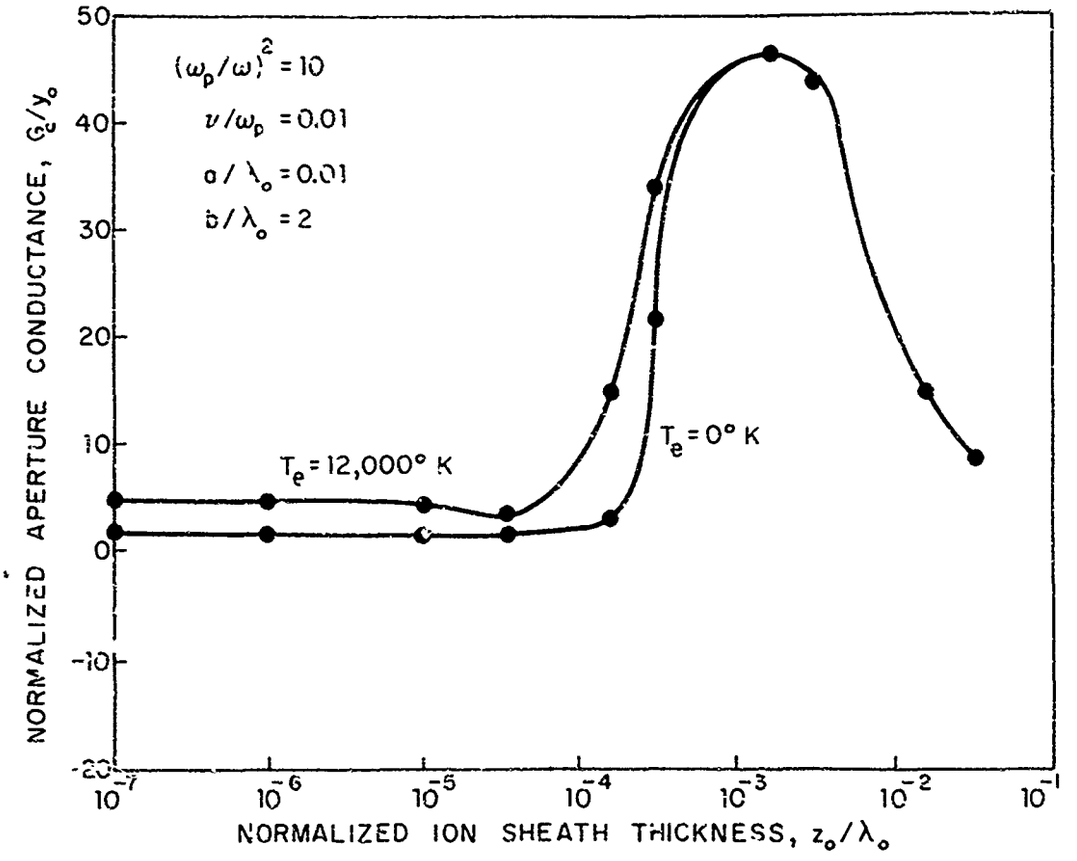

Figure II-18. Normalized conductance of aperture radiating into overdense plasma: effect of ion sheath thickness.

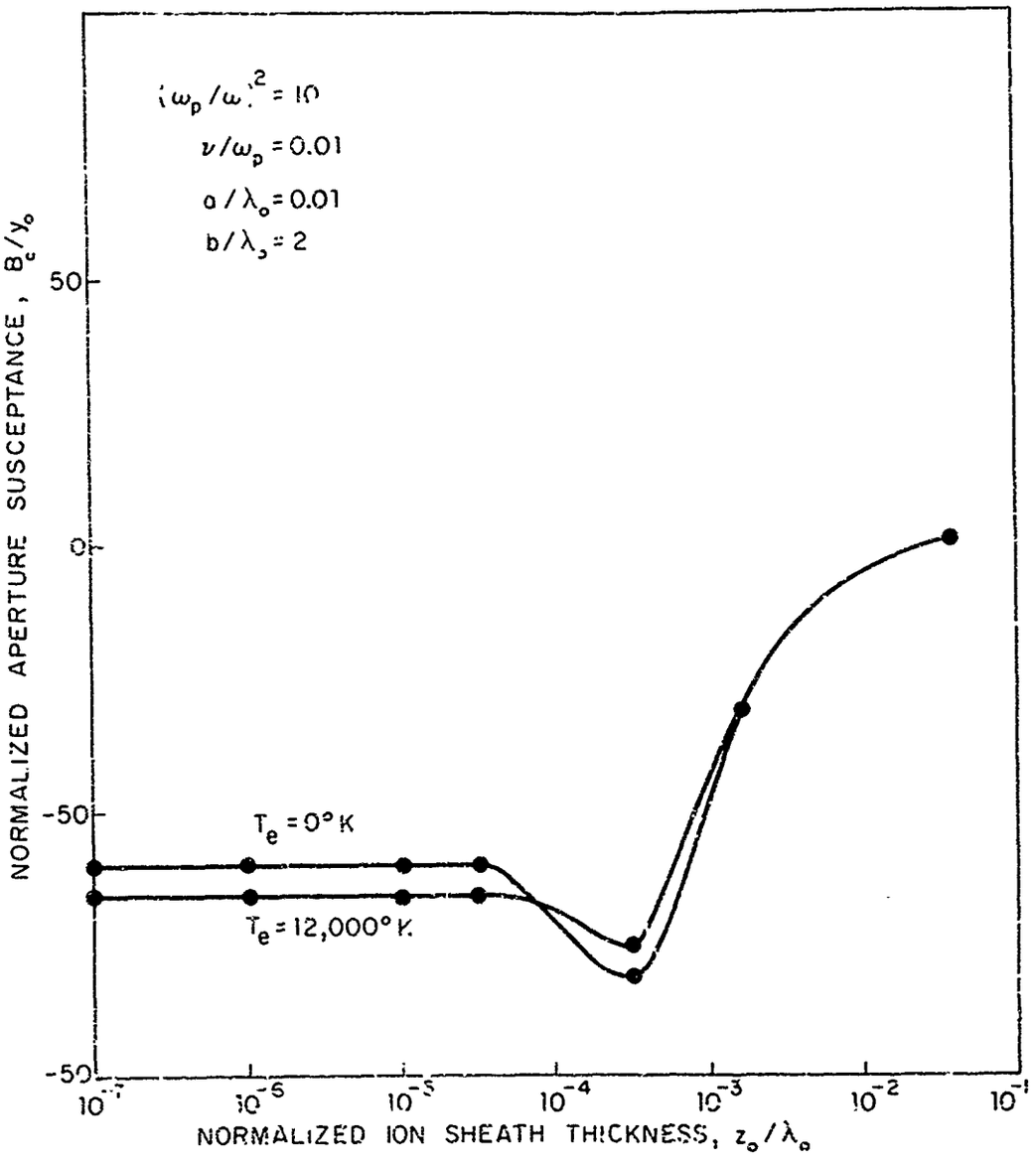

Figure II-19. Normalized susceptance of aperture radiating into overdense plasma; effect of ion sheath thickness.

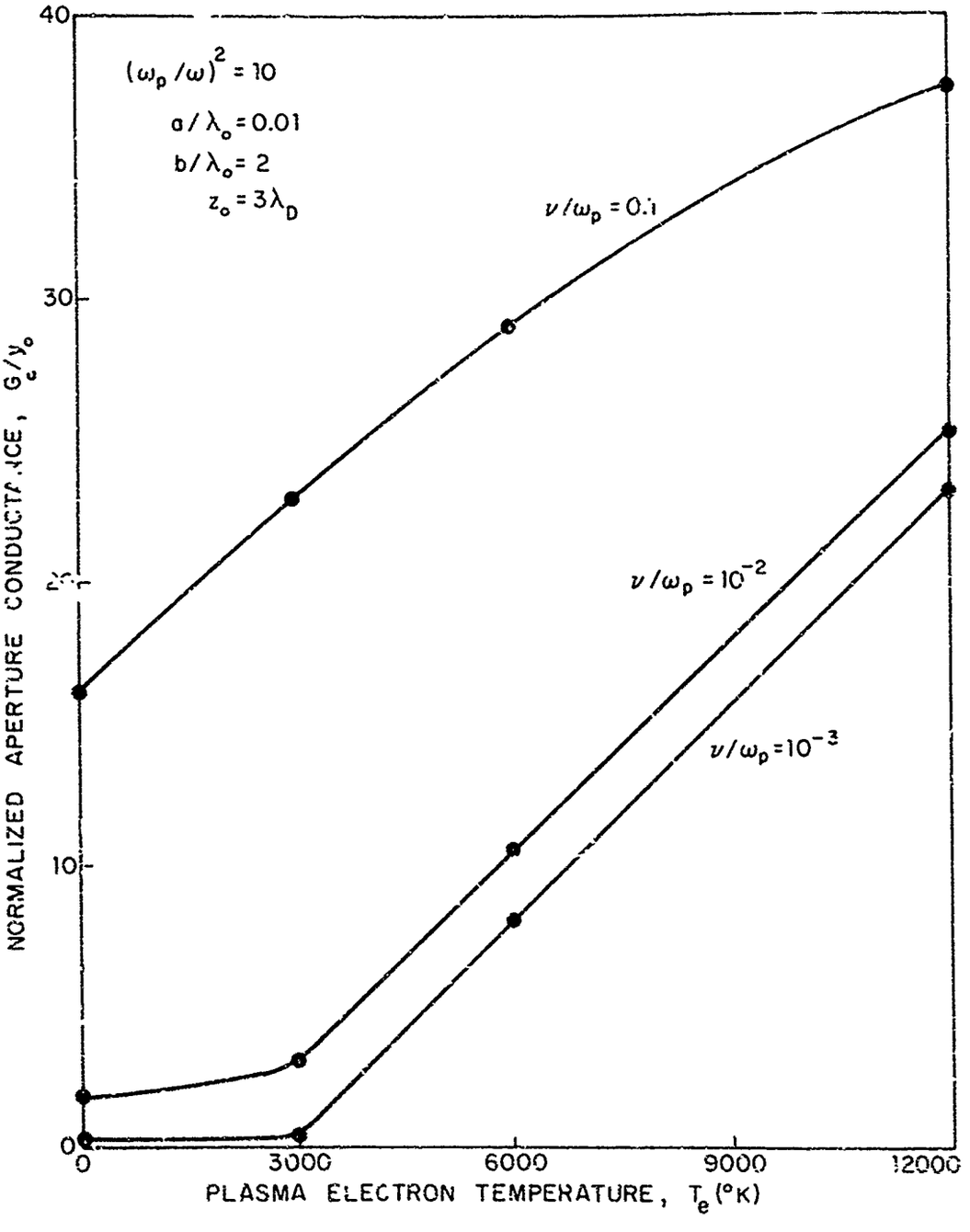

Figure II-20. Normalized conductance of sheathed aperture radiating into overdense plasma; effect of electron temperature.

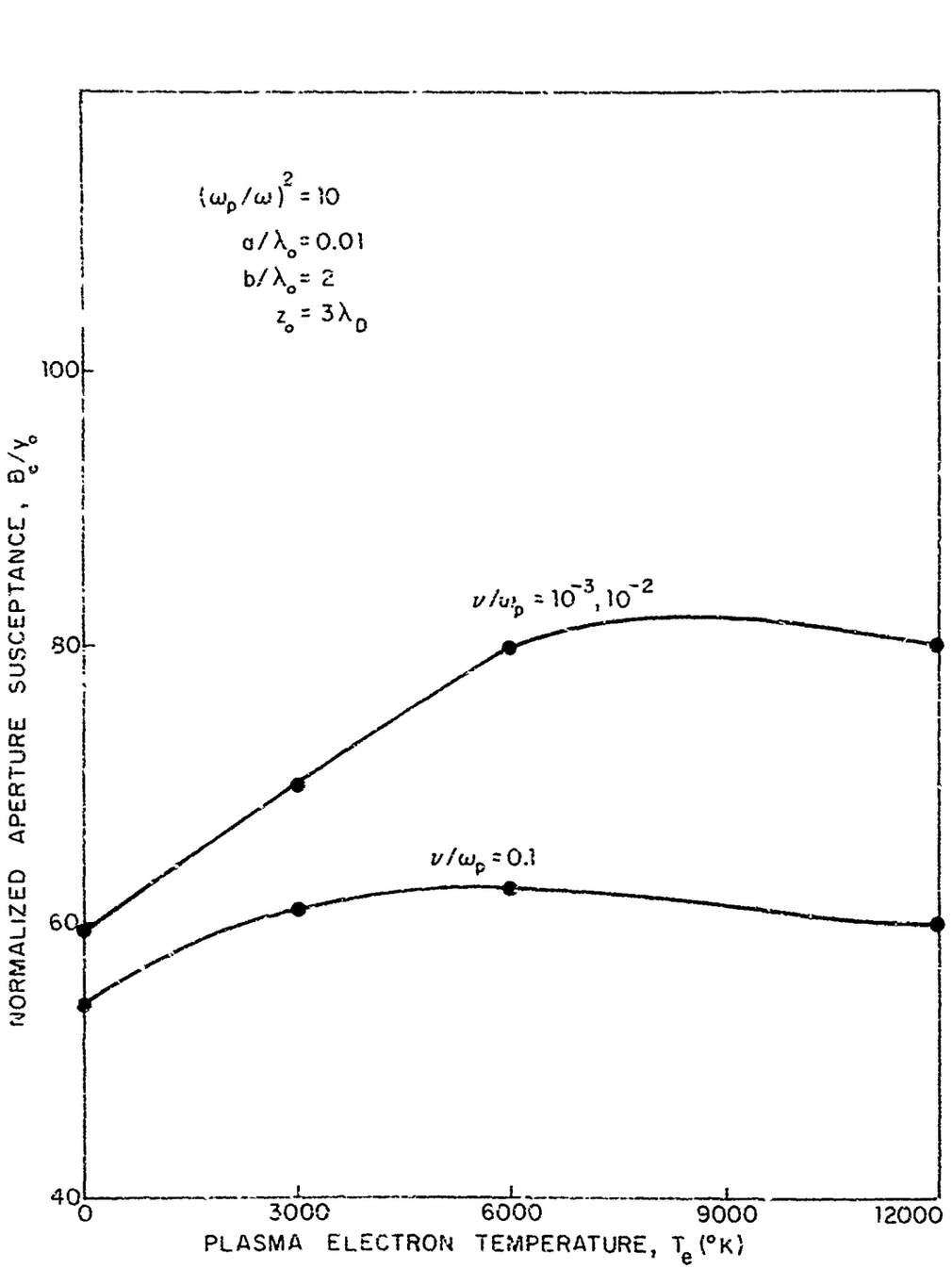

Figure II-21. Normalized susceptance of sheathed aperture radiating into overdense plasma; effect of electron temperature.

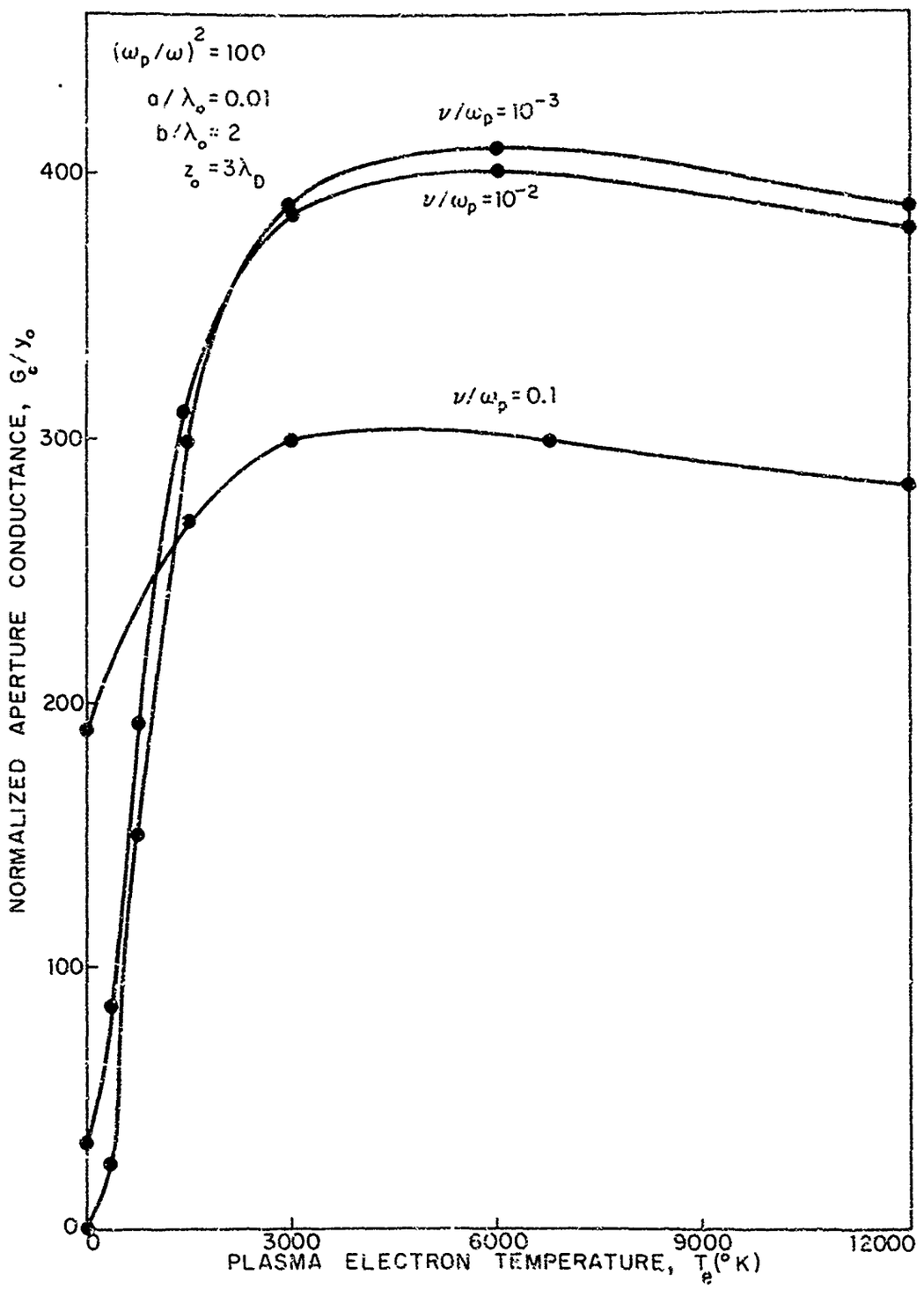

Figure II-22. Normalized conductance of sheathed aperture radiating into very overdense plasma: effect of electron temperature.

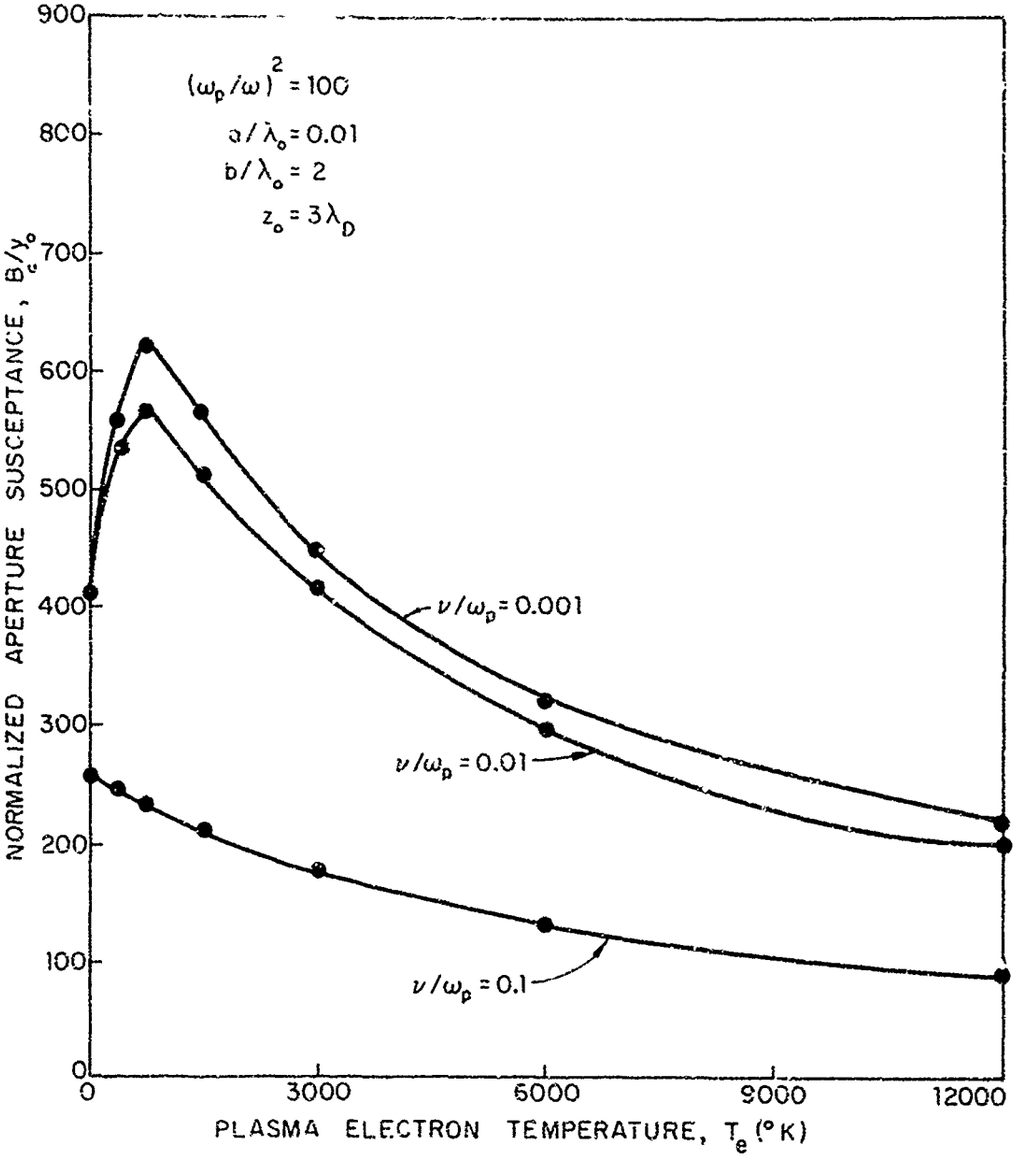

Figure II-23. Normalized susceptance of sheathed aperture radiating into very overdense plasma; effect of electron temperature.

The conductance and susceptance of the sheath covered aperture are found to vary linearly with the aperture length as in the sheathless case. In like manner, plasma electron temperature effects upon the admittance of a sheath covered aperture are reduced as the aperture width is increased. These results are not illustrated.

The aperture admittance, for a given aperture excitation frequency, is significantly affected by relatively small changes in the plasma electron density. This is shown in Figures II-24 and II-25 where calculated aperture conductance and susceptance values, respectively, are shown as functions of frequency for two slightly different plasma layers. The curves labelled "(1)" are admittance values calculated for a plasma layer having an electron density N_o equal to 1.2×10^{12} cm^{-3}, a collision frequency ratio ν/ω_p equal to .01, an electron temperature T_e equal to 12,000°K and a sheath thickness z_c equal to three Debye lengths. The curves labelled "(2)" are admittance values calculated for a plasma layer having an electron density of 2.5×10^{12} cm^{-3} with the other parameters unchanged. The plasma frequencies associated with the electron densities are 10 and 14 GHz, respectively. It is apparent from Figures II-24 and II-25 that significantly different aperture conductances and susceptances occur for a modest change in plasma electron density.

Figures II-2 through II-25 have shown that, in some cases, the admittance of an aperture antenna is significantly affected by the electron density, electron collision frequency and electron temperature of a contiguous plasma layer, using the rigid boundary condition. The following chapter will consider the aperture admittance expression for the case when all electrons incident upon the ground plane are absorbed.

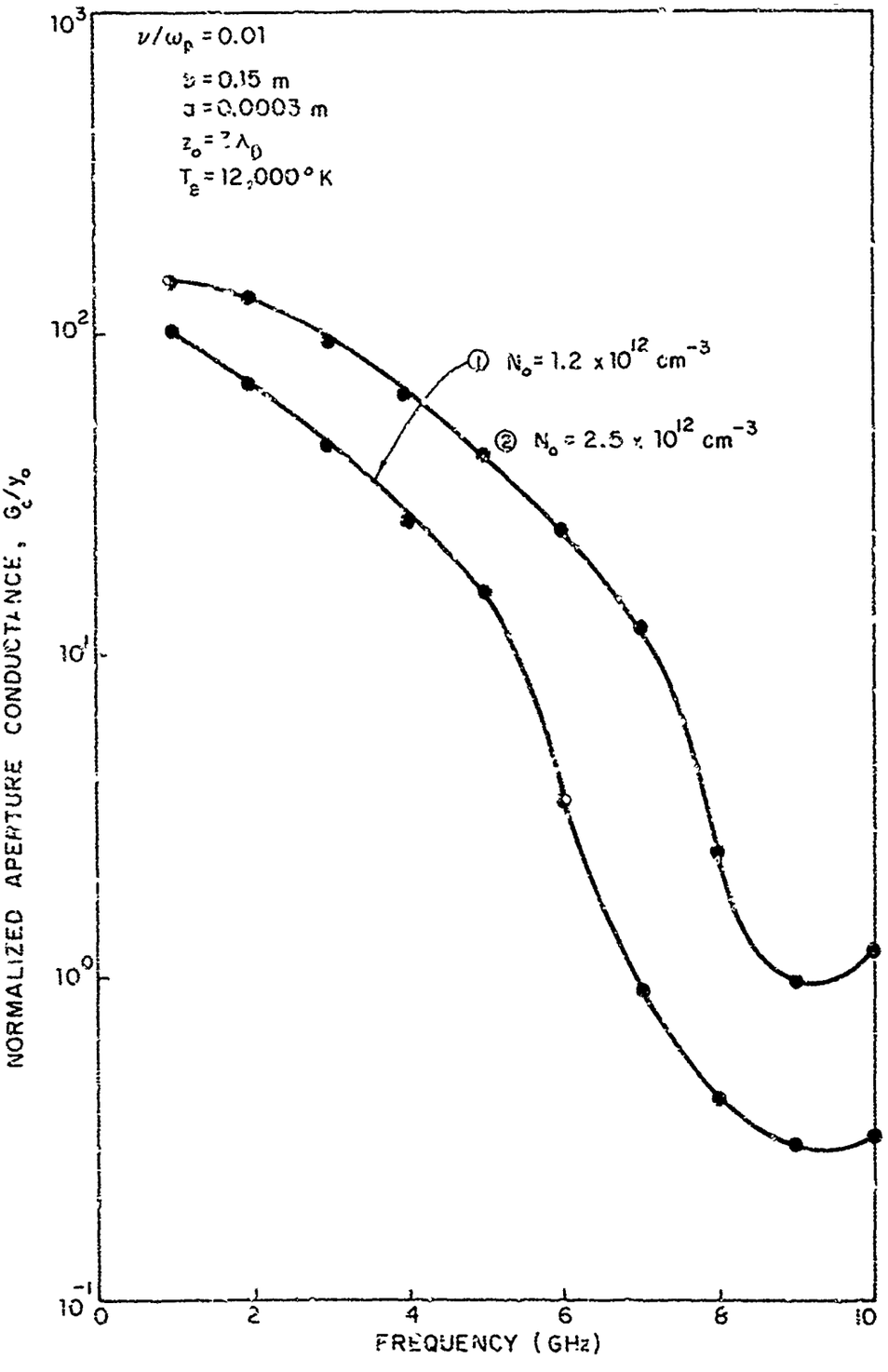

Figure II-24. Normalized conductance of sheathed aperture radiating into overdense plasma; effect of frequency.

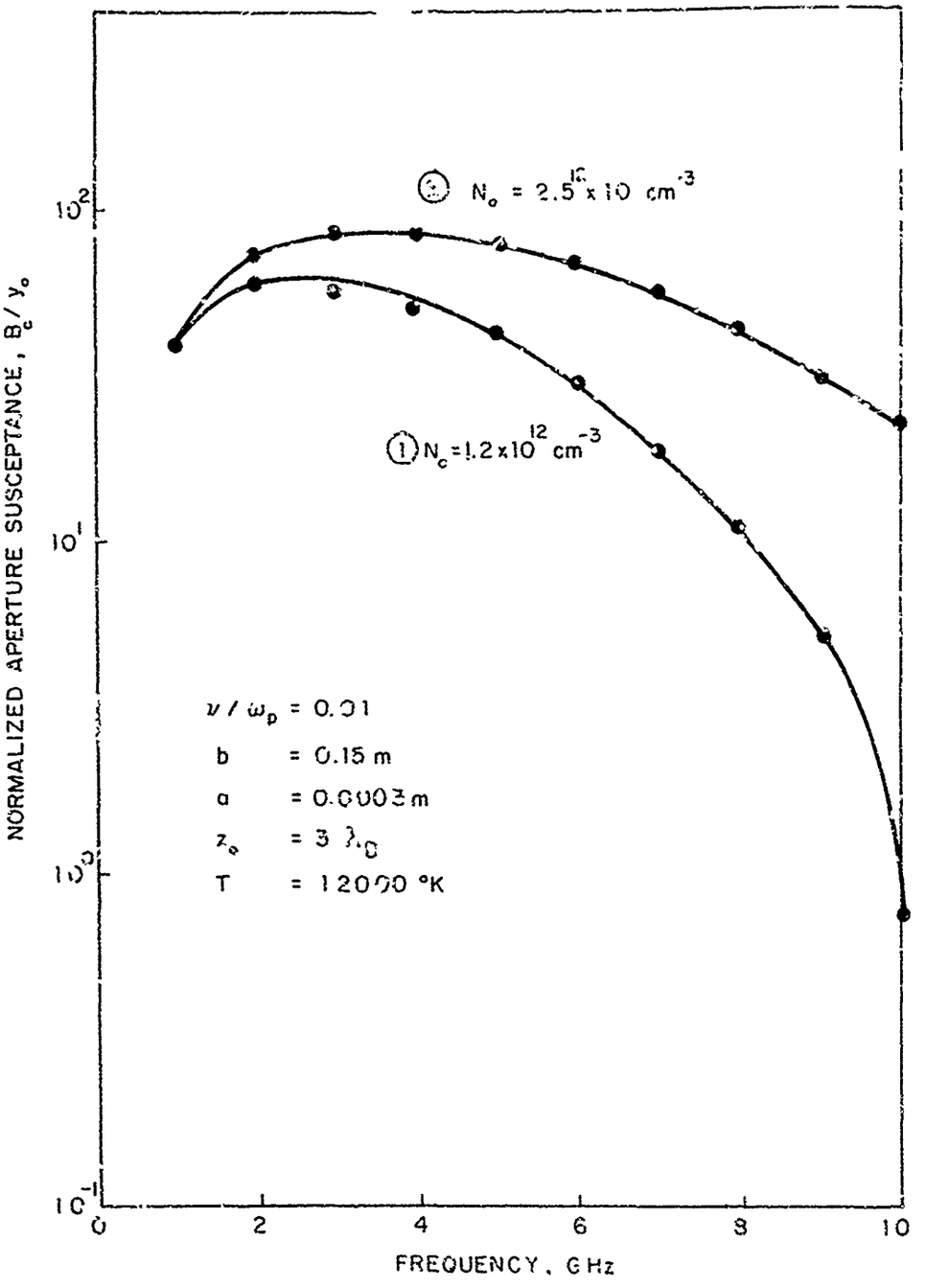

Figure II-25. Normalized susceptance of sheathed aperture radiating into overdense plasma; effect of frequency.

CHAPTER III

APERTURE ADMITTANCE FOR AN ABSORBING BOUNDARY

All electrons coming within several Debye lengths of the aperture-ground plane surface were assumed repelled in the previous chapter. This is not an unreasonable representation for a thin ion sheath and has been widely used in the literature. The chief difficulty with this representation is that the exact location of the sheath edge is not known in an actual situation (Wait 1966).

The electron density near a conducting boundary can be made nearly uniform by eliminating the ion sheath. The ion sheath can be eliminated by making the potential of the conducting boundary equal to the plasma space potential (Wasserstrom et al. 1965). Nearly all the electrons striking the conducting surface are then absorbed. An "absorptive boundary condition" has been developed (Balmain 1965) using a two-sided velocity distribution in the Boltzmann transport equation. Balmain used this absorptive boundary condition in his analysis of parallel plate and spherical RF plasma probes. The absorptive boundary condition also has been used by Wait (1966) in his idealized study of the waves that can propagate along a plasma-conductor interface. This boundary condition generally has not been used in antenna analysis.

A. Aperture Admittance Formula The development of the admittance formula proceeds in the same general manner as before except that now only a single layer plasma geometry is considered. The potential functions Ψ_z and Ψ_z^* for this case are written

$$\Psi_z = \frac{1}{(2\pi)^2} \iint_{-\infty}^{\infty} \bar{G}(k_x,k_y,z) \exp[i(k_x x+k_y y)]dk_x dk_y \qquad \text{(III-1)}$$

$$\psi_z \hat{=} \frac{1}{(2\pi)^2} \iint_{-\infty}^{\infty} \bar{\bar{F}}(k_x,k_y,z) \exp[i(k_x x+k_y y)]dk_x dk_y \qquad \text{(III-2)}$$

$$P = \frac{1}{(2\pi)^2} \iint_{-\infty}^{\infty} \bar{\bar{P}}(k_x,k_y,z) \exp[i(k_x x+k_y y)]dk_x dk_y \qquad \text{(III-3)}$$

where

$$\bar{\bar{G}}(k_x,k_y,z) = A(k_x,k_y) \exp(ik_{ez}z) \qquad \text{(III-4)}$$

$$\bar{\bar{F}}(k_x,k_y,z) = C(k_x,k_y) \exp(ik_{ez}z) \qquad \text{(III-5)}$$

$$\bar{\bar{P}}(k_x,k_y,z) = P_o(k_x,k_y) \exp(ik_{pz}z) \qquad \text{(III-6)}$$

with

$$k_{ez} = \sqrt{k_e^2-k_x^2-k_y^2} \qquad \text{(III-7)}$$

$$k_{pz} = \sqrt{k_p^2-k_x^2-k_y^2} \qquad \text{(III-8)}$$

$$k_e^2 = \omega^2\mu_o\varepsilon \qquad \text{(III-9)}$$

$$k_p^2 = \frac{\omega^2}{u^2}\left[1 - \left(\frac{\omega_p}{\omega}\right)^2 + i\,\nu/\omega\right] \quad . \qquad \text{(III-10)}$$

The propagation coefficients k_{ez} and k_{pz} are defined in the first quadrant of the complex plane.

The components of $\dot{E}$ and $\dot{J}$ are defined by equations (II-10) to (II-15) as before.

The boundary conditions imposed at $z = 0$ are continuity of E_x and E_y together with the absorptive boundary condition (Balmain 1965; Wait 1966)

$$v_z(o) = -\sqrt{\frac{2}{\pi}}\ \frac{P(o)}{uN_o m} \quad . \tag{III-11}$$

These boundary conditions can be written from equation (II-8) and equations (II-10) through (II-15) together with equations (II-62) through (II-67) in the form

$$\frac{-(\varepsilon_o-\varepsilon)}{N_o e\varepsilon}\left[\frac{(k_x^2+k_y^2)}{o}\bar{\bar{G}}(o) + \frac{\omega\varepsilon_o k_{pz}\bar{\bar{P}}(o)}{N_o e}\right] = \sqrt{\frac{2}{\pi}}\ \frac{\bar{\bar{P}}(o)}{uN_o m} \tag{III-12}$$

$$\bar{\bar{E}}_x = i\left[-k_y\bar{\bar{F}}(o) - \frac{k_x k_{ez}\bar{\bar{G}}(o)}{\omega\mu_o\varepsilon} + \frac{k_x(\varepsilon_o-\varepsilon)\bar{\bar{P}}(o)}{N_o e}\right] \tag{III-13}$$

$$\bar{\bar{E}}_y = 0 = i\left[k_x\bar{\bar{F}}(o) - \frac{k_y k_{ez}\bar{\bar{G}}(o)}{\omega\mu_o\varepsilon} + \frac{k_y(\varepsilon_o-\varepsilon)\bar{\bar{P}}(o)}{N_o e\varepsilon}\right] \tag{III-14}$$

The aperture field Fourier transform E_x is defined by equation (II-40).

The quantities $F(o)$, $G(o)$ and $\bar{P}(o)$ are obtained from equations (II-73) through (II-75) in the form

$$\bar{\bar{F}}(o) = \frac{-iE_x}{(DET)}\left[\frac{k_y k_{ez}}{\omega\mu_o\varepsilon}\left\{\frac{\omega\mu_o k_{pz}}{N_o e} + \frac{\sqrt{\frac{2}{\pi}}\ e\varepsilon}{um(\varepsilon_o-\varepsilon)}\right\} + \frac{k_y(k_x^2+k_y^2)(\varepsilon_o-\varepsilon)}{N_o e u_o\varepsilon}\right] \quad . \tag{III-15}$$

$$\bar{\bar{G}}(o) = \frac{-i\bar{\bar{E}}_x k_x}{(DET)}\left[\frac{\omega\varepsilon_o k_{pz}}{N_o e} + \sqrt{\frac{2}{\pi}}\ \frac{e\varepsilon}{um(\varepsilon_o-\varepsilon)}\right] \qquad \text{(III-16)}$$

$$\bar{F}(o) = \frac{iE_x k_x (k_x + k_y)}{\mu_o (DET)} \qquad \text{(III-17)}$$

where

$$DET = \frac{-(k_x^2+k_y^2)^2(\varepsilon_o-\varepsilon)}{N_o e u_o \varepsilon} - \frac{(k_x^2+k_y^2)k_{ez}}{\omega\mu_o\varepsilon}\left[\frac{\omega\varepsilon_o k_{pz}}{N_o e} + \frac{\sqrt{\frac{2}{\pi}}\ e\varepsilon}{um(\varepsilon_o-\varepsilon)}\right] \qquad \text{(III-18)}$$

The Fourier transform of H_y at $z = 0$ can be determined from equation (II-11) along with equations (II-76) and (II-77). The result is

$$\bar{\bar{H}}_y = \frac{-ik_x \bar{\bar{G}}(o)}{\mu_o} - \frac{ik_y k_{ez} \bar{\bar{F}}(o)}{\omega\mu_o}$$

$$= \bar{\bar{E}}_x k_x^2 \left[\varepsilon k_{pz} + \frac{\sqrt{\frac{2}{\pi}}\ \varepsilon^2 N_o e^2}{um(\varepsilon_o-\varepsilon)\varepsilon_o}\right]$$

$$+ \frac{\bar{\bar{E}}_x k_y^2 k_{ez}}{\omega\mu_o(k_x^2+k_y^2)} \quad . \qquad \text{(III-19)}$$

The time-averaged, outward normal flow of power per unit area through the aperture is given by

$$\vec{S} = \frac{1}{2}\left[E_x H_y^* + \mathcal{P} v_z^*\right]\Big|_{z=0^+} \hat{z} \quad . \tag{III-52}$$

The complex conjugate of the power radiated by the aperture can be expressed using Parseval's theorem in the form

$$W^* = \frac{1}{2}\int_{-\frac{a}{2}}^{\frac{a}{2}}\int_{-\frac{b}{2}}^{\frac{b}{2}} (E_x^* H_y + \mathcal{P}^* v_z)\,dx\,dy$$

$$= \frac{1}{2}\int_{-\infty}^{\infty}\int (\vec{E}_x^* \vec{H}_y + \vec{\mathcal{P}}^* \vec{v}_z)\,dk_x\,dk_y \quad . \tag{III-20}$$

The conjugate admittance Y^* is defined by

$$W^* = \frac{1}{2} V_o^2 Y^* \tag{III-55}$$

Equations (II-40), (II-55), (II-72), (II-80) and (II-81) are combined and a change of variables identical to that in equations (II-56) through (II-61) is performed with the result

$$Y^* = Y_o (k_o b)^2 \int_0^{\infty}\int_0^{2\pi} \left[\frac{\sin\left(\frac{ak_o \beta \cos\alpha}{2}\right)}{\left(\frac{ak_o \beta \cos\alpha}{2}\right)}\right]^2 \left[\frac{\cos\left(\frac{bk_o \beta \sin\alpha}{2}\right)}{\pi^2 - (bk_o \beta \sin\alpha)^2}\right]^2$$

$$\left\{\frac{\left[\frac{\varepsilon}{\varepsilon_o}\sqrt{\frac{k_p^2}{k_o^2} - \beta^2} + \sqrt{\frac{2}{\pi}}\left|\frac{\omega_p}{\omega}\right|^2 \left|\frac{c}{u}\right| \frac{\varepsilon^2}{(\varepsilon_o - \varepsilon)\varepsilon_o}\right]\cos^2\alpha}{\beta^2 \frac{(\varepsilon_o - \varepsilon)}{\varepsilon_o} + \sqrt{\frac{\varepsilon}{\varepsilon_o} - \beta^2}\left[\sqrt{\frac{k_p^2}{k_o^2} - \beta^2} + \sqrt{\frac{2}{\pi}}\left|\frac{\omega_p}{\omega}\right|^2 \left|\frac{c}{u}\right| \frac{\varepsilon}{\varepsilon_o - \varepsilon}\right]}\right.$$

$$+ \frac{\sqrt{\frac{2}{\pi}} \left|\frac{\omega_p}{\omega}\right|^2 \left|\frac{c}{u}\right| \left|\frac{\varepsilon}{\varepsilon_o}\right|^2 \beta^2 \cos^2\alpha}{\left[\beta^2 \frac{(\varepsilon_o - \varepsilon)}{\varepsilon_o} + \sqrt{\frac{\varepsilon}{\varepsilon_o} - \beta^2}\left[\sqrt{\left|\frac{k_p}{k_c}\right|^2 - \beta^2} + \sqrt{\frac{2}{\pi}}\left|\frac{\omega_p}{\omega}\right|^2 \left|\frac{c}{u}\right| \frac{\varepsilon}{\varepsilon_o - \varepsilon}\right]\right]^2}$$

$$+ \sqrt{\frac{\varepsilon}{\varepsilon_c} - \beta^2} \sin^2\alpha \Bigg\} \beta d\alpha d\beta \quad . \qquad \text{(III-21)}$$

The numerical integration of equation (III-21) is performed in the same manner as that of equation (III-61).

B. Numerical Results Aperture admittance values have been computed for several values of plasma parameters and aperture length for the case when the ion sheath is collapsed by a dc bias and the absorptive boundary condition is valid. These admittance values are compared with those obtained for the case of an ion sheath of zero thickness and the "hard" boundary condition in Figures III-1 through III-6.

It is observed that the absorptive boundary eliminates electron temperature effects upon aperture susceptance and decreases electron temperature effects upon the conductance. Nonzero electron temperature effects upon the aperture conductance are seen to decrease with decreasing aperture exciting frequency. Figures III-1 through III-4 show that the aperture admittance varies linearly with aperture length when the absorptive boundary condition is employed as well as when the hard boundary condition is used.

The aperture susceptance is seen to be constant over a rather large range of electron collision frequency values while the zero temperature aperture conductance varies linearly with electron collision frequency over a large range of values when the absorptive boundary condition is employed. This admittance behavior is shown in Figures III-5 and III-6 and is similar to that observed when the hard boundary condition is employed for a zero electron temperature plasma.

The admittance calculations indicate that while eliminating the ion sheath reduces the uncertainties which exist concerning the exact sheath thickness, the effect of the nonzero electron temperature upon the admittance is decreased. Nevertheless, aperture admittance measurements made at frequencies only slightly below the plasma frequency are significantly affected by the plasma electron temperature.

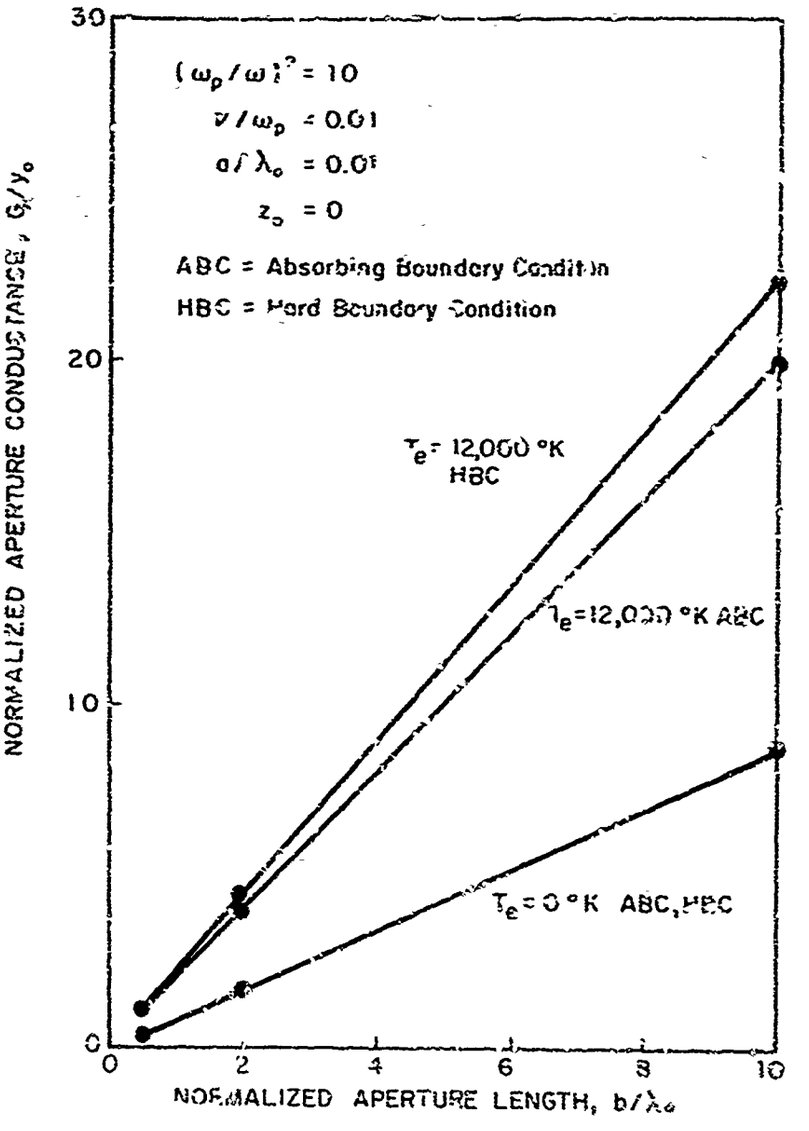

Figure III-1. Normalized conductance of aperture radiating into overdense plasma; effect of aperture length and boundary conditions.

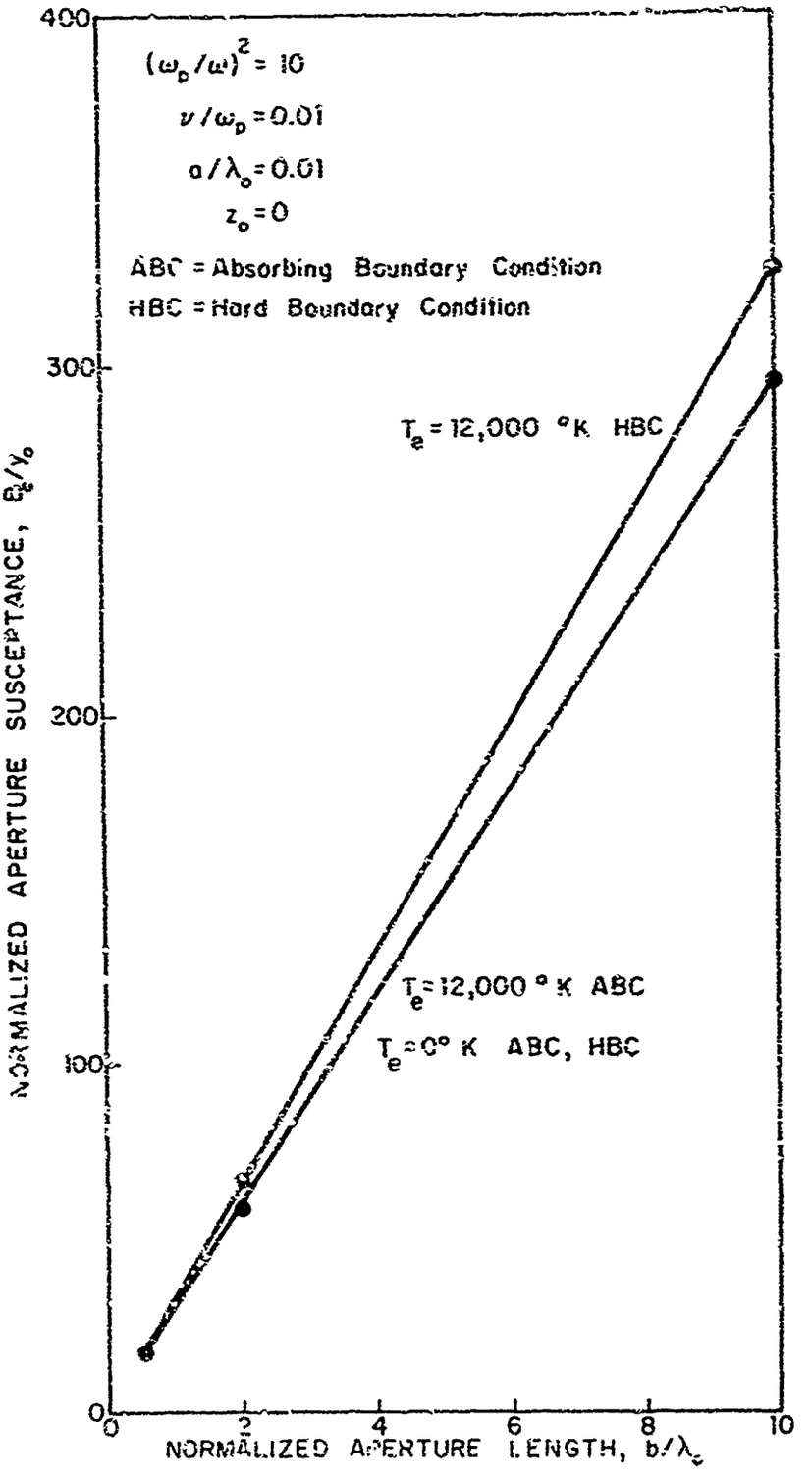

Figure III-2. Normalized susceptance of aperture radiating into overdense plasma; effect of aperture length and boundary conditions.

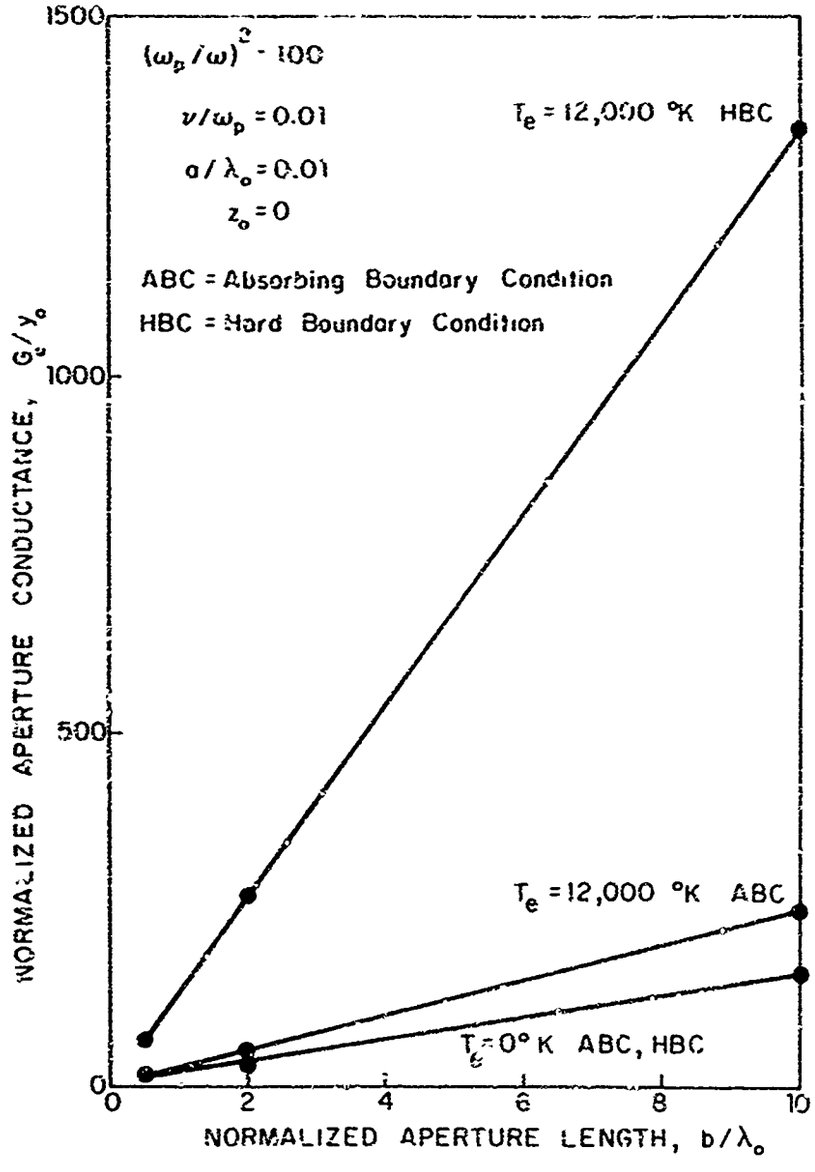

Figure III-3. Normalized conductance of aperture radiating into very overdense plasma; effect of aperture length and boundary conditions.

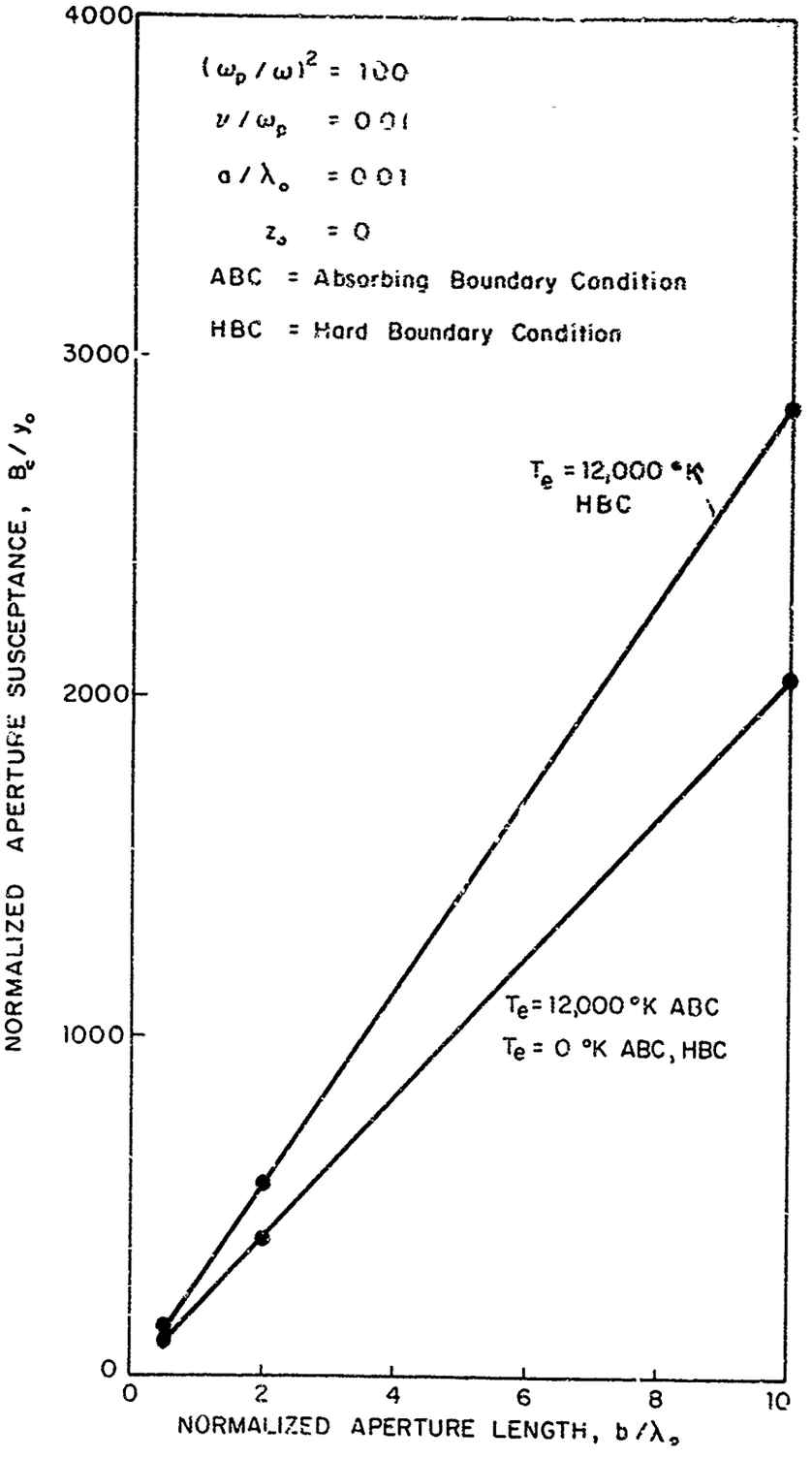

Figure III-4. Normalized susceptance of aperture radiating into very overdense plasma; effect of aperture length and boundary conditions.

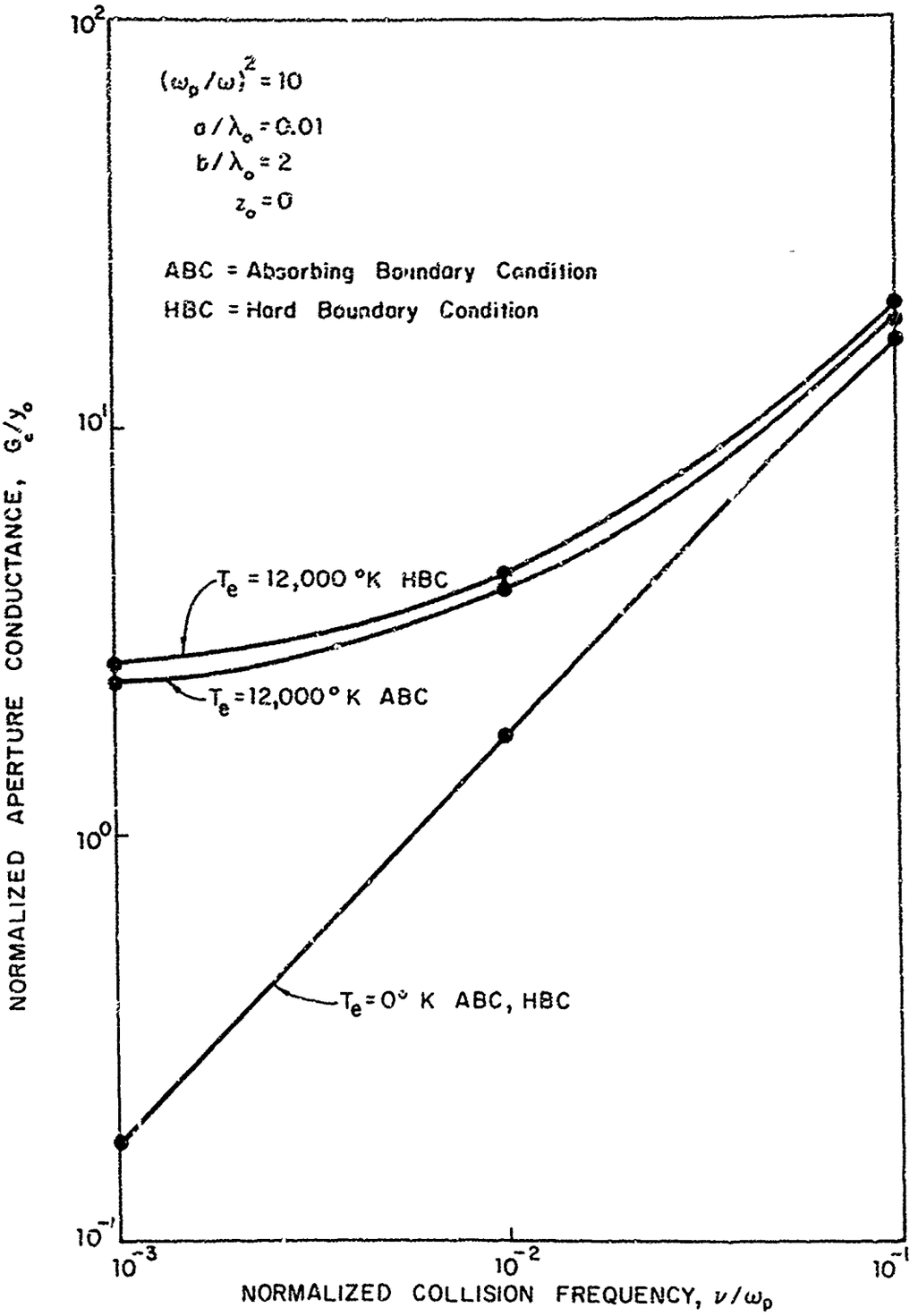

Figure III-5. Normalized conductance of aperture radiating into overdense plasma; effect of plasma losses and boundary conditions.

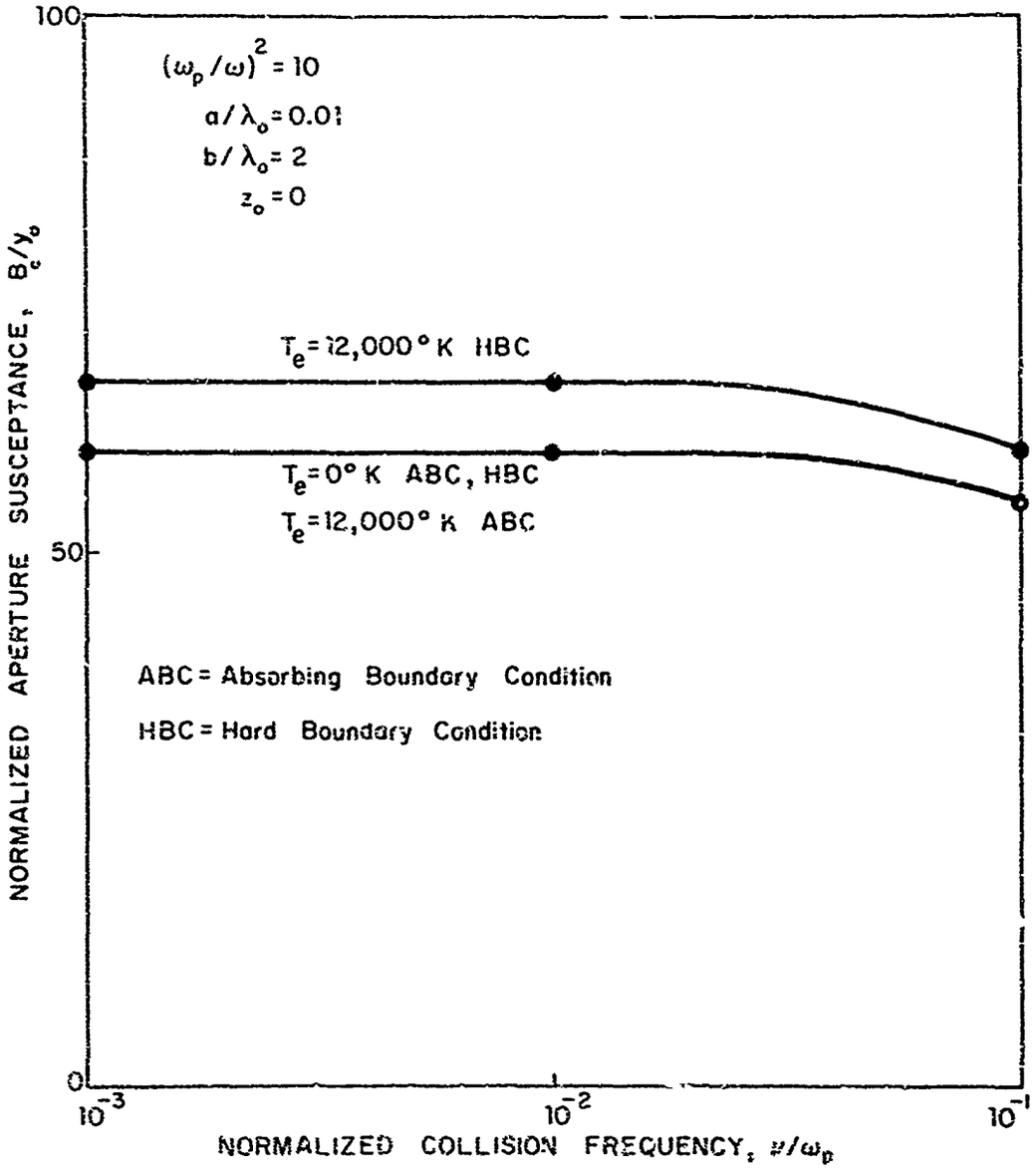

Figure III-6. Normalized susceptance of aperture radiating into overdense plasma; effect of plasma losses and boundary conditions.

CHAPTER IV

DETERMINATION OF REENTRY PLASMA PROPERTIES FROM APERTURE ADMITTANCE MEASUREMENTS

The calculations discussed in the previous chapter have shown the effect of a plasma layer upon aperture antenna admittance. The plasma electron temperatures experienced during reentry significantly affect aperture admittance only when the aperture is excited at a frequency below the plasma frequency and only for aperture widths very small compared to a free space wavelength. The aperture admittance, under these conditions, has been found to be linearly related to the aperture length for both zero and nonzero values of the plasma electron temperature.

These results are in contrast to those obtained when the aperture is excited at a frequency above the plasma frequency. Significant effects of the plasma electron temperature upon the aperture admittance are observed only when the plasma electron temperature is considerably greater thar that encountered during reentry and only when the aperture length is at least several free space wavelengths.

Ion sheath effects upon the admittance of a thin aperture have been found to be appreciable and must be included in any realistic study. The admittance calculations also have shown that the plasma electron temperature has a greater effect upon aperture antenna admittance when electrons are reflected at the surface of the ground plane compared to that when electrons are absorbed by the ground plane.

Aperture admittance was calculated in Chapters II and III under the assumption that the plasma layer is infinitely thick. In reality, the thickness of a reentry plasma layer is at most only of the order of centimeters or tens of centimeters. However, plasma layer thicknesses of several centimeters are sufficient to approximate an infinitely thick plasma when the wave frequency is below the plasma frequency. Consequently,

the antenna-plasma layer model used in the previous chapter is a valid representation for reentry plasma layers, provided the antenna is excited at a frequency below the plasma layer and provided the plasma layer is essentially uniform over a distance of several centimeters.

Aperture admittance measurements made for plasma layers not uniform over distances of several centimeters require much more sophisticated analysis techniques. Plasma layers of this type often are produced by blunted reentry vehicles at altitudes above about 45 km and by sharply pointed reentry vehicles above about 15 km. For these cases, admittance measurements generally must be made over a wide range of frequencies or at a number of carefully chosen discrete frequencies. Methods of diagnosing the properties of grossly nonuniform reentry plasmas have been proposed using admittance measurement techniques based on incompressible or cold plasma theory. It has not been possible to implement these methods experimentally (Mayhan 1968b, 1969).

A. Thin Apertures The aperture admittance expressions (equations (II-61) and III-21)) do not allow one to determine the reentry plasma properties directly from admittance measurements, using a closed form expression. However, it will be shown in this section that it is possible, using an iterative technique, to determine the plasma layer electron density, collision frequency and electron temperature from aperture admittance measurements made at frequencies below the plasma frequency. The technique is not particularly sophisticated and is included merely to show that plasma parameters can be obtained from admittance measurements.

The basic assumption employed in the following technique for the determination of plasma properties from aperture admittance measurements is that only one value of plasma electron density and electron collision frequency can result in a given value of complex aperture admittance if the excitation frequency and electron temperature are specified. While this assumption has not been rigorously proved true, it has not been found to be untrue in any cases investigated during the current study.

The plasma diagnostic technique, based on aperture antenna admittance measurements, is outlined in flow chart form in Figure IV-1. Values of aperture admittance are assumed to be known (measured) at two frequencies below the plasma frequency. Only one value of admittance is considered at

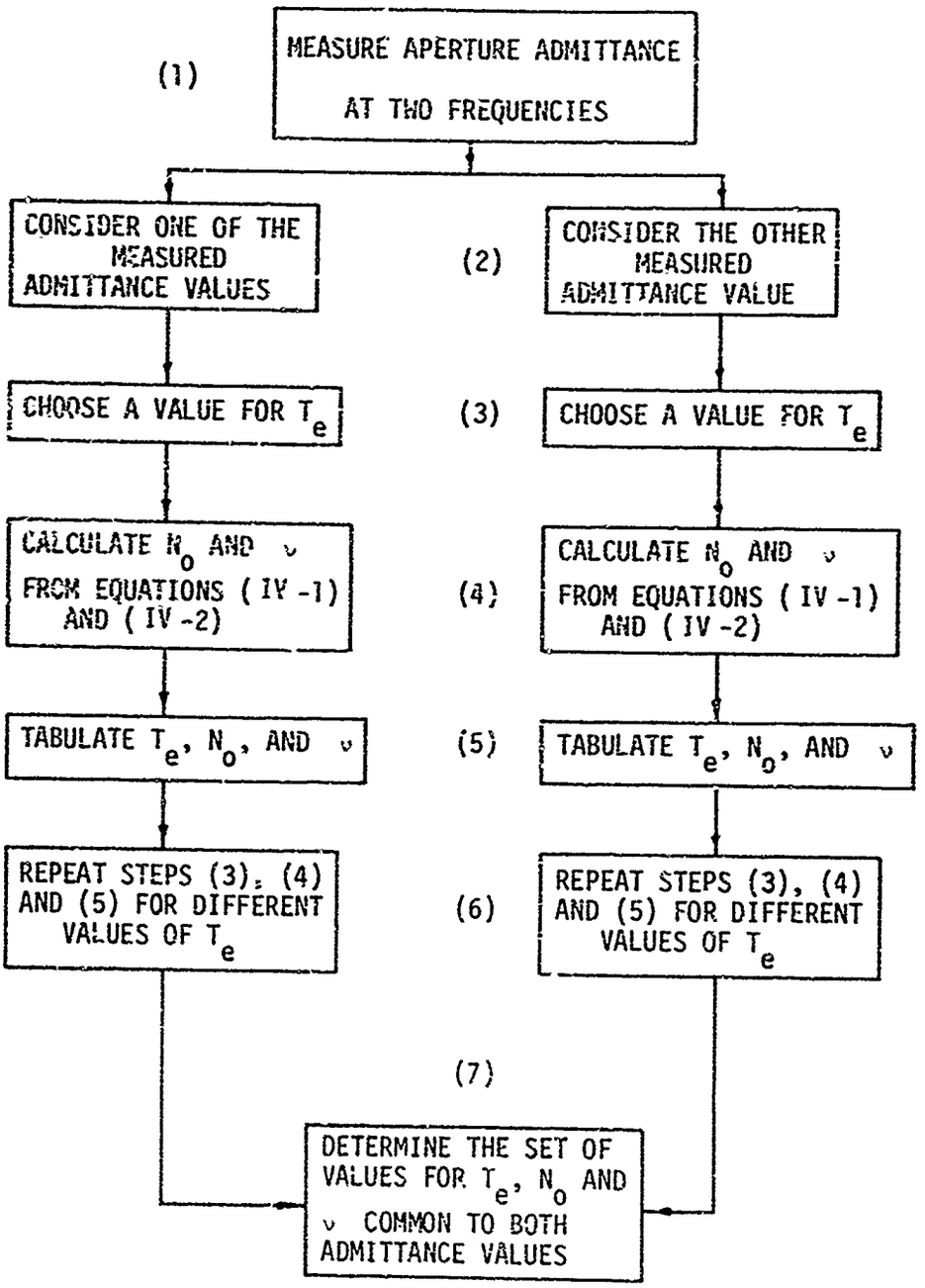

Figure IV-1. Flow chart of a reentry plasma diagnostic method based on two-frequency aperture admittance measurements.

a time. An approximate value of the plasma electron temperature T_e is chosen, leaving the plasma electron density N_o and collision frequency ν required to produce the measured admittance value with T_e specified at frequency ω, as the unknowns. The values of N_o and ν are then calculated using the Newton-Raphson iterative technique (McCracken and Dorn 1964) to determine the roots of the equations

$$G_c(N_o,\nu) - G_m = 0 \qquad \text{(IV-1)}$$

$$B_c(N_o,\nu) - B_m = 0 \qquad \text{(IV-2)}$$

where G_m and B_m are the measured values of aperture conductance and susceptance, respectively, and G_c and B_c are the values calculated using equation (II-61). The Newton-Raphson iterative technique is discussed in Appendix III.

Additional realistic values for T_e are selected for the same measured value of admittance and the corresponding values of N_o and ν are calculated. This provides sets of values for T_e, N_o and ν, all of which correspond to the measured value of aperture admittance.

The procedure is repeated for the admittance value measured at a second frequency. The result is sets of T_e, N_o and ν values for both measured admittance values. The set of T_e, N_o and ν values common to both admittance values is that of the reentry plasma layer.

The admittance calculations performed in Chapter III have shown that eliminating the ion sheath with a dc potential essentially eliminates electron temperature effects upon aperture admittance in addition to eliminating the uncertainty associated with the ion sheath thickness, particularly when the antenna excitation frequency is only slightly below the plasma frequency. This feature offers another possibility concerning the use of aperture admittance measurements for reentry plasma diagnostics. This second technique is outlined in Figure IV-2.

The value of aperture admittance measured when the ion sheath has been eliminated and at a frequency about a factor of ten below the plasma

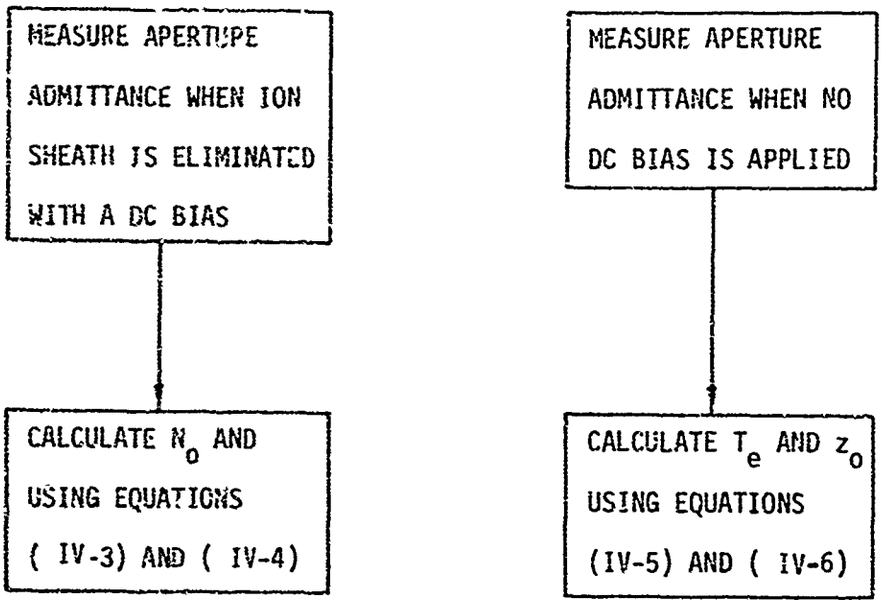

Figure IV-2. Flow chart of a reentry plasma diagnostic method based on single-frequency aperture admittance measurements.

frequency is affected only slightly by the plasma electron temperature. This admittance measurement can be used to calculate the plasma layer electron density N_o and electron collision frequency ν by solving the equations

$$G_c(T_e,z_o) - G_m = 0 \tag{IV-3}$$

$$B_c(T_e,z_o) - B_m = 0 \quad . \tag{IV-4}$$

using the Newton-Raphson iterative technique. The quantities G_c and B_c are the values of aperture conductance and susceptance, respectively, calculated using equation (III-21) with $u = 0 (T_e = 0)$. The subscript m denotes measured values of conductance and susceptance.

The potential used to eliminate the ion sheath is then removed and the aperture admittance is measured again, at the same frequency. The only unknowns then are the plasma electron temperature and ion sheath thickness. These quantities are then determined by solving the set of equations

$$G_c(T_e,z_o) - G_m = 0 \tag{IV-5}$$

$$B_c(T_e,z_o) - B_m = 0 \quad . \tag{IV-6}$$

The values G_c and B_c are calculated using equation (II-61). The advantage of this technique is that only single frequency admittance measurements need be made. As far as it is possible to determine from the open literature, the admittance of thin apertures never has been measured during reentry. Consequently, the efficacy of the above mentioned techniques for determining the reentry plasma electron density, collision frequency and electron temperature cannot be demonstrated using reentry data.

The admittance of open-ended-waveguide antennas was measured during the reentry of a Trailblazer II rocket (Caldecott et al. 1967). The calculations in Chapter II have shown electron temperature effects upon the admittance of apertures of this width to be negligible. However, the plasma flow field at the antenna locations was separated from the aperture by a distance ranging up to several millimeters due to aerodynamic boundary layer effects and can be analyzed in a manner similar to that outlined above.

The Trailblazer II flight on which the open-ended-waveguide admittance was measured will be described in detail and the admittance date analyzed. First, however, the admittance characteristics of an open-ended-waveguide antenna are discussed.

B. Waveguide Antennas The admittance of an open-ended-waveguide antenna can be calculated using equation (II-61) with appropriate values of the aperture dimensions a and b. The value of the electron acoustic velocity u is set equal to zero. Figures IV-3 and IV-4 show that plasma boundary layer thicknesses or plasma stand-off distances of millimeter order have an effect upon the calculated admittance of an open-ended-waveguide antenna excited at a frequency below the plasma frequency. The waveguide antenna susceptance is observed to be virtually independent of the plasma layer collision frequency for a given value of plasma boundary layer thickness z_o. The waveguide conductance, however, varies linearly with the plasma layer collision frequency over a large range. This behavior of waveguide antenna admittance is analogous to that of the dipole (King 1961; Miller 1968a) and is observed for frequencies in the range $1 < (\omega_p / \omega)^2 \leq 6$.

It is apparent, in this frequency range, that plasma layer electron density and boundary layer thickness principally affect the waveguide antenna susceptance. Waveguide antenna susceptance measurements made at two frequencies in the range $1 < (\omega_p/\omega)^2 < 6$ would be sufficient to determine the value of these quantities. Similarly, the waveguide antenna conductance is affected very much by the electron collision frequency. Measurements of the waveguide antenna conductance can be used to determine the plasma electron collision frequency, once the other plasma parameters are known.

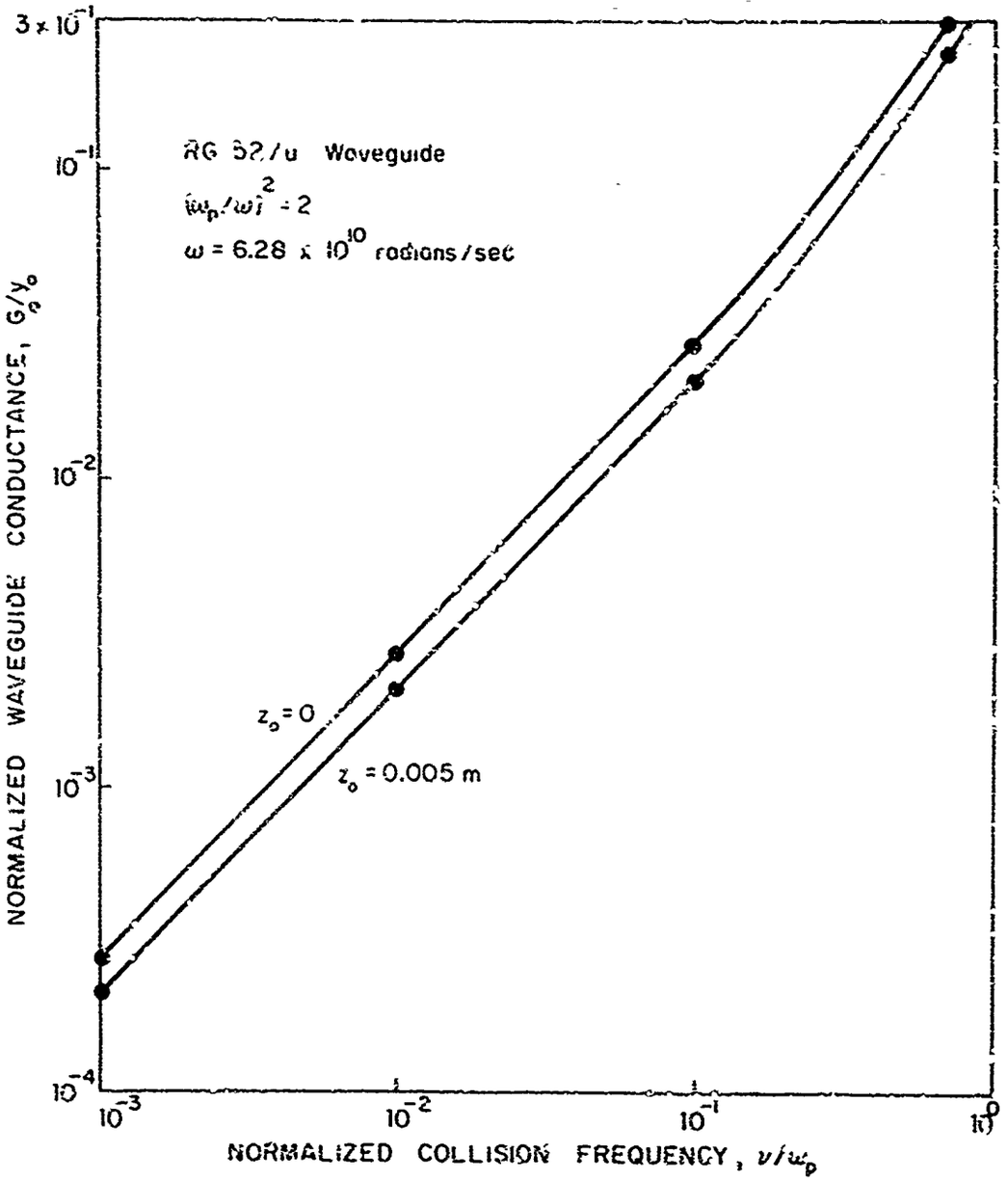

Figure IV-3. Normalized conductance of waveguide radiating into overdense plasma; effect of plasma losses.

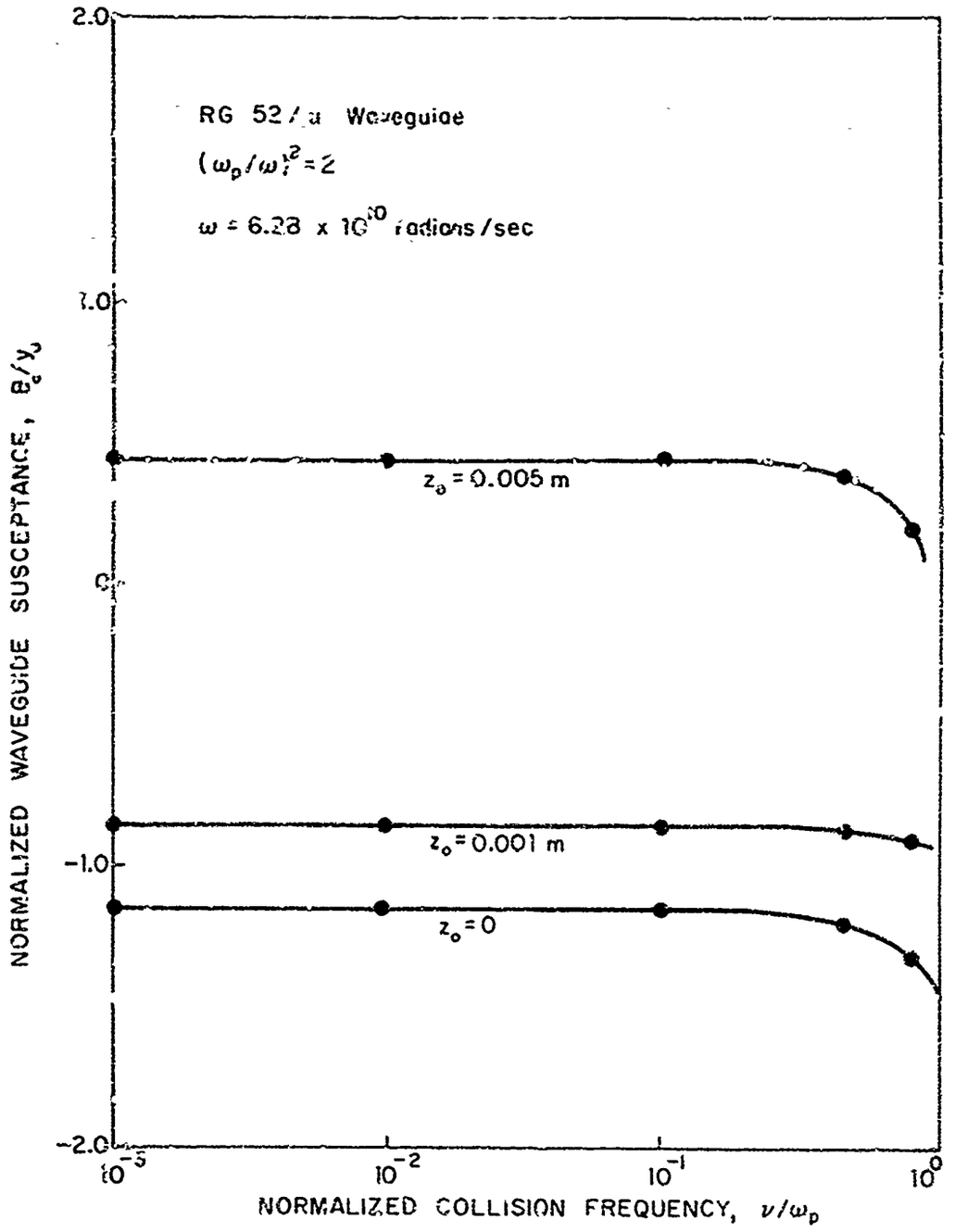

Figure IV-4. Normalized susceptance of waveguide radiating into overdense plasma; effect of plasma losses.

The determination of the reentry plasma properties is slightly more complicated if the admittance measurements are made at frequencies not in the range specified above. The procedure then is similar to that outlined initially (page 63) for thin apertures. Figure IV-5 shows a block diagram representation of the reentry plasma diagnostic technique.

Values of waveguide antenna admittance again are assumed to be known (measured) at two frequencies below the plasma frequency. Ideally, the two frequencies should differ by at least 20 per cent of the plasma frequency. Only one value of admittance is considered at a time. An approximate value of the boundary layer thickness z_o is chosen. The plasma electron density N_o and electron collision frequency ν required to produce the measured admittance value at frequency with z_o specified are determined using the Newton-Raphson technique to determine the roots of the equations

$$G_c(N_o,\nu) - G_m = 0 \qquad \text{(IV-7)}$$

$$B_c(N_o,\nu) - B_m = 0 \qquad \text{(IV-8)}$$

where G_c, G_m, B_c, and B_m have the same meanings as before. The values of G_c and B_c are calculated using (II-61) with $u = 0 (T_e = 0)$.

Other realistic values of z_o also are chosen for the same admittance value and the corresponding values of N_o and ν are determined. This provides sets of values for z_o, N_o and ν all of which correspond to the measured value of waveguide antenna admittance.

The procedure is repeated for the second admittance value. The result is sets of z_o, N_o and ν values for both measured admittance values. The set of z_o, N_o and ν values common to both admittance values is that of the reentry plasma layer.

C. Trailblazer II The Trailblazer II rocket used in reentry test studies (Caldecott et al. 1967; Mayhan et al. 1968) is a four-stage vehicle. The first two stages fire upward in the conventional manner.

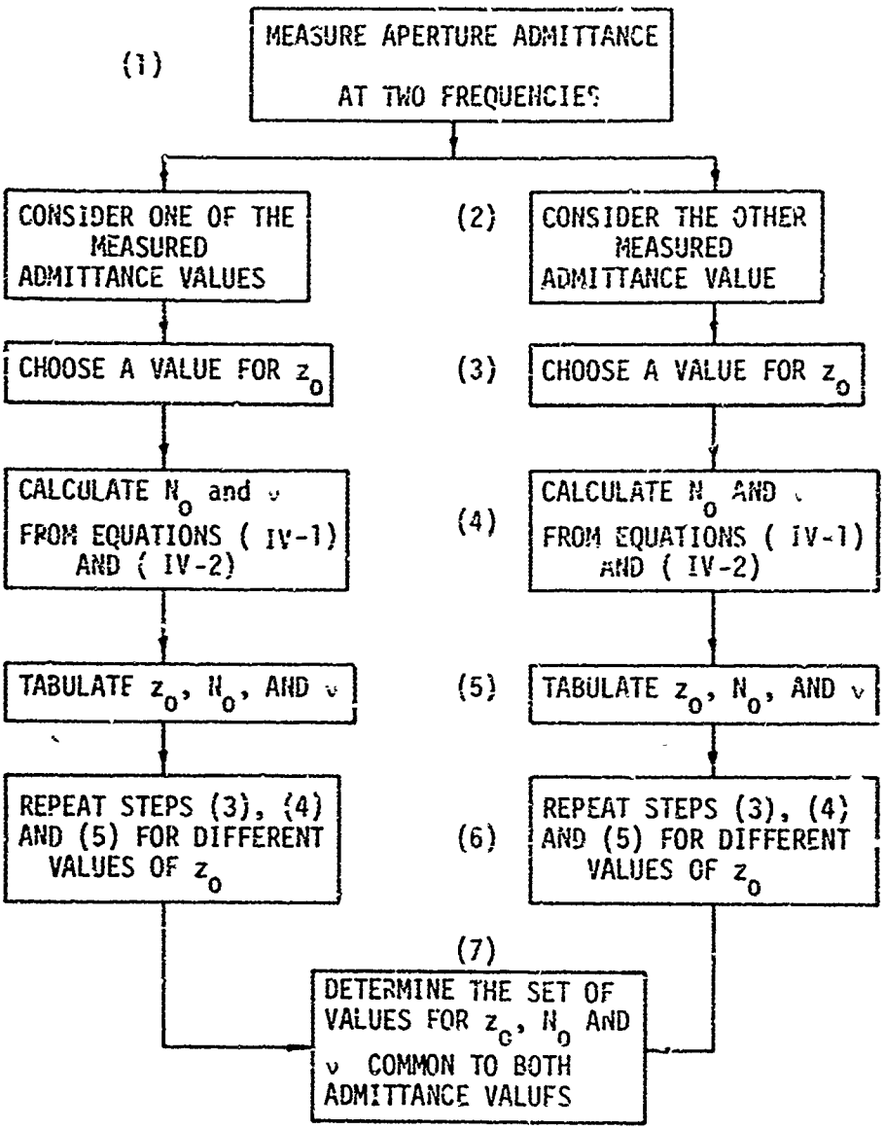

Figure IV-5. Flow chart of a reentry plasma diagnostic method based on two-frequency waveguide antenna admittance measurements.

The third and fourth stage engines face backward and drive the payload package back into the earth's atmosphere along a trajectory nearly parallel to that followed during the ascending part of the flight. The Trailblazer II vehicle is capable of injecting a 27 kg payload into a reentry trajectory at a velocity of 5.4 km per second. The payload reenters the atmosphere about 240 km from the launch point, minimizing the down-range support needed. The Trailblazer II trajectory is shown in Figure IV-6.

The complex admittances of two open-ended waveguide antennas operating at 2850 and 5600 MHz, respectively, were measured using reflectometers specially designed for this purpose (Bohley et al. 1963). The antennas were located at the aft edge of the payload package hemispherical nosecone. The location of the antennas with respect to the stagnation point was changing constantly because the payload was spin stabilized at 13.75 revolutions per second and reentered with an initial attack angle α_a of 10.5°. Both antennas passed through positions A, B and C, shown in Figure IV-7, during each revolution, depending upon the antenna location. The telemetry used to relay the admittance data back to earth operated at a frequency of 9.21 GHz and a power of 1100 watts peak. The telemetry antennas were located away from the most severe plasma conditions. Waveguide antenna admittance was measured continually during reentry.

The reentry plasma was relatively thick and dense at altitudes between about 50 and 30 km. Consequently, plasma properties at these altitudes can be estimated from the measured admittance values, using the technique outlined previously (page 72). The values of reentry plasma electron density N_o, collision frequency ν and boundary layer thickness z_o, determined in this manner for several values of reentry vehicle altitude, are presented in Table IV-1, together with the reentry vehicle velocity and the measured values of waveguide antenna admittance.

The plasma layer values determined from the waveguide antenna admittance measurements are in agreement with those predicted by pre-flight air chemistry and fluid flow calculations. The pre-flight calculations used simplified air chemsitry models and neglected the reencry vehicle angle of attack. The predicted values of electron density N_o, collision frequency ν and boundary layer thickness z_o were in the ranges

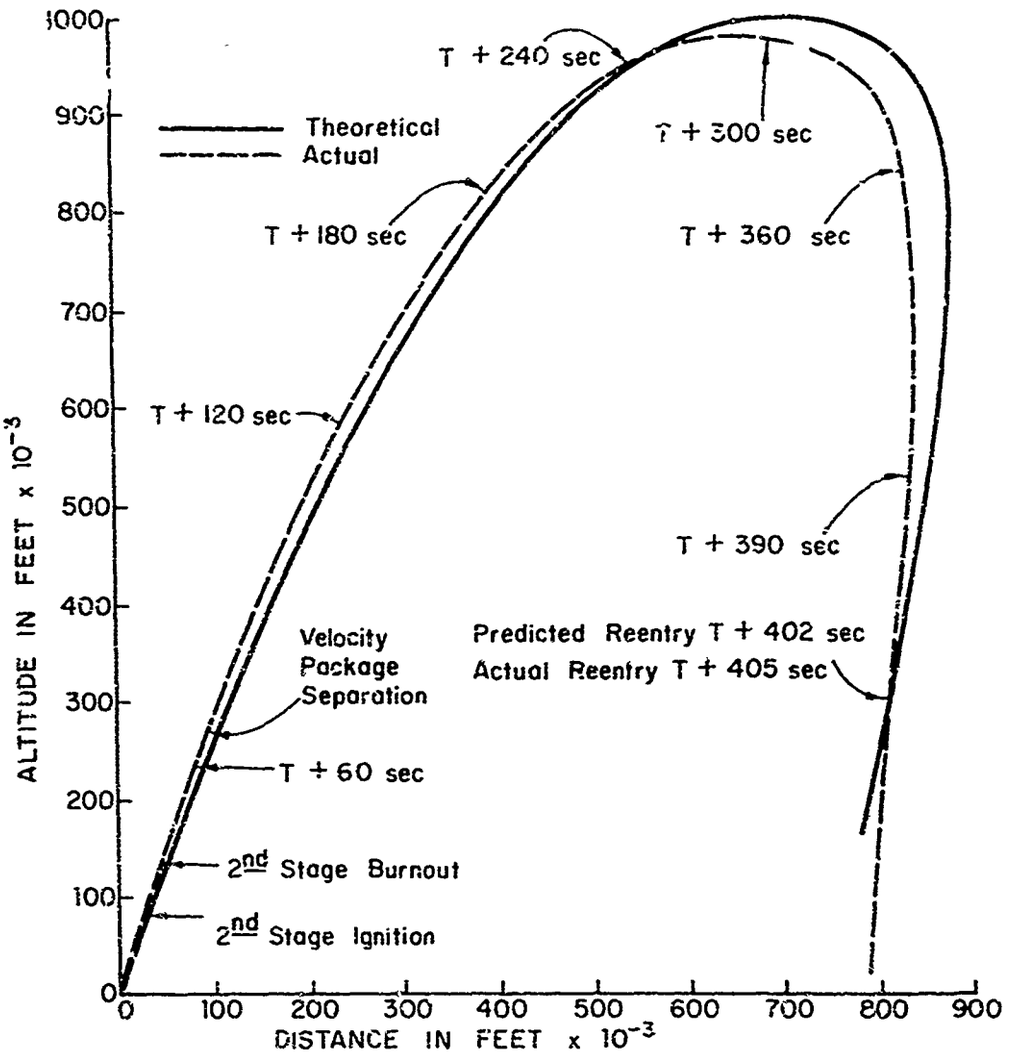

Figure IV-6. Trailblazer II flight trajectory (Caldecott et al. 1967, Figure 13).

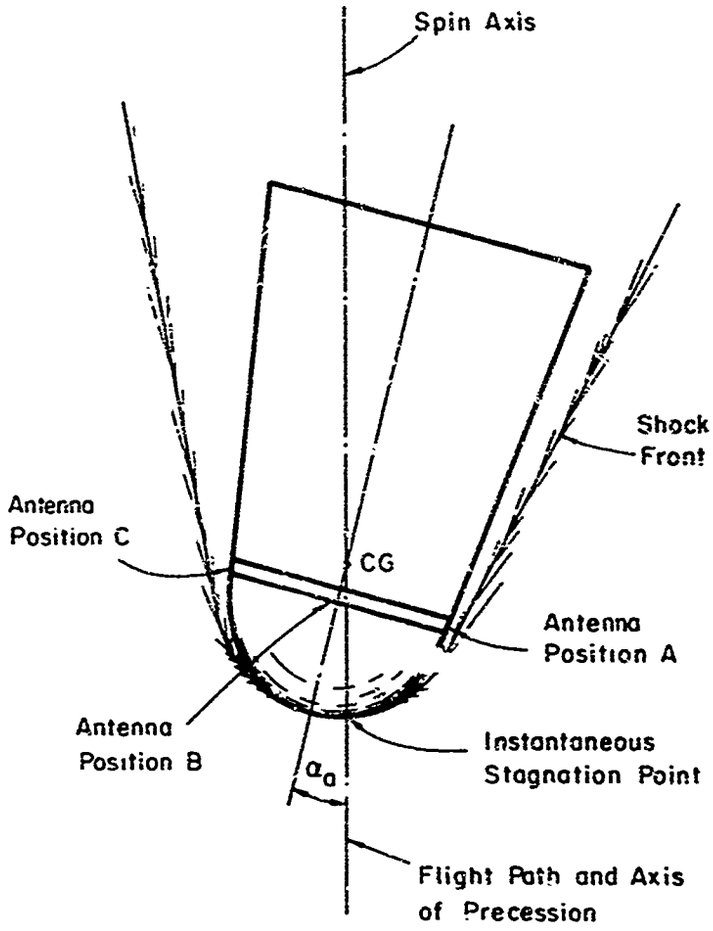

Figure IV-7. Relative antenna positions during reentry (Caldecott et al. 1967, Figure 3).

TABLE IV-1

TRAILBLAZER II REENTRY PLASMA PROPERTIES AND FLIGHT DATA

Altitude* (km)	Velocity* (km/sec)	Admittance* 2.85 GHz	Y/Y_o 5.60 GHz	Electron Density N (cm^{-3})	Collision Frequency ν (sec^{-1})	Boundary Layer Thickness a_o (m)
50	6	.45-i.48	.16-i.14	$6x10^{11}$	$3x10^{9}$	$2.0x10^{-3}$
47	6	.50-i.45	.19-i.16	$8x10^{11}$	$4x10^{9}$	$1.5x10^{-3}$
37	6	.55-i.37	.25-i.17	$1xi0^{12}$	$6x10^{9}$	$2.0x10^{-3}$

*Altitude, velocity and admittance values obtained from Caldecott et al. (1967).

$$5\times10^{11} < N_e < 1\times10^{13} \text{ cm}^{-3}$$

$$2\times10^{8} < \nu < 5\times10^{9} \text{ sec}^{-1}$$

and

$$0 < z_o < 5 \text{ mm}$$

respectively (Mayhan et al. 1968). Better agreement between pre-flight predictions and values determined from admittance measurements cannot be expected using simplified analyses.

It is noteworthy that the pre-flight predicted plasma values were used by Mayhan et al. (1968) to calculate the antenna admittance values expected during reentry. The measured admittance values were in only qualitative agreement with the predicted values. However, this agreement was considered sufficient to establish the validity of the air chemistry and fluid flow calculations. No further use was made of the measured admittance values by Mayhan et al.

The calculation of Trailblazer II reentry plasma properties from waveguide antenna admittance measurements has demonstrated the feasibility of using relatively simple techniques for reentry plasma diagnostics. Waveguide antenna admittance measurements, however, are insensitive to the plasma electron temperatures experienced during reentry and to ion sheath or boundary layer thicknesses less than about a millimeter. The admittance of a thin aperture is affected by these factors, making it more useful for reentry plasma diagnostics.

CHAPTER V

CONCLUSIONS AND RECOMMENDATIONS FOR FUTURE WORK

Admittances of surface mounted aperture antennas in a reentry plasma environment have been investigated extensively in this report. As a result, a number of significant conclusions can be stated and several recommendations for future work can be made.

Conclusions The following significant conclusions can be stated as a result of the current study:

1. The values of electron density, electron collision frequency, electron temperature and/or stand-off distance for reentry plasma can be decermined directly from measurements of the admittance of an aperture antenna located on the surface of a reentry vehicle.
2. The excitation frequency of the aperture should be less than the plasma frequency when admittance measurements are used for reentry plasma diagnostics.
3. The aperture length can be as small as 0.5 of a free space RF wavelength when admittance measurements are used for reentry plasma diagnostics.
4. The reentry plasma electron temperature can be determined from aperture antenna admittance measurements if the aperture width is about 0.01, or less, of a free space RF wavelength.
5. The effect of the plasma electron temperature upon aperture admittance depends upon whether the aperture ground plane absorbs or reflects incident electrons.
6. The reentry plasma electron temperature can be determined from aperture admittance measurements if the plasma is in contact with the aperture ground plane or is separated from the ground plane by less than 0.001 of a free space RF wavelength.

7. The admittance of an open-ended-waveguide antenna can be used to determine the plasma electron density, electron collision frequency and plasma stand-off distance when aerodynamic boundary layer effects cause the reentry plasma to be separated from the vehicle surface. This finding has been verified by a companion study at Colorado State University (Davidson 1970).
8. Values of waveguide antenna admittance measured at two frequencies during the reentry of a Trailblazer II payload package were used, in the current study, to determine the values of electron density, electron collision frequency and plasma stand-off distance associated with the reentry plasma. These values are consistent with the values determined by analytical means.

Recommendations for Future Work The analyses carried out in the current study have been based on the assumption of a planar geometry. This is a valid assumption as long as the reentry vehicle surface is reasonably flat over a distance of several wavelengths. The usefulness of the current study could be extended, however, by making aperture admittance calculations for finite sized apertures on non-planar conducting surfaces. Diagnostic measurements then could be made at locations on the reentry vehicle, such as the stagnation region, where the surface definitely is non-planar and where diagnostic measurements could most easily be related to theoretical predictions.

The admittance calculations also have been performed under the assumption that the plasma layer is uniform and infinite in extent. While this assumption often is reasonable when the aperture excitation frequency is less than the plasma frequency, it would be desirable to develop methods for determining the spatial variation of the plasma properties using aperture admittance measurements.

Mention has been made of theoretical techniques (Mayhan 1968, 1969), based on cold plasma theory, wherein aperture admittance measurements can be used to determine the properties of a thin, inhomogeneous reentry plasma layer. These proposed techniques involve rather complex experimental and data analysis problems and have not been demonstrated experimentally. The inclusion of electron temperature effects would not make the techniques significantly more complicated as long as the plasma electron temperature

could be taken to be approximately constant. Experimental admittance values for this type of plasma diagnostics probably would have to be measured on a swept frequency basis using techniques similar to those described by Davidson et al. (1969).

The admittance values discussed previously all have been calculated using linearized, hydrodynamic, compressible plasma theory. This hydrodynamic approach has been widely used in the literature in preference to the kinetic theory approach. Kinetic plasma theory can provide a more complete and accurate description of wave propagation in a plasma but is very difficult to apply to practical problems.

Kinetic plasma theory has been used by Kuehl (1966, 1967) to calculate the radiation resistance of a short filamental antenna in a warm, isotropic, collisionless plasma. He found that the transverse component of radiation resistance predicted by kinetic plasma theory agrees quite well with that predicted by hydrodynamic plasma theory except for frequencies below the plasma frequency. The longitudinal component of radiation resistance predicted by the two methods are similar only for frequencies which are large compared to the plasma frequency.

The analyses performed by Kuehl involved many highly idealized assumptions concerning the antenna and plasma. Nevertheless, Kuehl's results indicate the need for more sophisticated kinetic theory investigations of the performance of antennas in plasmas. Antenna admittance values obtained using kinetic plasma theory and those obtained using hydrodynamic plasma theory should be compared with experimentally measured values to determine the conditions under which each theory provides valid results.

REFERENCES

Balmain, K. G. (1966), "Impedance of a Radio-Frequency Plasma Probe with an Absorptive Surface," Radio Science, 1, (New Series), 1.

Bohley, P., R. Caldecott, R. McGown and R. C. Taylor (1963), "Automatic Impedance Plotter for Missile Application," Report 1565-1, Antenna Laboratory, The Ohio State University Research Foundation.

Caldecott, R., P. Bohley and R. M. Nerem (1967), "Reentry Communications: Antenna Impedance and Radar Reflections Recorded During the Reentry of a Trailblazer Rocket Vehicle on 14 February 1966," Report 2146-7 ElectroScience Laboratory, The Ohio State University Research Foundation.

Compton, R. T., Jr. (1964), "The Admittance of Aperture Antennas Radiating into Lossy Media," Report 1691-5, Antenna Laboratory, The Ohio State University Research Foundation.

Davidson, R. P. (1970), "Antenna Diagnostics of Reentry Plasmas," Ph.D. thesis, Colorado State University.

Davidson, R. P., R. J. Churchill and J. P. Rybak (1969), "Swept Frequency Microwave Measurements in Simulated Re-Entry Environments," AIAA Paper No. 69-701, Presented at the AIAA Fluid and Plasma Dynamics Conference, San Francisco, California, June 16-18, 1969.

Galejs, J. (1965), "Admittance of a Waveguide Radiating into a Stratified Plasma," IEEE Transactions on Antennas and Propagation, AP-13, 64.

Galejs, J. (1966), "Slot Admittance for Compressible Plasma Layers," Radio Science, 1, (New Series), 457.

Galejs, J. (1969), Antennas in Inhomogeneous Media, Pergamon Press, New York.

Harrington, R. F. (1961), Time-Harmonic Electromagnetic Fields, McGraw-Hill Book Company, New York.

Hessel, A., N. Marcuvitz and J. Shmoys (1962), "Scattering and Guided Waves at an Interface Between Air and a Compressible Plasma," IRE Transactions on Antennas and Propagation, AP-10, 48.

Huber, P. W., and T. E. Aims (1964), "The Entry-Communications Problem," Astronautics and Aeronautics, 2, 30.

Jacavanco, D. J. (1969), "Electron Reduction in the Reentry Plasma Sheath," AFCRL-69-0154, U. S. Air Force Cambridge Research Laboratories.

King, R. W. P. (1961), "Dipoles in Dissipative Media," Technical Report 336, Cruft Laboratory. Harvard University.

Kritz, A. H. and D. Mintzer (1950), "Propagation of Plasma Waves Across a Density Discontinuity," Physical Review, 117, 382.

Kuehl, H. H. (1966), "Resistance of a Short Antenna in a Warm Plasma," Radio Science, 1, (New Series) No. 8, 971.

Kuehl, H. H. (1967), "Computations of the Resistance of a Short Antenna in a Warm Plasma," Radio Science, 2 (New Series), No. 1, 73.

Mayhan, J. W. (1967), "Properties of Planar Antennas Radiating into Linear Inhomogeneous Media with Application to Plasma Diagnostics," Report 2146-8, ElectroScience Laboratory, The Ohio State University Research Foundation.

Mayhan, J. W. (1968), "Plasma Diagnostics Using the Reflection Coefficient of Planar Antennas," Report 2146-11, ElectroScience Laboratory, The Ohio State University Research Foundation.

Mayhan, J. W. (1969), "Plasma Identification Using the Reflection Coefficient of Planar Antennas," Report 2748-1, ElectroScience Laboratory, The Ohio State University Research Foundation.

Mayhan, J. W., R. Caldecott and P. Bohley (1968), "Antenna Impedance in a Reentry Environment," IEEE Transactions on Antennas and Propagation, AP-16, 573.

McCracken, D. D. and W. S. Dorn (1964), Numerical Methods and Fortran Programming, John Wiley and Sons, New York.

Miller, E. K. (1968a), "The Admittance of the Infinite Cylindrical Antenna Immersed in a Lossy, Compressible Plasma," IEEE Transactions on Antennas and Propagation, AP-16, 111.

Oster, L. (1960), "Linearized Theory of Plasma Oscillations," Review of Modern Physics, 32, 141.

Richmond, J. A. (1966), "Scattering by Wire Loops and Square Plates in the Resonance Region," Report 2097-1, Antenna Laboratory, The Ohio State University Research Foundation.

Seshadri, S. R. (1965a), "Radiation From an Electromagnetic Source in a Half Space of Compressible Plasma-Surface Waves," IEEE Transactions on Antennas and Propagation, AP-12, 340.

Sommerfeld, A. (1952), Lectures on Theoretical Physics, Academic Press, New York.

Stratton, J. R. (1941), Electromagnetic Theory, McGraw-Hill Book Company, New York.

Swift, C. T. (1967), "Input Admittance of a Rectangular Waveguide-Fed Aperture Radiating into an Inhomogeneous Lossy Dielectric Slab," NASA TN D-4158, Langley Research Center.

Tanenbaum, B. S. (1967), Plasma Physics, McGraw-Hill Book Company, Inc., New York.

Thomas, G. B., Jr. (1953), Calculus and Analytic Geometry, Addison-Wesley Publishing Company, Cambridge, Massachusetts.

Villeneuve, A. T. (1965), "Admittance of Waveguide Radiating into Plasma Environment," IEEE Transactions on Antennas and Propagation, AP-13, 135.

Wait, J. R. (1966), "On the Theory of Wave Propagation in a Bounded Compressible Plasma," Canadian Journal of Physics, 44, 293.

Wasserstrom, E., C. M. Su and R. F. Probstein (1965), "Kinetic Theory Approach to Electrostatic Probes," Physics of Fluids, 8, 56.

APPENDIX I

THE PLASMA ION SHEATH

An important concept in plasma physics is that of the plasma ion sheath which occurs in a plasma near a wall. The discussion of the plasma ion sheath in this section is meant to be heuristic and is not mathematically rigorous. A more thorough discussion of the plasma ion sheath is given by Tanenbaum (1967). The present discussion is a summary of that work.

Charged particles incident upon a surface are, for the most part, lost to the plasma. The ions and electrons incident upon the surface generally recombine and return to the plasma as neutrals. Also, some electrons are able to enter the conduction band of a metal surface. The particle flux hitting a wall can be calculated from a knowledge of the velocity distribution function for the particles near the wall.

Assuming a one-sided Maxwellian velocity distribution function near the wall, the electron flux Γ_e and Γ_i incident upon the wall are (Tanenbaum 1967)

$$\Gamma_e = N_o \left(\frac{KT_e}{2\pi m_e} \right)^{\frac{1}{2}} \tag{AI-1}$$

$$\Gamma_i = N_o \left(\frac{KT_i}{2\pi m_i} \right)^{\frac{1}{2}} . \tag{AI-2}$$

The electron flux to the wall generally is one or two orders of magnitude larger than the ion flux as a result of the large difference between (T_e/m_e) and (T_i/m_i) in most plasmas. Because of the large difference between the electron flux and the ion flux, an electrically isolated surface in contact with a plasma develops a negative charge and, hence, a negative potential with respect to the plasma. This negative potential

provides an attractive force for the ions in the plasma and a repulsive force for the electrons. The ion flux to the wall increases and the electron flux decreases until the two fluxes are equal and the negative potential at the wall attains a fixed value.

The electron density in the region near the wall is lower, by about one or two orders of magnitude, than the electron density in the main body of the plasma. Furthermore, near the wall the electron density is less than the ion density. This region of electron density and ion density unbalance is referred to as the plasma ion sheath.

The thickness of the plasma ion sheath is of the order of several Debye distances. The Debye distance λ_D is defined by the mks relations

$$\lambda_D = 69\sqrt{\frac{T_e}{N_o}} \quad . \tag{AI-3}$$

A Debye distance for typical reentry plasma parameters is of the order of 10^{-6} meter.

APPENDIX II

A NUMERICAL INTEGRATION TECHNIQUE

The integration of equations (II-61) and (III-21) (pages 16 and 53, respectively) must be performed numerically, as pointed out previously. A Simpson's rule technique is suitable for the α integration. However, the integrand varies rapidly for some values of β and slowly for other values. Consequently, a numerical integration technique employing fixed intervals is not efficient for evaluating the β integration. Ideally, the intervals should be small where the integrand varies rapidly, and should be large where the integrand varies slowly.

A computer program in which the size of the integration intervals is adjusted to the variation of the integrand has been developed at Ohio State University (Richmond 1966). The program is said to combine "the simplicity of the trapezoidal rule with the efficiency of the fifth-order Newton-Cotes Formula." The program handles both real and complex integrals of the form

$$\int_{AA}^{BB} f(x)dx \qquad \text{(AII-1)}$$

The computer program in Fortran IV is given in Figure AII-1. The variables ERRR and NX are the per cent error allowed in the integration and the number of "gross intervals" to be used, respectively. Only the basic principles of this program will be discussed.

```
      PROGRAM INT
      COMPLEX SSS, SS, TRAP, SIMP, FNCP, TRAZ, SIMZ, FNCZ
      READ (5,1) AA, BB, ERRR, NX
    1 FORMAT (3E20.3, I3)
      FN = NX
      DEL = (BB-AA)/FN
      SSS = CMPLX (0.0,0.0)
      ERR = .01*ERRR/FN
      A = AA
      DO 40 NXX = 1,NX
      MXX = 0
      B = A + DEL
      SS = CMPLX (0.0,0.0)
      MX = 2
      DX = DEL/2.
      LX = 1
      X = A
      GO TO 15
    5 TRAZ = DX*SS
      MX = 1
      LX = 1
      DX = DEL
   10 SS = CMPLX (0.0,0.0)
      LX = LX + 1
      DX = .5*DX
      X = A + DX
   15 DO 20 IX = 1,MX
   18 SS = SS + F(X)
   20 X = X + 2.*DX
      IF(LX.EQ.L) GO TO 5
      MX = 2*MX
   21 TRAP = .5*TRAZ + DX*SS
      DIF = CABS(TRAP-TRAZ)
      IF(DIF.GE.DIP) MXX = MXX + 1
      DIP = DIF
   22 SIMP = (4.*TRAP-TRAZ)/3.
   23 FNCP = (16.*SIMP-SIMZ)/15.
   24 ER = CABS(1.-FNCZ/FNCP)
      TRAZ = TRAP
      SIMZ = SIMP
      FNCZ = FNCP
   25 IF(LX.GT.4) GO TO 10
   26 IF(MXX.GT.4) GO TO 30
   27 IF(ER.GT.ERR) GO TO 10
   30 SSS = SSS + FNCP
   40 A = A + DEL
   50 WRITE(6,60) AA,BB,ERRR,SSS
   60 FORMAT(5E20.8)
      END
```

Figure AII-1. A digital computer program for numerical integration (Richmond 1966).

Let the range of integration $AA < x < BB$ be divided into M equal intervals, and let f_k represent the integrand value at the end points of these intervals as in Figure AII-2. Using the trapezoidal rule (McCracken and Dorn 1964) with $M = 1$, the integral is given by

$$TRAP_1 = DX(0.5f_1 + 0.5f_5) \tag{AII-2}$$

where $DX = BB-AA$. Dividing the integration range into two intervals, the trapezoidal rule yields

$$TRAP_2 = \frac{DX}{2}(0.5f_1 + f_3 + 0.5f_5) \tag{AII-3}$$

while if four intervals are used one obtains

$$TRAP_3 = \frac{DX}{4}(0.5f_1 + f_2 + f_3 + f_4 + 0.5f_5) \quad . \tag{AII-4}$$

Equations (AI-3) and (AI-4) can be written in the forms

$$TRAP_2 = 0.5\ TRAP_1 + \frac{DX}{2} f_3 \tag{AII-5}$$

$$TRAP_3 = 0.5\ TRAP_2 + \frac{DX}{4}(f_2 + f_4) \quad , \tag{AII-6}$$

The general relation is

$$TRAP_{i+1} = 0.5\ TRAP_i + \left(\frac{DX}{2^i}\right) SS \tag{AII-7}$$

where SS is the summation of the integrand values required for $TRAP_{i+1}$ not included in $TRAP_i$. Equation (AII-7) appears in the computer program as statement 2i where TRAP and TRAZ denote $TRAP_{i+1}$

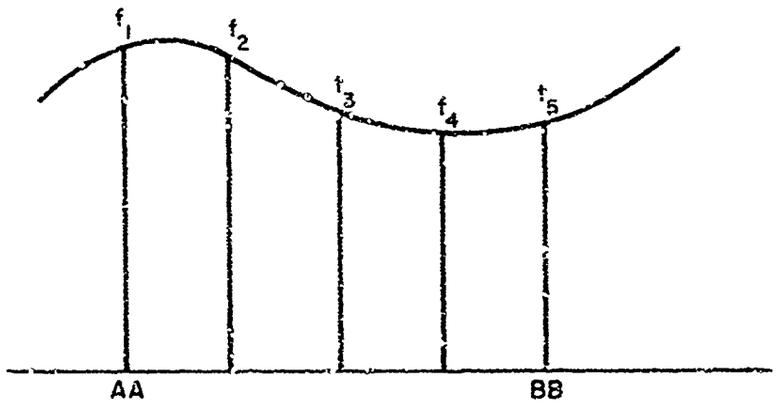

Figure AII-2. A plot of the function f(x).

and $TRAP_i$, respectively, The quantity SS is evaluated in statements 15 through 20.

Simpson's rule (McCracken and Dorn 1964) yields the following results when used to evaluate the integral for two and four intervals:

$$SIMP_2 = \frac{DX}{6}(f_1 + 4f_3 + f_5) \qquad \text{(AII-8)}$$

$$= \frac{1}{3}(4TRAP_2 - TRAP_1)$$

and

$$SIMP_3 = \frac{DX}{12}(f_1 + 4f_2 + 2f_3 + 4f_4 + f_5)$$

$$= \frac{1}{3}(4TRAP_3 - TRAP_2) \quad . \qquad \text{(AII-9)}$$

Simpson's rule integration is seen to be performed through a linear combination of two successive trapezoidal-rule integrations. This is carried out in statement 22.

The fifth-order Newton-Cotes formula for numerical integration generally is more efficient than the trapezoidal rule or Simpson's rule and can be obtained from a linear combination of two successive Simpson-rule integrations in the form

$$FNCP_i = \frac{1}{15}(16\ SIMP_i - SIMP_{i-1}) \quad . \qquad \text{(AII-10)}$$

This equation appears in the program as statement 23.

The process of repeatedly doubling the number of intervals is terminated when the results converge to the specified accuracy and is controlled by statement 27.

The number of "gross intervals," denoted by NX, can have a significant influence on the time required by the computer to perform the integration. The integration range (AA to BB) is divided into NX equal segments of length DEL. The computer integrates over each of these segments, one at a time. The value of the total integral is denoted by SSS and is obtained by summing the subintegrals (statement 30).

Intervals of equal length are used over the entire range from AA to BB if NX is unity. Values of NX larger than unity results in the computer using small intervals over the segments where the integrand varies rapidly and larger intervals over the segments where the integrand varies less rapidly. The calculation time can be minimized by a proper choice of NX, although the choice is not critical and does not affect the accuracy of the integration.

APPENDIX III

THE NEWTON-RAPHSON ITERATIVE METHOD

Equations (IV-1) and (IV-2) (page 64) form a set of two nonlinear, integral equations in two unknowns. It is impossible to reduce the problem so that the value of the variables N_o and ν can be determined directly in closed form. The Newton-Raphson method (McCracken and Dorn 1964) is an iterative method for finding the roots of such equations.

Let the set of equations be represented by

$$F(x,y) = 0 \tag{AIII-1}$$

$$G(x,y) = 0 \tag{AIII-2}$$

and let x_n, y_n be some approximate root. A better approximation to the root can be obtained by writing a truncated Taylor series expansion of the form

$$F(x_{n+1}, y_{n+1}) = 0 = F(x_n, y_n) + \frac{\partial F}{\partial x}(x_n, y_n)dx + \frac{\partial F}{\partial y}(x_n, y_n)dy \tag{AIII-3}$$

$$G(x_{n+1}, y_{n+1}) = 0 = G(x_n, y_n) + \frac{\partial G}{\partial x}(x_n, y_n)dx + \frac{\partial G}{\partial y}(x_n, y_n)dy \quad . \tag{AIII-4}$$

The defining relations for dx and dy are obtained by solving equations (AII-3) and (AII-4) and can be written in the form

$$dx = \frac{-F(x_n, y_n)\frac{\partial G}{\partial y}(x_n, y_n) + G(x_n, y_n)\frac{\partial F}{\partial y}(x_n, y_n)}{J(x_n, y_n)} \tag{AIII-5}$$

$$dy = \frac{F(x_n,y_n)\frac{\partial G}{\partial x}(x_n,y_n) - G(x_n,y_n)\frac{\partial F}{\partial x}(x_n,y_n)}{J(x_n,y_n)} \qquad \text{(AIII-6)}$$

where

$$J(x_n,y_n) = \frac{\partial F}{\partial x}(x_n,y_n)\frac{\partial G}{\partial y}(x_n,y_n) - \frac{\partial F}{\partial y}(x_n,y_n)\frac{\partial G}{\partial x}(x_n,y_n) \qquad \text{(AIII-7)}$$

It is assumed that $J(x_n,y_n)$ is not equal to zero.

A better approximation to the root of equation (AIII-1) and (AIII-2) is then given by

$$x_{n+1} = x_n + dx = x_n - \left[\frac{F\frac{\partial G}{\partial y} - G\frac{\partial F}{\partial y}}{J}\right]\Bigg|_{x_n,y_n} \qquad \text{(AIII-8)}$$

$$y_{n+1} = y_n + dy = y_n + \left[\frac{F\frac{\partial G}{\partial x} - G\frac{\partial F}{\partial x}}{J}\right]\Bigg|_{x_n,y_n} \qquad \text{(AIII-9)}$$

Successively better and better approximations to the root of equations (AIII-1) and (AIII-2) are obtained by repeatedly employing equations (AIII-8) and (AIII-9). In general, the selection of initial values for x and y is not critical.

Unclassified

Security Classification

DOCUMENT CONTROL DATA - R & D

(Security classification of title, body of abstract and indexing annotation must be entered when the overall report is classified)

1 ORIGINATING ACTIVITY (Corporate author) Colorado State University Department of Electrical Engineering Fort Collins, Colorado 80521	2a. REPORT SECURITY CLASSIFICATION Unclassified 2b GROUP

3 REPORT TITLE

MICROWAVE REENTRY PLASMA DIAGNOSTICS

4 DESCRIPTIVE NOTES (Type of report and inclusive dates)

Scientific. Interim.

5 AUTHOR(S) (First name, middle initial, last name)

James P. Rybak

6 REPORT DATE January 1971	7a. TOTAL NO OF PAGES 110	7b. NO OF REFS 34
8a. CONTRACT OR GRANT NO F19628-70-C-0035 PROJECT THEMIS b Project, Task, Work Unit Nos. 7260 n/a n/a c. DoD Element 61102F d. DoD Subelement 681310	9a. ORIGINATOR'S REPORT NUMBER(S) Scientific Report No. 3 9b. OTHER REPORT NO(S) (Any other numbers that may be assigned this report) AFCRL-71-0012	

10 DISTRIBUTION STATEMENT

1-This document has been approved for public release and sale; its distribution is unlimited.

11 SUPPLEMENTARY NOTES TECH., OTHER	12. SPONSORING MILITARY ACTIVITY Air Force Cambridge Research Laboratories L. G. Hanscom Field (LZ) Bedford, Massachusetts 01730

13 ABSTRACT

An analysis of surface-mounted aperture antenna admittance has been performed in this study to determine the conditions under which admittance measurements can be used for reentry plasma diagnostics. The primary contribution of the present work is the determination that the admittance of a thin, microwave aperture antenna, located on the surface of a reentry vehicle, can be used to obtain the values of the electron density, electron collision frequency, ion sheath thickness and electron temperature of the reentry plasma. It is further demonstrated, by using admittance measurements made during a reentry test flight as reported by Mayhan et al. (1968 IEEE Trans. Antennas and Propagation, AP-17, 573), that open-ended-waveguide antenna admittances can be used to determine the plasma electron density, electron collision frequency and plasma stand-off distance when the reentry plasma is separated, due to aerodynamic boundary layer effects, from the surface of the reentry vehicle.

DD FORM 1 NOV 65 1473

Unclassified

Security Classification

Unclassified

Security Classification

KEY WORDS	LINK A		LINK B		LINK C	
	ROLE	WT	ROLE	WT	ROLE	WT
Reentry						
Plasma Sheath						
Plasma Diagnostics						
Microwave Antennas						
Reentry Vehicles						

Unclassified

Security Classification